DEVELOPMENT OF ANALYTE SENSITIVE POLYMERS FOR USE IN MINIATURE BIOMEDICAL SENSORS

by

Seung-Hei Cho

A dissertation submitted to the faculty of
The University of Utah
in partial fulfillment of the requirements for the degree of

Doctor of Philosophy

Department of Chemical Engineering

The University of Utah

August 2014

The University of Utah Graduate School

STATEMENT OF DISSERTATION APPROVAL

The dissertation of **Seung-Hei Cho**

has been approved by the following supervisory committee members:

Jules J. Magda	, Chair	**April 25, 2014** Date Approved
Eric G. Eddings	, Member	**April 29, 2014** Date Approved
Mikhail Skliar	, Member	**April 25, 2014** Date Approved
Loren Rieth	, Member	**April 28, 2014** Date Approved
Prashant Tathireddy	, Member	**April 28, 2014** Date Approved

and by **Milind Deo** , Chair/Dean of

the Department/College/School of **Chemical Engineering**

and by David B. Kieda, Dean of The Graduate School.

ABSTRACT

Analyte-detecting sensors have been developed in many fields. Chemical sensors, and especially biomedical sensors, deserve special attention because they can simplify time-consuming, costly and site-limited medical procedures. Sensor efficiency depends on its analyte sensing material, signal transducing device and data processing system. The biggest barrier to devise biomedical sensors is the development of analyte sensing material with a high selectivity for target molecules.

The motivation of this research was to develop biomolecule-sensitive polymers that can be used in biomedical sensors. Thus, this thesis covers all stages of chemical sensor development, from developing target analyte sensitive materials to merging the developed materials with a signal transducing system. First, the potential application of a zwitterionic glucose-responsive hydrogel as a body implantable continuous glucose monitoring system was examined. After using thermodynamics to confirm the glucose sensing mechanism, synthesis of the hydrogels was optimized and analyzed using statistical methods (design of experiments (DOE)). Thermodynamics study showed that mixing contribution was an important factor to glucose selectivity as well as elastic contribution. By the DOE study, we confirmed that sensitivity of the hydrogels was determined by the molar ratio of cationic and anionic functional groups, and response time depended on the amount of cross-linker. A hydrogel degradation study was also performed to determine the effect of gamma ray sterilization and neutron irradiations on

the hydrogel cross-linking network for biomedical applications. Results showed that gamma ray affected cross-linking networks of UV cured hydrogels. However, the neutron irradiation effect was not considerable. In addition, ferromagnetic particles-embedded, zwitterionic glucose-responsive hydrogels were developed to enable the response processing by a magnetoresistive transducer. The hydrogel with horizontally aligned ferromagnetic particles showed good sensitivity in the physiological glucose range (~10 mM). Moreover, response time was reduced by almost seven-fold with twice thicker samples (800 um) than samples (400 um) with a pressure sensor measurement.

A second project optimized the synthesis of a glutathione (GSH)-sensitive polymer. The selectivity of the polymer for GSH was improved by synthesizing a GSH-imprinted polymer and adopting a cobalt ion-mediated chelating binding structure as analyte binding sites.

TABLE OF CONTENTS

LIST OF TABLES

NOMENCLATURE

μ	Mobility ($cm^2/v.s$)
μ_1	The chemical potential of water in the hydrogel at ambient pressure
$\mu_{1,0}$	The chemical potential of water in the reference solution that surrounds the hydrogel
1X PBS	Dublecco's phosphate buffered saline solution
3-APB	3-Acrylamido phenylboronic acid
AAm	Acrylamide
AA	Acrylic acid
AIBN	2,2'-Azobis-isobutyronitirle
ANOVA	Analysis of variance
APS	Ammonium Persulfate
B	Magnetic flux density (Wb/m^2)
B	Magnetic flux density (T)
B	The concentration of bound target molecule at equilibrium = [mM]
B_{max}	The total number of binding sites, same as N_t
BNCT	Boron neutron capture therapy
BIS	*N,N*-methylenebisacrylamide
C	The weight fraction of the polymer in the hydrogel
C_{gel}	The concentration of ions within the hydrogel
CGMS	Continuous glucose monitoring systems
CGS	Continuous glucose sensors
Co-MIP	Cobalt ion-imidazole interaction mediated binding complex with MIP
Co-NIP	Cobalt ion-imidazole interaction mediated binding complex with NIP
C_{sol}	The concentration of ions in outside the hydrogel

DDS	Drug Delivery System
DMAPAA	*N*-[3-dimentylamino)propyl]acrylamide
DMSO	Dimethyl sulfoxide
DOE	Design of experiments
EGDMA	Ethylene glycol dimethacrylate
F	Functional monomer
FAD	Flavin adenine dinucleotide
FFD	Fractional factorial design
FNIF	The fast neutron irradiation
G	Network elastic shear modulus
GDH	Glucose-1-dehydrogenase
GOx	Glucose oxidase
GSH	Glutathione
GSSH	Oxidized glutathione
H	Magnetic field strength = [kA/m]
HbAlc	Hemoglobin Alc
HEPES	4-(2-hydroxyethyl)piperazine-1-ethanesulfonic acid
HHMP	2-hydroxy-4'-(2-hydroxyethoxy)-2-methyl propiophenone
ISF	Interstitial fluid
k_1	Response rate
m	Geometric effect factor (length/width of current flow)
MAA	Methacrylic acid
MEMS	Micromechanical systems
MeOH	Methanol
MIP	Molecularly imprinted polymer
n_1	The number of moles of water
n_{cr}	Effective number of cross-linked chains in the network
NIP	Non-molecularly imprinted polymer
q	Electric charge (Coulombs)
q(I)	Wave vector
R	The gas constant

R_B	Resistance under magnetic field (ohm)
R_o	Resistance under non-magnetic field (ohm)
RSM	Response surface methodology
SANS	Small angle neutron scattering
T	Tesla
T	Temperature (K)
TEMED	*N,N,N',N'*-tetramethylethylenediamine
TI	The thermal neutron irradiation
T.P.	Transition Point (transition temperature)
UUTR	Utah TRIGA reactor
v	The concentration of the polymer elastic chains
$\boldsymbol{V}$	Rate vector (m/s)
V_1	The molar volume of water
VI	1-vinylimidazole
V_m	The volume of the relaxed network
V-pyrol	1-vinyl-2-pyrrolidinone
wt.%	Weight percentage
ΔF_{el}	The elastic free energy by the polymer structure stretching
ΔF_{ion}	The mixing free energy of water molecules and counterions within the hydrogel
ΔF_{mix}	The mixing free energy of water molecules and the polymer network
ΔF_{tot}	The total change of free energy
Λ	The deformation constant
ξ	The polymer-polymer correlation length
ρ_B	Resistivity under magnetic field (ohm·cm)
ρ_o	Resistivity under non-magnetic field (ohm·cm)
σ	The nominal stress
χ_1	The Flory-Huggins parameters for ternary interaction
χ_o	The Flory-Huggins parameters for binary interaction
Π_{mix}	The osmotic pressure of mixing
Π_{el}	The osmotic pressure of elastic
Π_{ion}	The osmotic pressure of ion mixing

N_t	The total number of binding sites, maximum binding = [mmole/g]
F	The concentration of free(unbound) target molecule at equilibrium = [mM]
K_a	Binding affinity to glutathione = [1/mM]
K_{ag}	Binding affinity to oxidized glutathione
K_D	Dissociation constant = [mM]

ACKNOWLEDGEMENTS

It has been five years since I started the Ph.D. program at the University of Utah. There were many difficulties during this program. However, I overcame many hindrances because of my professors and friends.

Foremost, I sincerely thank my adviser, Dr. Magda, for his supporting and mentoring for the last five years. I will never forget the support from Dr. Tathireddy, and Dr. Rieth. I could not proceed with my research without these three professors at the University of Utah. I also appreciate my committee members: Dr. Skliar, and Dr. Eddings for their advice. I also sincerely thank Dr. Young Moo Lee. He cheered me up when I was disappointed with myself.

I thank Jeff for being a best friend and coworker. I also thank Eunkyung, Genayo, Seungah, Tram, Vasiliy, and Yunlu. They always stand by me whenever I need them. I also thank Cheryl for taking care of me like a mom. Most importantly, I want to say here, “I love my mom and dad, and my sisters with all my heart.”

CHAPTER 1

INTRODUCTION

1.1 Motivation

The motivation for this research is developing chemical sensors for bio/medical applications because we can save many lives without complicated and expensive medical operations with a simple device.

Chemical sensors are defined as "a self-contained device that is capable of providing real time analytical information about a test sample" [1]. Ideally, chemical sensors gather analytical/numerical data such as concentration regarding chemical species, such as pollutants, explosives, biomolecules, etc. Recently, it has been acknowledged that biomolecule sensors (biosensors) can diagnose diseases and monitor patients more quickly and easily than traditional medical procedures. The development of biosensors for medical applications has accelerated for two reasons. First, the molecular risk factors or byproducts of many diseases have been identified. Second, physical sensor technology for transducing chemical sensor responses has also been developed. The main driver of biomedical sensor development is the merging of information and technology by micromechanical systems (MEMS).

This dissertation focuses on the development of biosensor-applicable biopolymers. Specifically, signal producing (via changing of pressure or magnetic field)

glucose sensitive hydrogels were studied for use as an implantable glucose sensor. In addition, a glutathione sensitive polymer was developed by using molecular imprinting technology. Moreover, this research is widely applicable for the development of other biosensors.

1.2. Background and Literature Review

1.2.1. Stimuli Responsive Hydrogels

Hydrogels are highly cross-linked polymeric networks that are capable of absorbing large amounts of water. Hydrogels are not soluble in water, although they can be degraded over time due to a breakdown of cross-linking structures [2], [3]. In addition, so-called stimuli-responsive hydrogels respond to external stimuli, such as temperature, pH, pressure and chemicals by using pendant functional groups. Because of these unique properties, as well as their good biocompatibility, hydrogels have been used as a drug delivery system [4], a cell culture membrane (scaffold) [5] and a biosensor [6]. Table 1.1 shows different applications of stimuli responsive hydrogels by type of stimulus and responsive pendants.

1.2.2. Thermodynamics of Hydrogel Swelling

The swelling mechanism of hydrogels can be explained by the total change of free energy ($\Delta \boldsymbol{F_{tot}}$). Hydrogels swell or shrink until $\Delta \boldsymbol{F_{tot}}$ reaches a minimum or, equivalently, the chemical potential of each mobile species becomes equal in coexisting phases [24]. $\Delta \boldsymbol{F_{tot}}$ comprises three types of free energies, including the mixing free energy of water molecules and the polymer network ($\Delta \boldsymbol{F_{mix}}$), the elastic free energy due to the polymer structure stretching ($\Delta \boldsymbol{F_{el}}$) and the mixing free energy of water molecules

Table 1.1 Classification of stimuli responsive hydrogels

Stimulus	Response Principle	Functional Pendant	Examples & Application
Temperature	Phase transition at LCST[a]	Poly(N-substituted acrylamide)	• Poly(N-isopropylacrylamide) [7] • Poly(*N,N'*-diethylacrylamdie) [8] • Poly(N-vinylisobutylamide) [9]
	Amphiphilic balance	Amphiphilic block copolymer	• Poly-ethylene oxide-propylene oxide-ethylene oxide tri-block copolymer [10]
pH	The net charge changes due to environment pH changes	Polyacrylic acid group	• Poly(acrylic acid): DDS[b] [11] • Poly(methacrylic acid): DDS [12]
		Amino groups	• Poly(vinylpyridine): DDS [13] • Poly(propylene imine): DDS [14]
		Polypeptides	• Poly(N-methacryloyl-$_L$-leucine): DNA delivery [15]
Glucose	Release entrapped GOx[c], catalase, and insulin by pH responsive material	pH responsive functional groups	• GOx trapped *N,N*-dimethylaminoethyl methacrylate : glucose sensor [16]
	Reversible hydrogen bonding between boronic acid and glucose	Boronic acid groups	• 3-acrylamidophenylboronic acid: in-loop insulin release system [17] • 3-acrylamidophenylboroic acid/tertiary amine groups: glucose sensor [18], [19], [20]
Electric field	Interaction of environment magnetic/electrical field and magnetic material	Conductive polymer	• Polythiophene: Actuator [21]
Magnetic field		Magnetic particles	• Chemically immobilized magnetic particles: artificial tissues [22]
Antigen	Binding of antigen and antibody	Modified antibody	• GAR IgG-NSA: protein drug delivery [23]

[a] LCST : Lower Critical Solution Temperature (Transition Point)
[b] DDS : Drug Delivery System
[c] GOx : Glucose Oxidase

and counterions within the hydrogel ($\Delta \boldsymbol{F_{ion}}$) (equation 1.1) [24]-[26].

$$\Delta F_{tot} = \Delta F_{mix} + \Delta F_{el} + \Delta F_{ion} \tag{1.1}$$

The swelling pressure (Π) of hydrogel is a differential of ΔF_{tot} with respect to water molar volume [24], [26].

$$\Pi = -\left(\frac{\Delta F_{tot}}{\partial n_1}\right)/V_1 = (\mu_{1.0} - \mu_1)/V_1 = \Pi_{mix} + \Pi_{el} + \Pi_{ion} \tag{1.2}$$

n_1: The number of moles of water

V_1: The molar volume of water

$\mu_{1.0}$: The chemical potential of water in the reference solution that surrounds the hydrogel

μ_1: The chemical potential of water in the hydrogel at ambient pressure

$\Pi_{mix}, \Pi_{el}, and\ \Pi_{ion}$: The osmotic pressure of mixing, elastic, and ion mixing

Π_{mix} is the osmotic pressure due to the polymer structure and solvent mixing, and can be expressed by the Flory-Hoggins equation (equation 1.3) [24].

$$\Pi_{mix} = -\frac{RT}{V_1}[\ln(1-\phi) + \left(1 - \frac{1}{p}\right)\phi + \chi\phi^2] \tag{1.3}$$

Π_{el} is the elastic pressure caused by stretching of the hydrogel polymer network, and this elastic pressure depends on the cross-linking structure within the hydrogel. It can be derived from the rubber elasticity theory (equation 1.4) [24].

$$\Pi_{el} = -ARTv\phi^{1/3} = -G \tag{1.4}$$

A: A constant that is dependent on the cross-linking structure

v: The concentration of the polymer elastic chains

G: A shear modulus defined as the ratio of shear stress to shear strain

Π_{ion} is driven by the difference of mobile ions inside and outside of the hydrogel. The ion concentration difference causes an osmotic pressure change between the

hydrogel and its environment. Thus, the ion concentration difference contributes to the hydrogel swelling pressure, and it can be estimated from the Donnan equilibrium theory (equation 1.5) [25].

$$\Pi_{ion} = RT\,(C_{gel} - C_{sol}) \tag{1.5}$$

C_{gel}: The concentration of ions within the hydrogel

C_{sol}: The concentration of ions in outside the hydrogel

1.2.3. Response Kinetics of Stimuli Responsive Hydrogels

There are several steps that must occur for a stimuli-responsive hydrogel to respond to its target analyte. First, analyte molecules must diffuse from the outside environment into the hydrogel matrix. Once the analyte binds the functional monomer within the backbone of the hydrogel, the hydrogel network [28] either loses or absorbs water due to changes in its structure and density. The response rate is determined by 1st order reaction kinetics (equation 1.6-1.7) [24].

Reaction kinetics of 1st order reactions

$$A + F \overset{k_1}{\leftrightarrow} AF \tag{1.6}$$

A: Analyte (A >> F)

F: Functional monomer

k_1: Response rate

Reaction rate

$$-\frac{d[F]}{dt} = k_1[F] \tag{1.7}$$

The response rate of stimuli responsive hydrogels is mainly dependent upon mass transportation of analyte and binding kinetics, as mentioned previously. However, the

response rate is mainly determined by polymer network relaxation because the binding of functional monomer and analytes is much faster than mass transportation of analyte. In addition, [28] reported that the effective diffusion coefficients within stimuli-responsive hydrogels are much smaller than the translational diffusion coefficients of analytes. Hence, the response times (response rate) of hydrogels can be reduced by reducing diffusion effects, either by increasing the surface area [29] or microfabrication of thinner hydrogels [30].

1.2.4. Glucose Sensors

According to the 2011 National Diabetes Fact Sheet [31], 35% of U.S. adults (ages 20 years and older) have prediabetes, and an additional 11.3% suffer from diabetes. Researchers anticipate that 52% of adults will have diabetes or prediabetes by 2020. While diabetes itself is not a fatal disease, it is among the top seven causes of death in the U.S. due largely to its connection to kidney failure, blindness, heart disease and stroke. Also, health care costs related to prediabetes and diabetes among adults were estimated at $194 billion in 2010 and the cost is expected to increase up to $3,351 billion by 2020 [32]. These numbers illustrate the need for new treatments that allow patients to do more than merely monitor their blood sugar levels to avoid fatal complications of the disease.

Currently, the most effective management method for diabetes involves monitoring glucose levels to maintain euglycemia. Therefore, various monitoring devices that can measure glucose concentrations in body fluids have been developed. Glucose monitoring systems mainly consist of three parts: a selective glucose recognition element, a signal transducer, and a signal processing system (Figure 1.1). Various glucose sensors

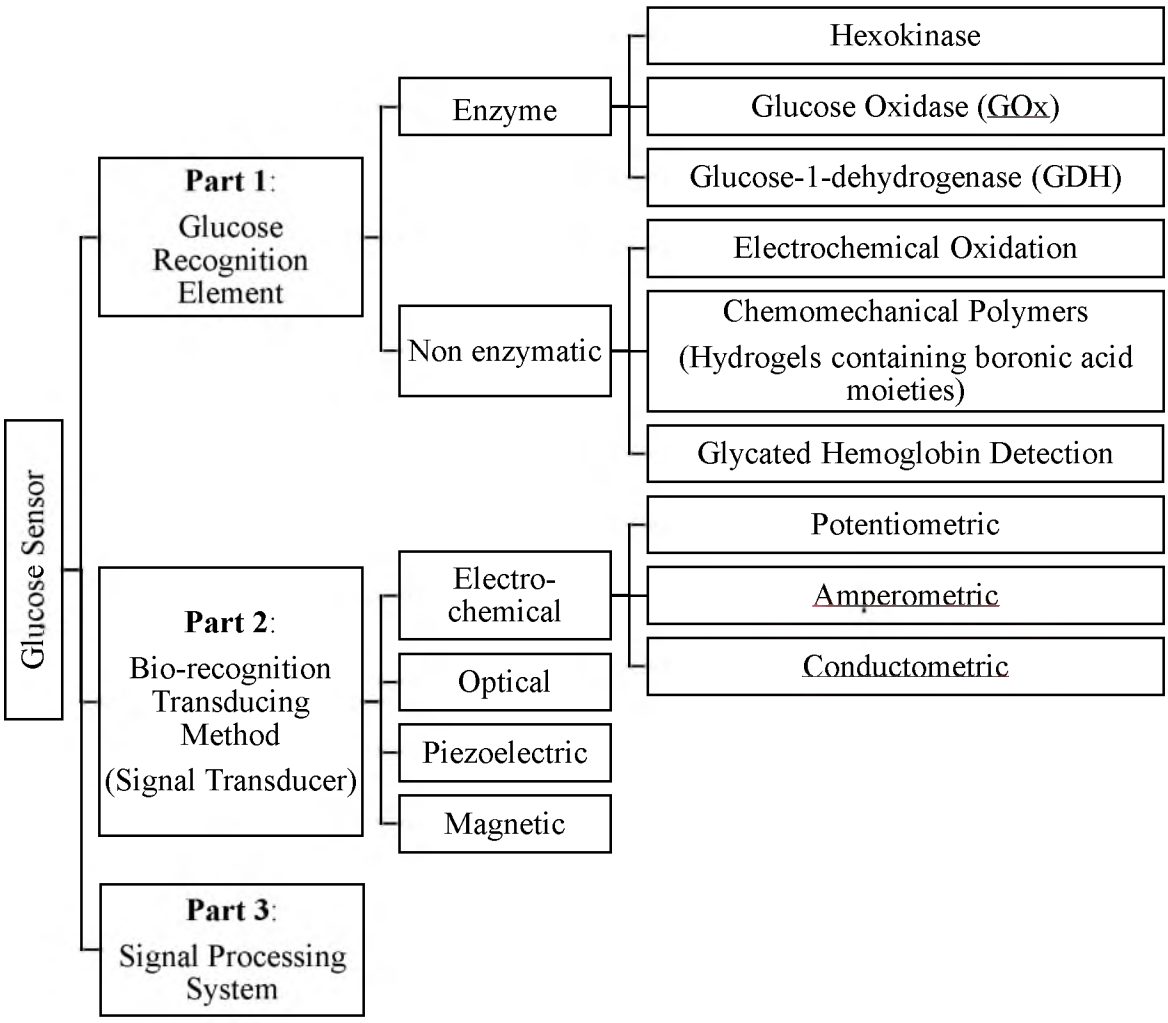

Figure 1.1 Illustration of the three main parts of glucose sensors and classification of types.

have been devised that combine different types of glucose recognition elements and signal transducers. The type of signal transducer used governs the choice of the signal processing system.

This type of glucometer is based on the oxidation of glucose molecules by immobilized enzymes (enzymatic glucose sensors). For example, GOx-flavin adenine dinucleotide (FAD) is reduced by glucose (equation 1.8), and the reduced GOx-FAD produces hydrogen peroxide in the presence of oxygen (equation 1.9). The amount of

consumed oxygen is quantified by electrodes. Currently, most 'point-of-care' type glucometers use this mechanism.

$$\text{Glucose} + \text{GOx-FAD}^{+} \rightarrow \text{Glucolactone} + \text{GOx-FADH}_2 \quad (1.8)$$

$$\text{GOx-FADH}_2 + \text{O}_2 \rightarrow \text{GOx-FAD} + \text{H}_2\text{O}_2 \quad (1.9)$$

However, enzymatic glucose sensors have limited stability and reproducibility, and are sensitive to oxygen levels. Stability is the most common problem because enzymatic activity can be adversely affected by changes in temperature and pH. Thus, the sensitivity of enzymatic glucose sensors fluctuates in response to changing environmental conditions [38].

Moreover, the lack of oxygen can decrease the sensitivity of enzymatic glucometers because oxygen is a reactant the glucose-enzyme reaction (equation 1.9). The reproducibility of enzymatic glucometers is another problem to be solved. Current glucometers are designed to be disposable because the immobilized enzymes do not reversibly react with glucose molecules. Once the enzymes are exposed to glucose, they lose activity. For these reasons, nonenzymatic glucose measurement systems are a viable alternative to enzymatic glucometers. One approach uses the electrochemical oxidation of glucose on a metal surface, such as Pt [39], Au [40], Ni [41], or chemically modified surface. Glucose is oxidized by catalytic metals such as Pt, and the Pt electrode measures the number of electrons produced by glucose oxidation (Figure 1.2) [39].

Another approach is to use polymers that generate chemomechanical responses in Fresponse to chemical stimuli. Glucose-responsive hydrogels containing boronic acid as a glucose receptor are the most notable example. Such hydrogels can serve as continuous glucose sensors (CGS, Section 1.2.5. Continuous Glucose Monitoring System) because

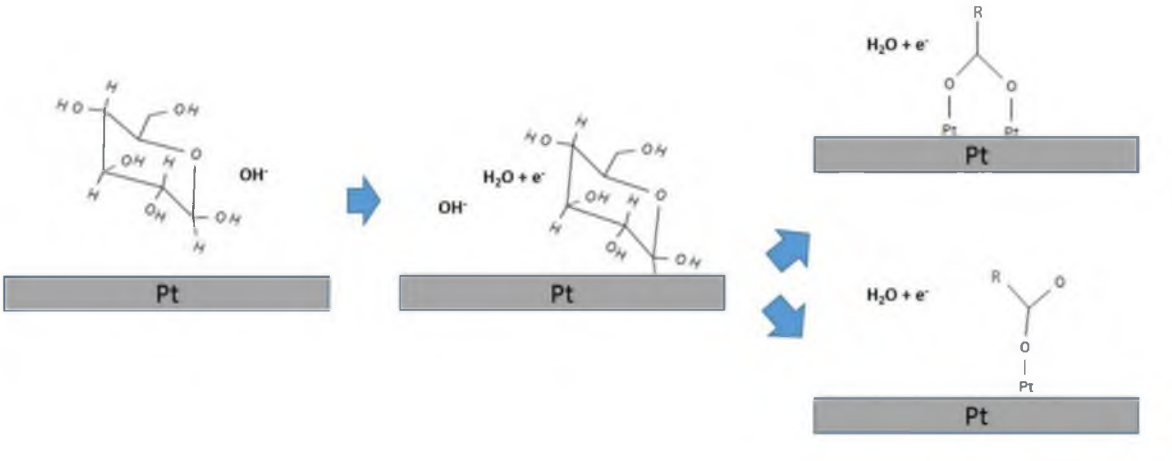

Figure 1.2 Schematic principle of electrochemical oxidation of glucose on a Pt surface (adapted from [39]).

they have good biocompatibility and stability. In addition, the sensitivity of glucose-responsive hydrogels is reproducible because the boronic acid moieties bind glucose molecules reversibly. Boronic acid-incorporated hydrogels have been used in conjunction with different types of signal transducing methods, such as fluorescence [43], a hologram [44], an electrode [45] and a piezoresistive pressure transducer [20]. Details of these transducers will be discussed in Section 1.2.6. (boronic acid incorporated glucose responsive hydrogels).

1.2.5. Continuous Glucose Monitoring System

The best treatment for diabetes is to maintain the euglycemic state of diabetics by monitoring blood sugar levels in real time. Ideally, blood sugar levels of patients should be monitored continuously. However, a point of care system is mostly used to check blood sugar levels. This requires patients to examine their blood sugar levels several times a day, such as before/after meal and exercises, and in the middle of a night. As a result, patients frequently become hyperglycemic or hypoglycemic. In addition, such

monitoring systems can be painful to use, as they require patients to prick their fingers to acquire the requisite blood sample. Continuous glucose monitoring systems (CGMS) have been developed to overcome these limitations (Figure 1.3). Therefore, CGMS should:

- Accurately monitor blood glucose level in real time
- Not be a cause of pain or infection
- Allow self-monitoring by nonprofessionals
- Be of minimal size

Most of the currently commercialized CGMS products are designed to be installed semi-invasively on a patient's body, such as the arm, thigh, flank, back or stomach. Current CGMS sensors read the concentration of glucose or hemoglobin A1c (HbA1c) of interstitial fluid (ISF) surrounding fat or muscle tissues. Many clinical reports have demonstrated that some CGMS products show good efficacy for controlling hyperglycemia and hypoglycemia. CGMS® Gold from Medtronic Minimed (Figure 1.3 (a)) was the first Food and Drug Administration (FDA) approved CGMS. CGMS® Gold was designed to monitor ISF glucose values by measuring HbA1c in ISF every 5 minutes. Using this device, patients decreased HbA1c levels by 1.1% versus 0.4% when using a finger prick device [46]. Another study reported that patients using a Dexcom STS sensor reduced their incidences of hypoglycemia (glucose<55mg/dl) and hyperglycemia (glucose>240 mg/dl) by 21% and 23%, respectively, when compared to a control group [47].

However, current CGMS technology also has limitations. The main problem is a lag time due to physiological time lags and signal processing times. As mentioned

Figure 1.3 Commercialized Continuous Glucose Monitoring Systems: (a) CGMS® Gold, Medtronic Minimed (adapted from [72]) (b) Dexcom® G4 Platinum (I. Signal Receiver, II. Sensor, III. Sensor Applicator), DEXCOM (adapted from [73]).

previously, semi-invasive CGMSs are designed to detect glucose or HbA1c in ISF, not blood plasma glucose. Glucose in plasma diffuses from capillaries into ISF, and then ISF glucose is removed by insulin-induced cellular uptake. This process takes about 10 minutes [48]. In addition, signal processing, such as signal transducing from a sensor to a receiver, requires several minutes before actual glucose values can be displayed. Although the lag time of CGMS products can be minimized by algorithms, numbers displayed on a CGMS are not actual real time values [49]. Because most CGMSs detect ISF glucose levels, the values from CGMS should be calibrated by actual plasma glucose values. Thus, CGMS users still have to use a finger prick glucometer to calibrate their CGMS three or four times a day. Numerous efforts have attempted to address these limitations. The ideal solution is to combine a completely invasive CGMS that can measure plasma glucose levels with a closed-loop system that releases insulin automatically. Therefore, the next generation CGMS must be implantable, and merged with a MEMS that contains a miniaturized feedback insulin pump.

1.2.6. Boronic Acid Incorporated, Glucose-Responsive Hydrogels

Developing boronic acid incorporated glucose-responsive hydrogels is a promising approach to devise effective, nonenzymatic continuous glucose sensors for several reasons. First, hydrogels have good biocompatibility, and their chemical structure can be modified for different applications.

Second, aromatic boronic acids are good materials for recognizing cyclic carbohydrates. Thermodynamically, the structure of anionized boronic acids is stabilized by forming chelating complexes with cyclic carbohydrates (Figure 1.4) [52].

Figure 1.5 illustrates the chelating complexes of anionized boronic acid moieties and cyclic carbohydrates within the hydrogel in an aqueous environment. Certain numbers of aromatic boronic acid groups are ionized in aqueous environment at the equilibrium state, especially under alkaline conditions because the pKa of boronic acid is about 8.6. The number of anions is maintained if the pH of the environment does not change. Once sugar molecules diffuse into the hydrogel matrix from the aqueous environment, esterification proceeds between 1, 2 or 3, 5, 6 position diols of the cyclic carbohydrate and the anionized boronic acid moieties. Then, more boronic acid moieties

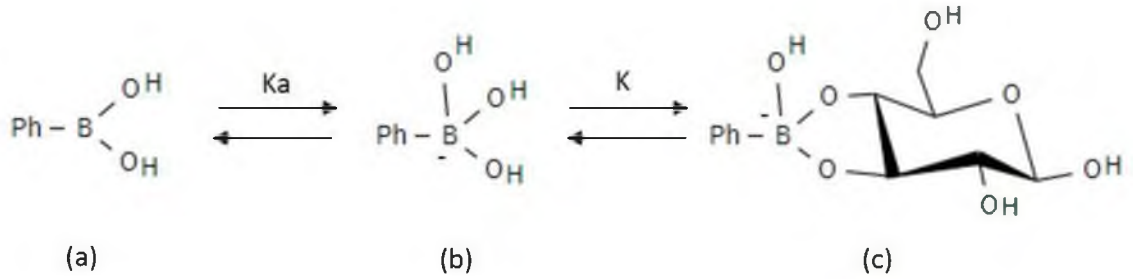

Figure 1.4 Aromatic boronic acid structure in aqueous media and anticipated binding complex formation with a sugar molecule (adapted from [50]): (a) Nonionized structure, (b) ionized structure, (c) chelating binding structure of boronic acid and glucose molecule (pyranose form).

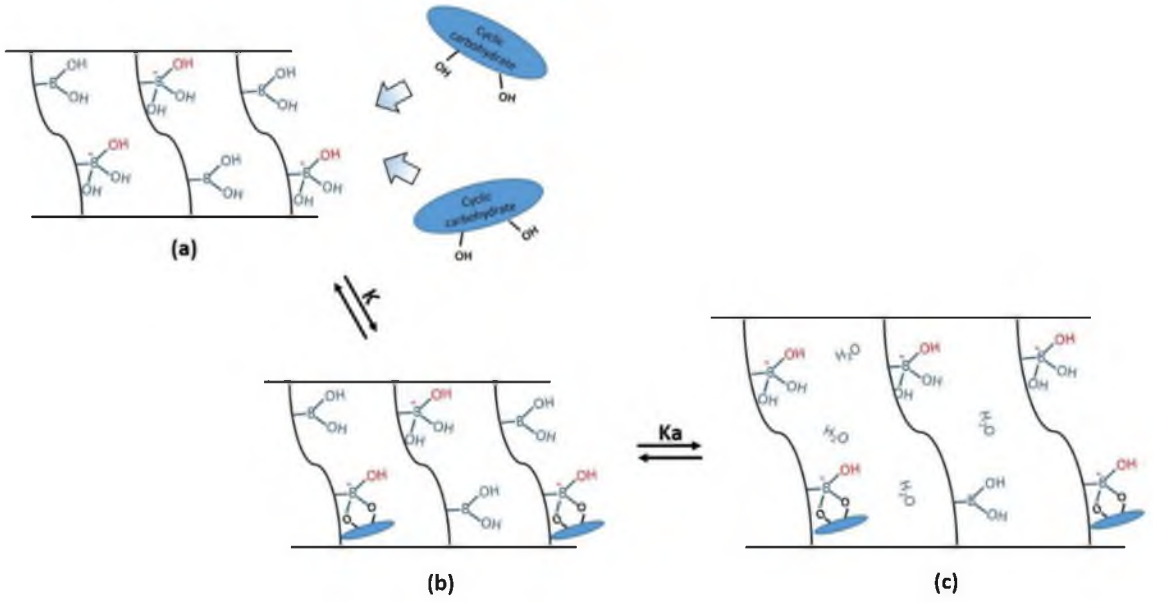

Figure 1.5 Illustration of chelating binding structures within the hydrogel matrix and swelling mechanism of boronic acid containing hydrogels (drawn based on the theory from [50], [51]): (a) Anionized aromatic boronic acids within the hydrogel matrix, (b) binding structure of boronic acid moieties and sugar molecules, (c) new equilibrium states of hydrogel after increasing the number of charged boronic acid moieties.

are ionized. This results in swelling of the hydrogel matrix via water absorption because the hydrophilicity of the hydrogel increases as the number of charged boronic acid moieties increases (Figure 1.5).

In addition, the esterification between boronic acids and diols of sugar molecules is a reversible reaction. As a result, aromatic boronic acid groups containing hydrogels reversibly swell in response to sugar molecules. However, there is a selectivity issue because the ionized boronic acid groups can also bind to other types of sugars, such as fructose, galactose or disaccharides. This is significant because [55] showed that fructose responses were 40 times greater than glucose. In addition, C.R. Lowe's group reported lactate interference with 3-acrylamidophenyl boronic acid (3-APB) containing hydrogels with a holographic sensor [53]. However, lactate interference was reduced by substituting

ortho binding boronic acid for 3-APB [54].

Fortunately, the glucose selectivity of boronic acid-containing hydrogels can be improved by incorporating zwitterions with cationic functional groups, such as tertiary amines, within the hydrogel structure [19], [56]. When 1, 2- diol and 3, 5 or 3, 5, 6–diol are in a cis orientation, diols of glucose form bis-binding complexes with two adjacent anionized boronic acid groups. The number of anionized boronic acid groups are stabilized by the incorporation of cationic groups. In this case, the glucose molecule serves as an extra cross-linker within the zwitterionic hydrogel (Figure 1.6). As a result, the hydrogel shrinks in response to glucose, whereas it swells in response to other types of sugar molecules. Recent studies have confirmed that cationic group-incorporated

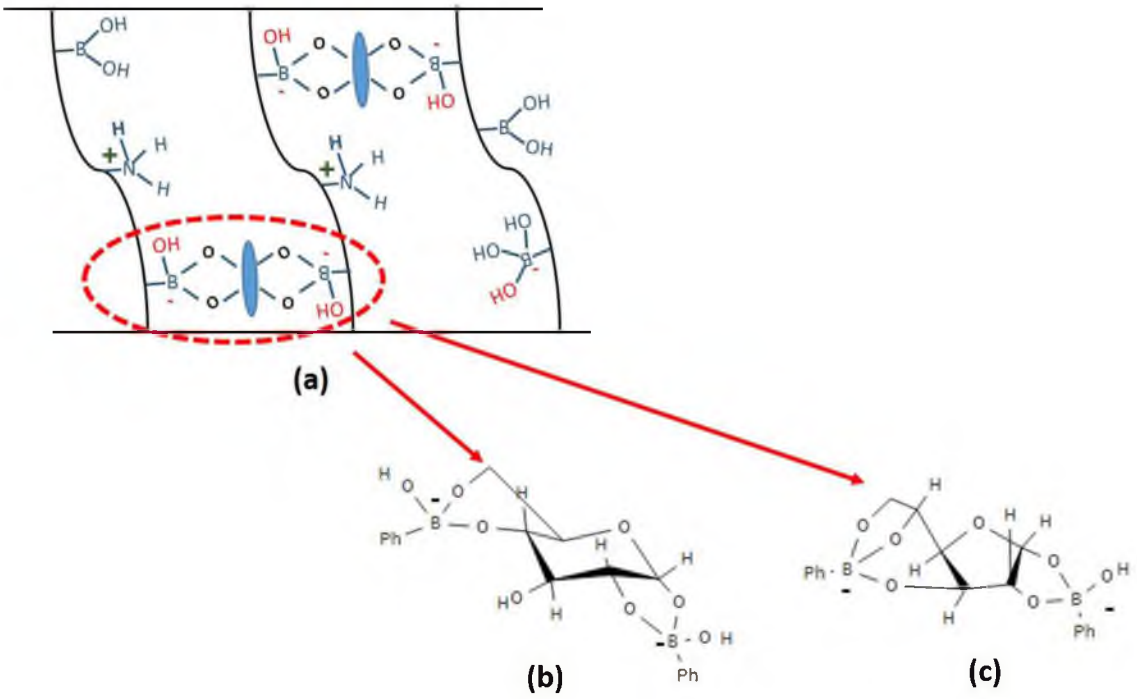

Figure 1.6 Illustration of a glucose binding complex within a zwitterionic glucose-responsive hydrogel (adapted from [18] and [52]): (a) Bis-diols binding structure within a hydrogel, (b) Pyranose form, (c) Furanose form.

hydrogels exhibit good glucose selectivity in an aqueous environment [18]-[20]. However, the binding structure and mechanism of glucose molecules and boronic acid groups within zwitterionic hydrogels have never been clearly studied. Also, there are additional barriers, such as response time, sensitivity, and pH interferences, to be overcome before zwitterionic hydrogels become commercially available. Thus, in this research, a thermodynamic analysis was performed to characterize the binding mechanism of glucose and boronic acid moieties (Chapter 2). In addition, the effect of chemical composition on the response of zwitterionic glucose sensitive hydrogels was studied using the design of experiments (DOE) method (Chapter 3) to improve glucose sensitivity and response time.

1.2.7. Measurement by a Piezoresistive Pressure Transducer

Load pressure changes will alter the electrical resistance of a piezoresistive device. Therefore, such devices can be used to measure the stimuli response of hydrogels, whose load pressures are altered by volume changes. The volume of a stimuli-responsive hydrogel will change through swelling or shrinking upon binding a target analyte. If the hydrogel is in a confined space, the volume changes drive loading pressure changes on the piezoresistive diaphragm. Thus, the stimuli response can be monitored continually by the piezoresistive device. Figure 1.7 shows how a piezoresistive pressure sensing system works with a stimuli-responsive hydrogel.

Previously, responses of hydrogels were mostly measured by weight changes or volume changes. In these cases, weight or volume was measured when the hydrogel reached a state of equilibrium. Hence, only the final swelling ratio can be used to develop

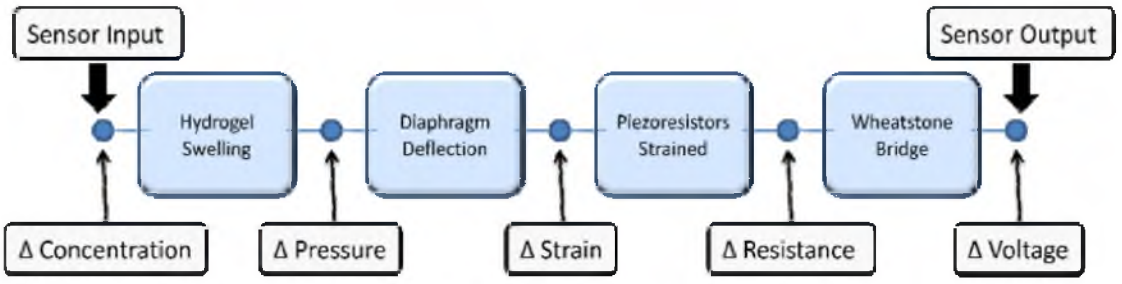

Figure 1.7 Schematic illustration of hydrogel based chemomechanical sensors (adapted from [57]).

new materials and the response cannot be monitored continuously. However, if changes in the volume of hydrogels can be transported to a pressure transducer, the response can be measured continuously and simultaneously. Also, scaling down the size of a sensor system using microfabricating technology can enhance the response rate of hydrogels. Several research groups have successfully developed hydrogel sensors with piezoresistive pressure transducers. For example, [58] made a pH sensitive hydrogel for CO_2 detection and then measured the pH response with a microscale pressure transducer. [59] synthesized hydration-sensing hydrogels in a micropressure transducer, and then measured the osmolality change response with the sensor. In this study, glucose responses of zwitterionic glucose sensitive hydrogels were measured by a piezoresistive pressure transducer. In addition, the hydrogel polymerization method was optimized by the UV curing method using microfabrication techniques (Chapter 2 - Chapter 4).

1.2.8. Signal Transducing Mechanism of a Magnetoresistive Sensor

Magnetoresistive sensors are a good method to transduce hydrogel responses. The principle of a magnetoresistive sensor is based on a Lorentz force (equation 1.10). According to the definition, magnetic flux affects the rate and force of moving charged

particles, such as electrons, within a current. Thus, if a magnetic force is applied or changed, a Lorentz force will be proportionally changed. Resistance also will be changed due to the length or direction changes of current flow (equation 1.11). Thus, a magnetoresistive sensor is a very sensitive and accurate signal transducing system.

$$Lorentz\ Force\ (F) = q\boldsymbol{V} \times \boldsymbol{B} \tag{1.10}$$

q: Electric charge (Coulombs)

$\boldsymbol{V}$: Rate vector (m/s)

$\boldsymbol{B}$: Magnetic flux density (Wb/m^2)

$$Resistance\ (R_B) = R_o \frac{\rho_B}{\rho_o} \{1 + m(\mu B)^2\} \tag{1.11}$$

R_B: Resistance under magnetic field (ohm)

R_o: Resistance under non-magnetic field (ohm)

μ: Mobility (cm^2/v.s)

ρ_B: Resistivity under magnetic field (ohm·cm)

ρ_o: Resistivity under non-magnetic field (ohm·cm)

B: Magnetic flux density (T)

m: Geometric effect factor (length/width of current flow)

1.2.9. Gamma Irradiation Effects on Polymer Structure

If a hydrogel is used in a medical device, it must be resistant to the sterilization methods commonly applied to medical devices. There are various sterilization methods, such as autoclaving, steam sterilization and gas sterilization for medical products. Most sterilization methods are performed at high temperature and pressure. These extreme environments easily melt or change the chemical structure of polymers. Therefore,

gamma ray irradiation has become the most popular sterilization process for medical application products. However, there are concerns that gamma ray irradiation may alter polymer, especially in cases where the polymer has a particular function, such as sensing glucose. Research has shown that gamma irradiation sterilization changes the rheological properties and functions of polymers when the polymer has functional groups such as amides and peptides [60], [61]. Therefore, before being used in clinical research, the stability of materials to gamma irradiation should be confirmed (Chapter 4).

1.2.10. Molecular Imprinted Polymers (MIPs)

Molecularly imprinted polymers (MIPs) are polymeric matrices containing reversible and selective binding sites obtained using imprinting technology. In general, five main components are required for preparing MIPs:

1. Template (target molecule): Molecules desired to be separated or sensed.

2. Functional monomer: Monomers having functional groups that can selectively form reversible binding structures with target molecules.

3. Solvent: A solvent for dissolving all components used for polymerization. The porosity of MIPs is mostly determined by the solvent used during polymerization. Thus, they are called porogenic solvents.

4. **Cross-linker**: Monomers form the cross-linked network structure within MIPs. The binding complexes of target molecules and functional monomers are trapped within MIPs by the cross-linking process during polymerization. Also, the cross-linker determines polymer morphology and rigidity.

5. Initiator: The radical polymerization method is used for preparing MIPs.

Initiators can be activated following exposure to a specific temperature or UV light. Following activation, they produce free radicals to initiate polymerization.

Figure 1.8 illustrates the procedures for MIPs preparation and the target molecule binding mechanism. In the molecular imprinting process, a cross-linked polymer is synthesized from a monomer in the presence of a template molecule. Initially, target molecules and functional monomers should be mixed in a porogenic solvent until binding structures are formed. Although complex formation can be driven by many types of binding forces, such as covalent, hydrogen, van der Waals, or dipole-dipole interactions, the binding complex should be reversible. Following binding, the binding complex is fixed by a cross-linker during polymerization. When the polymerization is finished, fixed target molecules are removed from the polymer, leaving behind a molecular cavity that will only bind to molecules having the identical size, shape and chemical structure of the

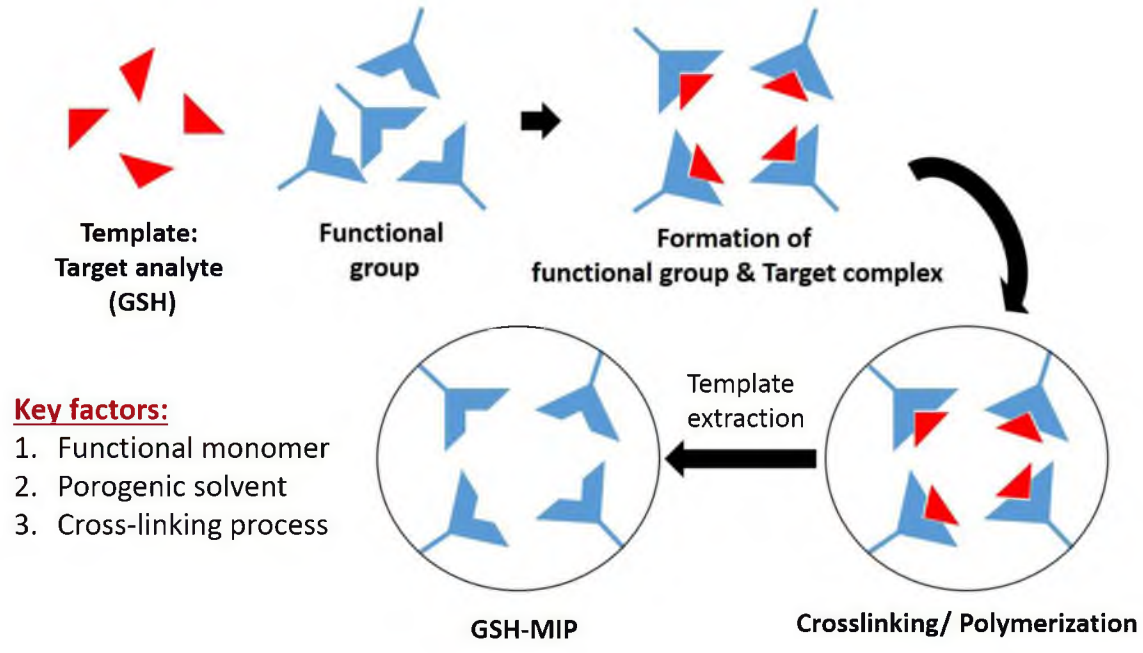

Figure 1.8 Illustration of MIPs preparation, and the binding mechanism of targets.

template molecule. This enables the synthesized polymer to bind the target selectively and reversibly. MIPs have good binding affinity and selectivity to target molecules because the polymer "remembers" the specific binding structure from the templating process. In addition, it was reported that MIPs have good physical strength, and good resistance to pressure and temperature changes [62].

The application of MIPs has proven advantageous in many areas. The most traditional and popular application is in chemical extraction/separation by chromatography and electrophoresis. A majority of studies report that the separation efficiency was improved by using MIPs, as compared to using gravity or pressure [63], [64]. More recent applications include biomedical device areas, such as drug delivery systems (DDS), drug discovery, cell culture scaffolds and biochemical sensors (Table 1.2).

One of the most attractive applications is chemical/biosensors because MIPs improve the sensitivity and selectivity of sensors. Biosensors are designed to quantify biological molecules, such as antibodies and enzymes. Initially, bioreceptors were used as biological target recognition elements. However, poor chemical stability and physical deformations of bioreceptors became the main barriers to biosensor development. Therefore, biomimetic receptors were adopted as recognition elements to solve the stability issue of bioreceptors, even though actual bio receptors exhibit a greater binding affinity for target analytes. Fortunately, many studies report that the sensitivity and selectivity of biomimetic sensors were improved by using MIPs. For example, [66] developed a glucose-sensing polymer by imprinting the binding structure of triazacyclononane-Cu^{2+} and glucose [66]. They confirmed that sensitivity was in the

Table 1.2 Applications of molecularly imprinted polymers (MIPs) (adapted from [65])

Area	Applications	Formation
Solid phase extraction (SPE)	• Chemical extraction • Purification • Environmental analysis • Food analysis • Biomaterial analysis • Chemical sensors	• Monolith • Surface imprint • Monodispersed spheres • Nano-scale spheres/particles
Medical devices	• Drug delivery (DDS) • Oral absorbers • Blood purification • Therapeutic monitoring • Scaffolds	• Monodispersed spheres • Porous membrane
Drug discovery	• Library screening tools • Library synthesis tools	• Nano-scale spheres/particles
Catalysts	• Enzyme like catalysts	• Monolith • Surface imprint • Monodisperse spheres
Separation	• Enantiomer separation	• Monolith • Monodispersed spheres

clinical range (0 to 25 mM of glucose) by measuring the pH level because their polymer produced electrons after binding glucose molecules. Although they employed glucose oxidase, which is mostly used in glucose sensors as a glucose receptor, they observed a similar level of sensitivity with their glucose-imprinted polymer. Based on a MIP [67] developed a morphine sensitive device. Interestingly, they developed a two-step morphine sensor by using the ability of MIPs to form reversible binding structures. Initially, morphine was bound to morphine-imprinted polymer. Following the addition of an excess amount of an electro-inactive competitor, bound morphine was released and quantified by an amperometric device. MIPs can also serve as protein sensors, which can be used for diagnostics, biomarkers, in the food industry (quality or fermentation control

purpose) and for environmental monitoring. However, protein sensors are more difficult to develop than other chemical/biochemical sensors due to the large proteins, as well as their structural sensitivity to changes in temperature, ionic strength, pH and radicals. In addition, proteins often have enantiomers. Therefore, it is difficult to achieve a good selectivity for the target protein. Some studies reported that MIPs can be used to solve the selectivity problem of protein sensors. For example, [68] designed surface plasmon resonance sensor (SPR) chips with lysozyme-imprinted thin films to evaluate MIP efficiency for protein detection. Their results showed that MIP enhanced target protein sensitivity up to three-fold relative to a non-imprinted polymer (NIP).

1.2.11. Glutathione Sensors

Glutathione is an endogenous tri-peptide consisting of glycine, cysteine and glutamic acid (Figure 1.9). In the body, glutathione efficiently detoxifies drugs and xenobiotics. In fact, glutathione is both a nucleophile and a reductant. Thus, glutathione reacts with electrophilic or oxidizing species before they can interact with critical cellular constituents, such as nucleic acids and proteins [69].

Glutathione deficiency contributes to oxidative stress, which plays a key role in aging and the pathogenesis of many diseases, such as seizures, Alzheimer's disease,

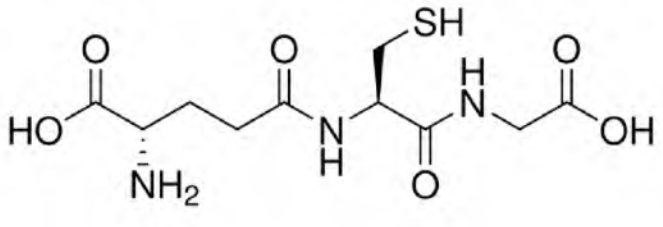

Figure 1.9. Chemical structure of reduced glutathione.

Parkinson's disease and diabetes [69]. Therefore, the use of glutathione sensors that can monitor glutathione level in cells/body fluid may prevent such diseases. Several studies have described glutathione sensors. [70] devised a glutathione sensor with an Au nanocluster (NC)-based fluorescent sensor. The sensing mechanism is based on the interaction of glutathione and Hg on the Au-NC surface. When the Au-NC-Hg system is exposed to glutathione molecules, fluorescence is enhanced due to the binding of glutathione and Hg. The Au-NC system could detect glutathione in the 0.04 to 16.0 μM range. Electrochemical sensors also have been used to develop glutathione-sensing systems. [71] made poly-aminophenol deposited glassy carbon (GC) electrodes for glutathione detection. GC electrodes detect glutathione by quantifying electrons that are produced following glutathione oxidation.

All previous studies reported that their sensors showed good sensitivity to glutathione. However, most of the studies did not examine sensor sensitivity. Glutathione sensors are used to monitor body fluids, such as blood plasma and saliva. Most bodily fluids contain cysteine, which can interfere with glutathione sensors that are based on the oxidation of the thiol group of cysteine. Therefore, highly glutathione-selective material was developed using glutathione imprinting methods in this dissertation. The sensitivity and selectivity of glutathione sensors will be discussed in Chapter 6.

1.3 Thesis Overview and Novelty

The main purpose of this research is to develop novel materials that can be used for medical devices or sensors. Specifically, this study focuses on enhancing the sensitivity and selectivity of glucose and glutathione sensors.

First, a zwitterionic glucose-responsive hydrogel will be discussed in Chapter 2 through Chapter 5. As mentioned previously, zwitterionic glucose sensitive hydrogels have good selectivity for glucose molecules [18]-[20]. However, the sensing mechanism within the hydrogels has not been extensively analyzed thus far. Only the binding structure between sugar molecules and boronic acids was studied, indirectly, in an aqueous phase [18], [50]-[52]. Therefore, the responses of zwitterionic glucose sensitive hydrogels to sugar molecules was analyzed thermodynamically to gain greater insights into the binding structure in Chapter 2.

Zwitterionic glucose-responsive hydrogels containing both 3-acrylamido phenylboronicacid (3-APB) and *N*-(3-dimethylaminopropyl acrylamide) (DMAPAA) showed good glucose selectivity in previous studies [18]-[20]. However, the precise ratio of the charged monomers that will optimize sensitivity and response time needs to be determined. Therefore, the design of experiments (DOE) technique was performed to determine the best composition for a zwitterionic glucose-responsive hydrogel. Although DOE has long been a useful product development tool in industry, only a few studies describe DOE techniques for the optimization of hydrogel/polymer [72]-[75]. In this study, DOE was performed using three factors (the molar ratio of cationic/anionic functional monomers, the amount of cross-linker, and concentration of pregel solution) to optimize two different hydrogel responses (swelling pressure and response time). Next, the effects of monomer composition and wt% on hydrogel responses were examined by a statistical analysis of hydrogel responses (Chapter 3). The statistical approach will be a valuable tool for developing glucose-responsive hydrogels for different applications.

The zwitterionic glucose sensitive hydrogel was developed for the purpose of

creating an implantable continuous glucose sensor (CGS). Thus, the CGS system must be sterilized by autoclaving, gamma irradiation or ethylene oxide gas. Gamma irradiation is the most common method to sterilize medical devices. However, previous studies reported that gamma irradiation can adversely affect chemical structures, especially the cross-linking networks of polymers [76], [77]. Therefore, degradation studies of zwitterionic glucose sensitive hydrogels were performed to characterize the effects of gamma irradiation (Chapter 4).

A piezoresistive pressure transducer was used for all glucose sensitive hydrogel studies in Chapter 2 - Chapter 4. A piezoresistive pressure sensor is one of the most promising signal transducing systems for pressure-producing, stimuli-responsive hydrogels because it has good sensitivity, and microfabrication is available for scaling down their size [20], [57], [58]. However, a magnetometer is also considered to be a good signal transducing device for a chemical sensor because it has good signal sensitivity and high signal resolution. In addition, it is possible to fabricate a miniaturized system. However, a chemical sensor with a magnetometer is rarely studied because it is difficult to develop materials that change their magnetic flux density in response to stimuli. Therefore, magnetic field-producing, zwitterionic glucose-responsive hydrogels were developed by embedding ferromagnetic particles within the hydrogels. The embedding method was optimized by computer simulation. Glucose responses were measured by a magnetoresistive transducer, and the results will be discussed in Chapter 5.

Second, the study of glutathione-imprinted polymers will be discussed in Chapter 6. Although the importance of monitoring glutathione levels in bodily fluids has been emphasized for a long time [69], only a few studies of glutathione sensors have been

reported [70], [71]. Moreover, the glutathione selectivity of sensors was not thoroughly discussed in previous studies [70], [71]. Thus, glutathione-imprinted polymers were developed for use as glutathione sensors in this research. The sensitivity and selectivity of glutathione-imprinted polymers was analyzed and will be discussed in Chapter 6. Finally, conclusions and future research directions will be discussed in Chapter 7.

1.4 References

[1] Banica, F. Chemical Sensors and Biosensors: Fundamentals and Applications, John Wileys & Sons, 2012.

[2] Lutolf, M. L. Designing Materials to Direct Stem Cell Fate. *Nature Materials* **2009,** 8, 6, 451-453.

[3] Hiemstra, C.; Zhong, Z.; Steenbergen, M. J.; Hennink, W. E.; Feijen, J. Release of Model Proteins and Basic Fibroblast Growth Factor from In Situ Forming Degradable Dextran Hydrogels. *Journal of Controlled Release* **2007,** 122, 1, 71-78.

[4] Peppas N. A.; Leobandung, W. Stimuli-Sensitive Hydrogels: Ideal Carriers for Chronobiology and Chronotherapy. *Journal of Biomaterials Science, Polymer Edition* **2004,** 15, 2, 125-144.

[5] Janorkar, A. V. Review: Polymeric Scaffold Materials for Two-Dimensional and Three-Dimensional in Vitro Culture of Hepatocytes. *ACS Symposium Series* **2010,** 1054, 1-32.

[6] Buenger, D.; Topuz. F.; Groll, J. Hydrogels in Sensing Applications. *Progress in Polymer Science* **2012,** 37, 12, 1678-1719.

[7] Schild, H. Poly(N-isopropylacrylamide): Experiment, Theory and Application. *Progress in Polymer Science* **1992,** 17,163-249.

[8] Qui, Y.; Park, K. Environment-Sensitive Hydrogels for Drug Delivery. *Advanced Drug Delivery Reviews* **2001,** 53, 321-339.

[9] Suwa, K.; Yamamoto, K.; Akashi, M.; Takano, K.; Tanaka, N.; Kunugi, S. Effects of Salt on the Temperature and Pressure Responsive Properties of Poly(N -vinylisobutyramide) Aqueous Solutions. *Colloid and Polymer Science* **1998,** 276, 6, 529-533.

[10] Malmsten, M.; Lindman, B. Water Self-Diffusion in Aqueous Block Copolymer Solutions. *Macromolecules* **1992,** 25, 5446-5450.

[11] Philippova, O. E.; Hourdet, D.; Audebert, R.; Khokhlov, A. R. pH-Responsive Gels of Hydrophobically Modified Poly(acrylic acid). *Macromolecules* **1997,** 30, 8278-8285.

[12] Torres-Lugo, M.; Peppas, N. A. Hydrogels for the Oral Delivery of Calcitonin. *Macromolecules* **1999,** 32, 6646-6651.

[13] Gohy, J.-F.; Lohmeijer, B. G. G.; Varshney, S. K.; Decamps, B.; Leroy, E.; Boileau, S; Schubert, U. S. Stimuli-Responsive Aqueous Micelles from an ABC Metallo-Supramolecular Triblock Copolymer. *Macromolecules* **2002,** 35, 26, 9748-9755.

[14] Sideratou, Z.; Tsiourvas, D.; Paleos, C. M. Quaternized Poly(propylene imine) Dendrimers as Novel pH-Sensitive Controlled-Release Systems. *Langmuir* **2000,** 16, 4, 1766-1769.

[15] Bignotti, F.; Penco, M.; Sartore, L.; Peroni, I.; Mendichi, R.; Casolaro, M.; D'Amore, A. Synthesis, Characterisation and Solution Behaviour of Thermo- and pH-Responsive Polymers Bearing l-Leucine Residues in the Side Chains. *Polymer* **2000,** 41, 23, 8247-8256.

[16] Traitel, T.; Cohen, Y.; Kost, J. Characterization of Glucose sensitive Insulin Release Systems in Simulated in Vivo Conditions. *Biomaterials* **2000,** 21, 1679-1687.

[17] Kataoka, K. ; Miyazaki, H.; Bunya, M.; Okano, T.; Sakurai, Y. Totally Synthetic Polymer Gels Responding to External Glucose Concentration: Their Preparation and Application to On-Off Regulation of Insulin-Release. *J. Am. Chem. Soc.* **1998,** 12694-12695.

[18] Alexeev, V. L.; Sharma, A. C.; Goponenko, A. V.; Das, S.; Lednev, I. K.; Wilcox, C.S.; Finegold, D.N.; Asher, S.A. High Ionic Strength Glucose Sensing Photonic Crystal. *Anal. Chem.* **2003,** 75, 2316-2323.

[19] Tierney, S.; Volden, S.; Stokke, B.T. Glucose Sensors Based on a Responsive Gel Incorporated as a Fabry-Perot Cavity on a Fiber-Optic Readout Platform. *Biosens. Bioelectron.* **2009,** 24, 2034–2039.

[20] Lin, G.; Chang, S.; Hao, H.; Tathireddy, P.; Orthner, M.; Magda, J.; Solzbacher, F. Osmotic Swelling Pressure Response of Smart Hydrogels Suitable for Chronically-Implantable Glucose Sensors. *Sensors & Actuators, B, Chem.* **2010,** 144, 332–336.

[21] Irvin, D. J.; Goods, S. H.; Whinnery, L. L. Direct Measurement of Extension and Force in Conductive Polymer Gel Actuators. *Chem. Mat.,* **2001,** 13, 4, 1143-1145.

[22] Zrinyi, M. Intelligent Polymer Gels Controlled by Magnetic Fields. *Colloid Polym* Sci **2000,** 278, 98-103.

[23] Miyata, T.; Asami, N; Uragami, T. A. Reversibly Antigen-Responsive Hydrogels. *Nature* **1999,** 399, 6738, 766-769.

[24] Flory P. Principles of Polymer Chemistry, Ithaca, NY: Cornell University, 1953.

[25] Horkay, F.; Tasaki, I.; Basser, P.J. Osmotic Swelling of Polyacrylate Hydrogels in Physiological Salt Solutions. *Biomacromolecules.* **2000,** 1, 84–90.

[26] Dusek, K.; Prins, W. Structure and Elasticity of Non-Crystalline Polymer Networks. *Adv. Polymer Sci.* **1969,** 6, 1-102.

[27] Gehrke, S. Synthesis, Equilibrium Swelling, Kinetics, Permeability and Applications of Environmentally Responsive Gels. *Adv. Polymer Sci.* **1993,** 110, 81-144.

[28] Han, I.S.; Han, M-H.; Kim, J.; Lew, S.; Lee, Y.J.; Horkay, F.; Magda, J.J. Constant-Volume Hydrogel Osmometer: A New Device Concept for Miniature *Biosensors. Biomacromolecules.* **2002,** 3, 1271–1275.

[29] Yang, Q.; Adrus, N.; Tomicki, F.; Ulbricht, M. Composites of Functional Polymeric Hydrogels and Porous Membranes. *J. Mater. Chem.* **2011,** 21, 9, 2783-2811.

[30] Lin, G.; Chang, S.; Kuo, C-H.; Magda, J.; Solzbacher, F. Free Swelling and Confined Smart Hydrogels for Applications in Chemomechanical Sensors for Physiological Monitoring. *Sens. Actuators, B, Chem.* **2009,** 136, 186–195.

[31] National Diabetes Fact Sheet. 2011. http://www.cdc.gov/diabetes/pubs/pdf/ndfs_2011.pdf.

[32] The United States of Diabetes: Challenges and opportunities in the decade ahead, 2010.

[33] Cho, J.; Ryoo, N.; Hahn, T.; Jeon, J. Evidence for a Role of Hexokinases as Conserved Glucose Sensors in both Monocot and Dicot Plant Species. *Plant Signaling & Behavior* **2009,** 4, 9, 908-910.

[34] Holtz, J. H.; Asher, S. A. Polymerized Colloidal Crystal Hydrogel Films as Intelligent Chemical Sensing Materials. *Nature* **1997,** 389, 6653, 829-832.

[35] Wang, J.; Musameh, M. Carbon Nanotube/Teflon Composite Electrochemical Sensors and Biosensors. *Analy. Chem.* **2003,** 75, 9, 2075-2079.

[36] Shan, C.;Yang, H.; Song, J.; Han, D.; Ivaska, A.; Niu, L. Electrochemical Determination of NADH and Ethanol Based on Ionic Liquid-Functionalized Graphene. *Analy. Chem.* **2009,** 81, 6, 2389-2382.

[37] D'Costa, E. J.; Higgins, I. J.; Turner, A. P. Quinoprotein Glucose Dehydrogenase and its Application in an Amperometric Glucose Sensor. *Biosensors* **1986,** 2, 71-87.

[38] Wilson, R.; Turner, A.P.F. Glucose Oxidase: an Ideal Enzyme. *Biosens. Bioelectrn* **1992,** 7, 3, 165-185.

[39] Benden, B.; Largeaud, F.; Kokoh, K. B.; Lamy, C. Fourier Transform Infrared Reflectance Spectroscopic Investigation of the Electrocatalytic Oxidation of D-glucose: Identification of Reactive Intermediates and Reaction Products. *Electrochimica Acta.***1996,** 41, 5, 701-709.

[40] Aoun, S.; Bang, G.; Koga, T.; Nonaka, Y.; Sotomura, T.; Taniguchi, I. Electrocatalytic Oxidation of Sugars on Silver-UPD Single Crystal Gold Electrodes in Alkaline Solutions. *Electrochemistry Communications* **2003,** 4, 317-320.

[41] You T, Niwa O, Chen Z, Hayashi K, Tomita M, Hirono S. An Amperometric Detector Formed of Highly Dispersed Ni Nanoparticles Embedded in a Graphite-like Carbon Film Electrode for Sugar Determination. *Anal Chem.* **2003,** 75, 19, 5191-6.

[42] Bamba, K.; Leger, J.-M.; Garnier, E.; Bachmann, C.; Servat, K.; Kokoh, K.B. Selective Electro-Oxidation of d-Glucose by RuCl2(azpy)2 Complexes as Electrochemical Mediators. *Electrochimica Acta* **2005,** 50, 3341-3346.

[43] Tony, D.; James, K.R.A.; Sandanayake, S.; Iguchi, R.; Shinkai, S. Novel Saccharide-Photoinduced Electron Transfer Sensors Based on the Interaction of Boronic Acid and Amine. *J. Am. Chem. Soc.* **1995,** 117, 8982-8987.

[44] Yang, X.; Lee, M.C.; Sartain, F.; Pan, X.; Lowe, C.R. Designed Boronate Ligands for Glucose-Selective Holographic Sensors. *Chem. Eng. J.* **2006,** 12, 8491-8497.

[45] Kikuchi, A.; Suzuki, K.; Okabayashi, O.; Hoshino, H.; Kataoka, K.; Sakurai, Y.; Okano, T. Glucose-Sensing Electrode Coated with Polymer Complex Gel Containing Phenylboronic Acid. *Anal. Chem.,* **2006,** 68, 823-828.

[46] Deiss, D.; Bolinder, J.; Riveline, J.P.; Battelino, T.; Bosi, E.; Tubiana-Rufi, N.;

Kerr, D.; Phillip, M. Improved Glycemic Control in Poorly Controlled Patients with Type 1 Diabetes using Real-Time Continuous Glucose Monitoring. *Diabetes Care* **2006,** 29, 2730–2732.

[47] Garg, S.; Zisser, H.; Schwartz, S.; Bailey, T.; Kaplan, R.; Ellis, S.; Jovanovic, L. Improvement in Glycemic Excursions with a Transcutaneous, Real-Time Continuous Glucose Sensor: A Randomized Controlled Trial. *Diabetes Care* **2006,** 29, 44–50.

[48] Thome-Duret, V.; Reach, G.; Gangnerau, M.N.; Lemonnier, F.; Klein, J. C.; Zhang, Y.; Hu, Y.; Wilson, G. S. Use of a Subcutaneous Glucose Sensor to Detect Decreases in Glucose Concentration Prior to Observation in Blood. *Anal Chem.* **1996,** 68, 21, 3822-3826.

[49] Keenan, D.B. ; Mastrototaro, J.J.; Voskanyan, G.; Steil, G.M. Delays in Minimally Invasive Continuous Glucose Monitoring Devices: A Review of Current Technology. *J. Diabetes Sci. Technol.* **2009,** 3, 5, 1207-1214.

[50] Kataoka, K.; Miyazaki, H.; Okano, T.; Sakurai, Y. Sensitive Glucose Induced Change of the Lower Critical Solution Temperature of poly[N,N-(dimethylacrylamide)-co-3-(acrylamido)-phenylboronic acid] in Physiological Saline. *Macromolecules* **1994,** 27, 1061-1062.

[51] Zhang, Y.; Guan, Y.; Zhou, S. Synthesis and Volume Phase Transitions of Glucose sensitive Microgels. *Biomacromolecules* **2006,** 7, 3196-3201.

[52] Nicholla, M.P.; Paul, P.K.C. Structures of Carbohydrate-Boronic acid Complexes Determined by NMR and Molecular Modelling in Aqueous Alkaline Media. *Org. Biomol. Chem.* **2004,** 2, 1434-1441.

[53] Lee, M. C.; Kabilan, S.; Hussain, A; Yang, X.; Blyth, J.; Lowe, C. R. Glucose sensitive Holographic Sensors for Monitoring Bacterial Growth. *Anal. Chem.* **2004,** 76, 19, 5748-5755.

[54] Yang, X.; Lee, M. C.; Sartain, F.; Pan, X.; Lowe, C. R. Designed Boronate Ligands for Glucose-Selective Holographic Sensors. *Chem. Eur. J.* **2006,** 8491-8497.

[55] Kawasaki, T.H.; Akanuma, H.; Yamanouchi, T. Increased Fructose Concentrations in Blood and Urine in Patients With Diabetes. *Diabetes Care* **2002,** 25, 353-357.

[56] Horgan, A.; Marshall, A.; Kew, S.; Dean, K.; Creasey, C.; Kabilan, S. Crosslinking of Phenylboronic Acid Receptors as a Means of Glucose Selective Holographic Detection. *Biosens. Bioelectron.* **2006,** 21, 9, 1838-1845.

[57] Lin, G. Development of pH and Glucose Hydrogels for Microfabricated Biomedical Sensor Array, Salt Lake City: University of Utah, **2010**.

[58] Herber, S.; Eijkel, J.; Olthuis, W.; Bergveld, P.; Van den Berg, A. Study of Chemically Induced Pressure Generation of Hydrogels under Isochoric Conditions using a Microfabricated Device. *Journal of Chem. Phy.* **2004,** 212, 2746-2751.

[59] Porter, T. L.; Stewart, R.; Reed, J.; Morton, K. Models of Hydrogel Swelling with Applications to Hydration Monitoring. *Sensors,* **2007,** 7, 1980-1991.

[60] Tyan, Y. C.; Liao, J. D.; Lin, S. P.; Chen, C. C. The Study of the Sterilization Effect of Gamma ray Irradiation of Immobilized Collagen Polypropylene Naonwoven Fabric Surfaces.*Wiley Periodicals* **2003,** 1033-1043.

[61] Andriola, A. K.; Brun-Graeppi, S.; Richard, C.; Bessodes, M.; Scherman, D.; Narita, T.; Ducouret, G. The Effect of Sterilization Methods on the Thermo-gelation Properties of Xyloglucan Hydrogels. *Poly. Degrad. Stabil.* **2010,** 95, 254-259.

[62] Vasapollo, G.; Sole, R. D.; Mergola, L.; Lazzoi, M. R.; Scardino, A.; Scorrano, S.; Mele, G. Molecularly Imprinted Polymers: Present and future prospective. *Int. J. Mol. Sci,* **2011,** 12, 5908-5945.

[63] Deng, Q. L.; Li, L. Y.; Zhang, L. H.; Zhang, Y. K. Molecularly Imprinted Macroporous Monolithic Materials for Protein Recognition. *Chin. Chem, Lett,* **2011,** 22, 1351-1354.

[64] Vallano, P. T.; Remcho, V. T. Highly Selective Separations by Capillary Electrochromatography: Molecular Imprint Polymer Sorbents. *J. Chromatogr. A* **2000,** 887, 125-135.

[65] Schirhagl, R. Bioapplications for Molecularly Imprinted Polymers. *Analy. Chem.* **2014,** 86, 250-261.

[66] Chen, G.; Guan, Z.; Chen, C. T.; Fu, L.; Sundaresan, V.; Arnold, F. H. A. Glucose Sensing Polymer. *Nature Biotechnol,* **1997,** 15, 354-357.

[67] Kriz, D.; Mosbach, K. Competitive Amperometric Morphine Sensor Based on an Agarose Immobilised Molecularly Imprinted Polymer. *Anal. Chim. Acta* **1995,** 300, 71-75.

[68] Matsunaga, T.; Hishiya, T.; Takeuchi, T. Surface Plasmon Resonance Sensor for Lysozyme Based on Molecularly Imprinted Thin Films. *Analy. Chimica. Acta.* **2007,** 591, 63-67.

[69] Pompella, A.; Visvikis, A.; Paolicchi, A.; Tata, V.; Casini, A. F. The Changing Faces of Glutathione, a Cellular Protagonist. *Biochemical Pharmacology* **2003,** 66, 1499-1503.

[70] Tian, D.; Qian, Z.; Xia, Y.; Zhu, C. Gold Nanocluster-Based Fluorescent Probes for Near Infrared and Turning on Sensing of Glutathione in Living Cells. *Langmuir* **2012,** 28, 3945-3951.

[71] Oztekin, Y.; Ramanaviciene, A.; Ramanavicius, A. Electrochemical Glutathione Sensor Based on Electrochemically Deposited Poly-maminophenol. *Electroanalysis* **2011,** 23, 701-709.

[72] MiniMed 530G User Guide, Paradigm REAL-Time Revel System Insulin Pump User Guide. http://www.medtronicdiabetes.com/treatment-and-products/continuous-glucose-monitoring.

[73] Dexcom G4 PLATINUM User Guide, May 2012. http://www.dexcom.com.

CHAPTER 2

THERMODYANMIC ANALYSIS OF THE SELECTIVITY ENHANCEMENT OBTAINED BY USING SMART HYDROGELS THAT ARE ZWITTERIONIC WHEN DETECTING GLUCOSE WITH BORONIC ACID MOIETIES

Reprinted from Sensors and Actuators B, 160/1, F. Horkay, S.H. Cho, P. Tathireddy, L. Rieth, F. Solzbacher, J. Magda, Thermodynamic analysis of the selectivity enhancement obtained by using smart hydrogels that are zwitterionic when detecting glucose with boronic acid moieties, 1369-1371, Copyright (2011), with permission from Elsevier.

Boronic acid-incorporated hydrogels have been extensively studied since [29] reported that hydrogels containing alkylamino phenyboronic acid reversibly bound glucose molecules in aqueous environment. Nevertheless, hydrogels have limitations for use as glucose sensors because boronic acids exhibit high binding affinity for other cyclic carbohydrates. [28] reported that the binding affinity of fructose was 40 times greater than glucose. However, glucose selectivity was achieved by adding cationic groups to the hydrogel. S. Kitano synthesized an acrylamide-based block copolymer with dimethylamino propylacrylamide (DMAPAA), m-amino phenylboronic acid (m-APB), and N-vinyl-2-pyrrolidone (NVP) to develop a glucose responsive drug delivery system for insulin release [30]. They found that the copolymer gel was transformed by addition of glucose. It was the first trial of a controlled release system for protein delivery. [12] observed that light emitted by boronic acid-containing crystalline colloidal array embedded in a photonic crystal was blue shifted by glucose, whereas it was red shifted by fructose. This was due to the fact that the gel was shrunk by bis-bidetate complex formation between glucose and two boronic acid molecules when cations stabilized the tetrahedral structure of the boronic acid moieties. Although many studies achieved glucose selectivity by using cationic groups in boronic acid-containing hydrogels, differences in the binding structure/mechanism in hydrogels have not been carefully examined. In this chapter, a thermodynamic explanation is presented for the binding mechanisms of different cyclic carbohydrates.

Zwitterionic hydrogels containing 3-acrylamido phenylboronic acid (3-APB) and N-(3-dimethyenebisacrylamide (DMAPAA) were synthesized by the radical polymerization method for this research. Total osmotic swelling pressure (Π_{tot}) was

measured by adding osmotic shrinking agent poly (vinylpyrrolidone) (PAA). Shear modulus for estimation of the elastic contribution factor (Π_{el}) was obtained by using a texture analyzer (TA.XT21 HR Texture analyzer, Stable Micro System, UK). In addition, small-angle neutron scattering (SANS) was used to confirm structural changes in the hydrogel network following binding of sugar molecules. Previous studies [12, 14, 20, 21, and 24] showed that differences in the number of cross-links by bis diols binding is the main reason for response differences. However, this study showed that the mixing contribution (Π_{mix}) is also an important factor. In particular, the ternary interaction parameter (χ_1) of a Flory-Huggins equation was significantly larger in a glucose solution (≈ 0.51) than in a fructose solution (≈ 0.45).

Sensors and Actuators B 160 (2011) 1363–1371

Contents lists available at SciVerse ScienceDirect

Sensors and Actuators B: Chemical

journal homepage: www.elsevier.com/locate/snb

Thermodynamic analysis of the selectivity enhancement obtained by using smart hydrogels that are zwitterionic when detecting glucose with boronic acid moieties☆

F. Horkay[a,*], S.H. Cho[b], P. Tathireddy[c], L. Rieth[c], F. Solzbacher[c,d,e], J. Magda[b,d,**]

[a] Section on Tissue Biophysics and Biomimetics, Program on Pediatric Imaging and Tissue Sciences, Eunice Kennedy Shriver National Institute of Child Health and Human Development, National Institutes of Health, Bethesda MD 20892-5772, USA
[b] Department of Chemical Engineering, University of Utah, Salt Lake City, UT 84112, USA
[c] Department of Electrical & Computer Engineering, University of Utah, Salt Lake City, UT 84112, USA
[d] Department of Materials Science & Engineering, University of Utah, Salt Lake City, UT 84112, USA
[e] Department of Bioengineering, University of Utah, Salt Lake City, UT 84112, USA

ARTICLE INFO

Article history:
Received 3 August 2011
Received in revised form
16 September 2011
Accepted 26 September 2011
Available online 1 October 2011

Keywords:
Glucose sensor
Smart hydrogel
Boronic acid
Monosaccharides
SANS

ABSTRACT

Because the boronic acid moiety reversibly binds to sugar molecules and has low cytotoxicity, boronic acid-containing hydrogels are being used in a variety of implantable glucose sensors under development, including sensors based on optical, fluorescence, and swelling pressure measurements. However, some method of glucose selectivity enhancement is often necessary, because isolated boronic acid molecules have a binding constant with glucose that is some 40 times smaller than their binding constant with fructose, the second most abundant sugar in the human body. In many cases, glucose selectivity enhancement is obtained by incorporating pendant tertiary amines into the hydrogel network, thereby giving rise to a hydrogel that is *zwitterionic* at physiological pH. However, the mechanism by which incorporation of tertiary amines confers selectivity enhancement is poorly understood. In order to clarify this mechanism, we use the osmotic deswelling technique to compare the thermodynamic interactions of glucose and fructose with a zwitterionic smart hydrogel containing boronic acid moieties. We also investigate the change in the structure of the hydrogel that occurs when it binds to glucose or to fructose using the technique of small angle neutron scattering.

1. Introduction

The development of novel glucose sensors continues to be one the most widely studied areas of sensor research, due to the continuing need for improvements in glucose sensors used in the management of diabetes [1,2] and in control of fermentation processes [3,4]. The first type of continuous glucose sensor developed over 20 years ago was an amperometric electrochemical glucose sensor that used the enzyme *glucose oxidase* (GOx) for glucose recognition [5,6]. This type of glucose sensor is relatively fast and small, and research on improvements to amperometric glucose sensors continues unabated [7–9]. However, even though GOx is highly specific to glucose, the use of GOx as a recognition element for glucose suffers from the following disadvantages: (1) the enzyme GOx is susceptible to denaturation with subsequent loss of activity; (2) GOx requires oxygen or another redox mediator and is thus unsuitable for anaerobic fermentation reactors [4]; (3) the reaction catalyzed by GOx continuously consumes the analyte (glucose) and produces a potentially harmful by-product (H_2O_2). This last point implies that sensors employing GOx are transport sensors rather than equilibrium sensors, with sensitivities that vary with the glucose diffusion coefficient. For these reasons, many of the newer glucose sensors under development use the boronic acid moiety rather than GOx as the recognition element for glucose [10–27]. This includes sensors based on optical [11–14,16,18,20,21,27], fluorescence [25,26], surface plasmon [23], and swelling pressure measurements [17,24]. Small molecules containing boronic acid have been known for over a century to strongly yet reversibly bind *cis*-diols on glucose and other monosaccharides to give cyclic boronic acid esters in aqueous media [28], as shown schematically in Fig. 1. Kataoka and co-workers appear to be the first research group to incorporate boronic acid moieties

☆ J. Magda, F. Solzbacher, and P. Tathireddy have financial interests in an early-stage startup company (pre-IPO) located in Salt Lake City, UT, USA (Blackrock Sensors, Inc.) that is licensing hydrogel-based sensing technology.

* Corresponding author: Tel.: +1 301 435 7229; fax: +1 301 435 5035.
** Corresponding author at: Department of Chemical Engineering, University of Utah, 50 s central campus dr, rm 3290, Salt Lake City, UT 84112, USA. Tel.: +1 801 581 7536; fax: +1 801 585 9291.
E-mail addresses: horkay@helix.nih.gov (F. Horkay), jj.magda@utah.edu (J. Magda).

0925-4005/$ – see front matter © 2011 Elsevier B.V. All rights reserved.
doi:10.1016/j.snb.2011.09.079

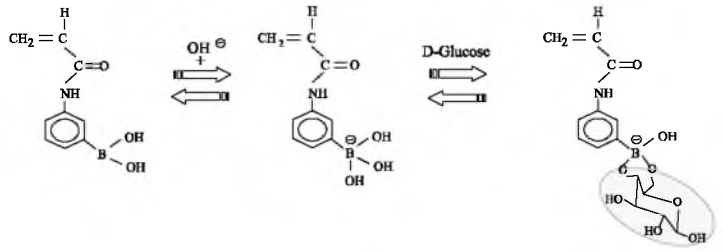

Fig. 1. From left-to-right, the interaction between the boronic acid moiety (on acrylamide monomer) and a hydroxyl group to form the charged boronate moiety; reversible binding between the boronate moiety and a diol such as D-glucose to form a cyclic boronic acid ester (tridentate binding is also possible).

into smart hydrogels, thereby obtaining "totally synthetic" polymer gels that reversibly swell in response to increases in the environmental glucose concentration [29]. At physiological pH (7.4), this hydrogel is a slightly charged poly(anion), because the pK_a value for isolated boronic acid groups is about 8.86 [30]. Unfortunately, this smart hydrogel and others of similar chemistry are actually more responsive to fructose than to glucose. This is not surprising, because small molecule spectroscopic studies show that the isolated boronic acid moiety has a binding constant with fructose that is about 40 times greater than its binding constant with glucose [28]. Thus, even though the normal physiological concentration of fructose is approximately 200 times smaller than that of glucose [31], some method of glucose selectivity enhancement is thought to be necessary. In the last 10 years, a number of research groups working on a variety of different types of glucose sensors have determined that beneficial effects can be obtained by using zwitterionic polymers or zwitterionic hydrogels obtained by incorporating pendant tertiary amines into the polymers or hydrogels nearby to the boronic acid moieties [12,14,18,20,21,24,27,30,32]. The chosen tertiary amines are Lewis bases that accept a proton to become cations at physiological pH. In addition, for polymers at least, the incorporation of tertiary amines facilitates the ionization of nearby boronic acid groups [33]. As an example of the benefits to glucose selectivity of this approach, consider the results of Horgan et al., who developed a holographic glucose sensor in which a diffraction grating is embedded within a glucose-responsive hydrogel [14]. The signal from this sensor is the measured change in the wavelength of diffracted light in response to an increase in the concentration of environmental glucose or fructose concentration from 0 to 5.7 mM, the normal glucose physiological value. When the holographic sensor was used with a smart hydrogel containing boronic acid but no tertiary amines, the optical response observed was a red shift of 761 nm for fructose, and a red shift of 40 nm for glucose. On the other hand, when the holographic sensor was used with a smart hydrogel containing an equimolar ratio of boronic acid and tertiary amine, the optical response observed was a red shift of only 13 nm for fructose, and a *blue shift* of 50 nm for glucose. The results of Horgan et al. are indicative of the two trends that have been observed by a number of different research groups [12,14,18,20,21,24,27,32] when tertiary amines are incorporated into glucose-responsive hydrogels containing boronic acid moieties: (1) an increase in the magnitude of hydrogel glucose response relative to the magnitude of the fructose or lactate response, and (2) a change in the *direction* of the hydrogel response to an increase in glucose concentration from swelling to shrinking. A thermodynamic model based on reversible cross-linking proposed by Alexeev et al. [12] that explains both of these trends has become widely accepted by other researchers in the field [14,18,20,21,24,27,32]. According to Alexeev et al. [12], glucose is relatively unique among monosaccharides in that it can bind simultaneously to two different boronic acid moieties, thereby forming reversible glucose-bis(boronate) cross-links in the hydrogel network. The associated thermodynamic model further assumes that the free energy of mixing (Π_{mix}) of glucose with the hydrogel is negligible implying that all glucose molecules bind onto the boronic acid groups and do not influence the thermodynamic interactions between the polymer and the solvent, and thus the glucose response of the zwitterionic smart hydrogel arises *solely* from the formation or breakage of glucose-mediated cross-links [12]. However, as far as we know, there is of yet no direct spectroscopic evidence that glucose-bis(boronate) cross-links form in hydrogels, though NMR studies on small organic molecules show that *both* glucose and fructose can simultaneously bind to two boronic acid groups [28]. We do not dispute the importance of glucose-mediated cross-links, but feel it is necessary in the following to re-examine the additional assumption that the change in the free energy of mixing (Π_{mix}) does not contribute significantly to zwitterionic hydrogel glucose response. To investigate the effect of glucose on the thermodynamic properties of these gels it is important to separate the elastic and mixing free energy components. To this end we made osmotic swelling pressure measurements on gels containing relatively low amounts (8 mol%) of boronic acid moieties. The low boronic acid content reduces the number of additional cross-links formed in the presence of glucose.

2. Thermodynamics

Unconfined neutral hydrogels swell until the total change in free energy, ΔF_{tot}, reaches a minimum or, equivalently, until the chemical potential of each mobile species becomes equal in the coexisting phases. The mixing of water with the polymer chains makes a negative contribution to the free energy (ΔF_{mix}), while the stretching of the hydrogel network makes a positive contribution (ΔF_{el}). Assuming these terms are independent, we can write [12,34–36]:

$$\Delta F_{tot} = \Delta F_{mix} + \Delta F_{el}. \quad (1)$$

In the case of charged hydrogels, the ions also contribute to ΔF_{tot}. However, at high ionic strength (0.16 M), the ionic contribution can be neglected [12], as shown by several experimental studies on highly swollen polyelectrolyte hydrogels (e.g., polyacrylic acid gels, DNA gels) [36,37] as well as molecular dynamics simulations [38].

In an osmotic swelling experiment the measurable quantities involve derivatives of the free energy, i.e.

$$\Pi_{tot} = -\frac{1}{V_1}\left(\frac{\partial \Delta F_{tot}}{\partial n_1}\right) = \Pi_{mix} + \Pi_{el}, \quad (2)$$

where Π_{tot} is the swelling pressure of the gel, Π_{mix} and Π_{el} are the mixing and elastic contributions of Π_{tot}, respectively, V_1 is the molar volume of solvent (water), and n_1 is the number of moles

of water. At swelling equilibrium with the pure solvent Π_{tot} must equal zero. One can study non-zero values of the total swelling pressure by equilibrating the hydrogel with an osmotic stressing agent of known osmotic pressure [36,37], or by squeezing the water out of the hydrogel using a known mechanical (hydrostatic) pressure [39].

According to a Flory–Huggins type equation, Π_{mix} is given by:

$$\Pi_{mix} = -\frac{RT}{V_1}[\ln(1-C) + C + \chi_0 C^2 + \chi_1 C^3], \quad (3)$$

where C is the weight fraction of the polymer in the hydrogel, χ_0 and χ_1 are the Flory–Huggins parameters for binary and ternary interactions, respectively, between the polymer network and the solution, R is the gas constant, and T is the temperature. The elastic contribution Π_{el} at a given gel volume V is given by [12,36]:

$$\Pi_{el} = -\frac{RTn_{cr}}{V_m}\left[\left(\frac{V_m}{V}\right)^{1/3} - \frac{1}{2}\left(\frac{V_m}{V}\right)\right] = -G, \quad (4)$$

where V_m is the volume of the relaxed network, n_{cr} is effective number of cross-linked chains in the network, and G is network elastic shear modulus. In their analysis of zwitterionic glucose-responsive hydrogels, the main assumption of Alexeev et al. [12] is that the hydrogel glucose response is dominated by the increase in n_{cr} with increase in glucose concentration; i.e. $|\Delta\Pi_{el}| \gg \Delta\Pi_{mix}$ for an increase in glucose concentration within the range of physiological interest (0–20 mM). It is this assumption that we check in the following sections.

3. Experimental methods

3.1. Materials

The monomers used for preparation of the gels were obtained as follows: acrylamide (AAM, Fisher Scientific), *N,N*-methylenebisacrylamide (BIS, Sigma–Aldrich), 3-acrylamidophenylboronic acid (3-APB, Frontier Scientific, Logan, UT, USA), and *N*-(3-dimethylaminopropyl acrylamide (DMAPAA). The monomers were used as received. Ammonium peroxydisulfate (APS, Sigma–Aldrich), *N,N,N′,N′*-tetramethylethylenediamine (TEMED, Sigma–Aldrich), 2,2-dimethoxy-2-phenylacetophenone (Sigma–Aldrich), 1-vinyl-2-pyrrolidinone (Sigma–Aldrich), D(+)-glucose (Mallinckrodt Chemicals), D(−)-fructose (Sigma–Aldrich), dimethyl sulfoxide (DMSO, Sigma–Aldrich), 4-(2-Hydroxyethyl)piperazine-1-ethanesulfonic acid (HEPES, Sigma–Aldrich), and Dulbecco's phosphate-buffered saline solution (1× PBS, Sigma–Aldrich) were also used as received. Market grade wire cloth mesh (type 304 stainless steel, 80 mesh, wire opening 178 μm, open area 31%) was obtained from Small Parts, Inc., Miramar, FL, USA.

3.2. Hydrogel synthesis

Zwitterionic glucose-sensitive hydrogels (GSHs) containing AAM/3-APB/DMAPAA/BIS at a nominal mole ratio of 80/8/10/2 were prepared by free radical cross-linking copolymerization. This is the same composition previously studied by Tierney et al. [20,21] and Lin et al. [24]. GSHs were prepared in molds of three different thickness values: 0.4 mm for samples used in glucose sensor tests, 1 mm for samples used for osmotic swelling pressure and SANS measurements, and 5 mm for samples used for shear modulus measurements. Samples 0.4 mm and 1 mm thick were prepared by either thermal or UV curing, whereas only thermal curing was used to prepare samples 5 mm thick. (In thicker samples UV curing does not result in homogeneous gels.) The polymer concentration in the pre-gel solution prior to curing was 13 wt.%, or 20 wt.% in a few selected cases. In brief, stock solutions were prepared of AAM and BIS in 1 mM HEPES buffer. Appropriate amounts of the two stock solutions were mixed in a vial with DMAPAA and TEMED in the case of thermal curing. In order to dissolve 3-APB into the pre-gel solution, 10 vol% of DMSO was added into the vial. In thermal curing, the free radical initiator APS was introduced after purging the vial with N_2 gas for 10 min, after which the pre-gel solution was rapidly injected into a cavity between two square plates (polycarbonate and poly(methyl methacrylate)) of surface area 60 cm^2. After approximately 12 h of reaction at room temperature, the hydrogel slab was removed from the mold and washed for at least two days with deionized water and 1× PBS buffer (pH 7.4, ionic strength 0.16 M) before testing. For UV curing, the photoinitator combination 2,2-dimethoxy-2-phenylacetophenone/1-vinyl-2-pyrrolidinone was used instead of the thermal initiator combination TEMED/APS. After purging with N_2 gas for 10 min, the pre-gel solution was injected into a cavity of known thickness between a glass plate and a poly(methacrylate) plate. Photopolymerization was induced by exposing the pre-gel solution through the glass plate to UV light (365 nm, 10 mW/cm^2) for 2.5 min. The GSHs obtained were first washed with DI water for about one day and then stored in 1× PBS buffer. The samples were also subjected to two cycles of ionic strength change between 0.16 M and 0.05 M PBS in order to further clean the hydrogels. The hydrogels were stored in 0.16 M PBS until testing. Prior to SANS measurements, the water in the hydrogel was exchanged with D_2O as described below. The solvent exchange did not cause appreciable change in the swelling degree. In order to estimate the water content, GSH samples were dried in an oven at 50 °C with the weight monitored as a function of time. A GSH sample synthesized in 1 mM HEPES buffer at 13 wt.% polymer and equilibrated with 1× PBS at pH 7.4 was shown to contain on average 88 wt.% water. A GSH sample synthesized in 1 mM HEPES buffer at 20 wt.% polymer and equilibrated with 1× PBS at pH 7.4 was shown to contain on average 85 wt.% water.

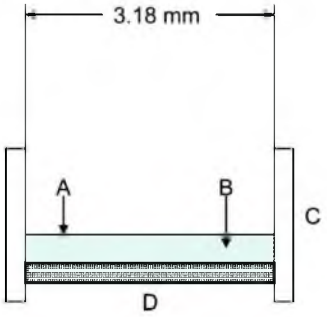

Fig. 2. Preliminary version of the chemomechanical sensor used in this study. A piezoresistive pressure transducer with a cylindrical sensing area (A) is completely covered with a disc-shaped hydrogel film (B) of approximate thickness 400 μ. The hydrogel is held in place by a cap (C) that has a top surface which is a replaceable wire mesh/porous membrane (D) (from reference [40]).

3.3. Sugar sensor construction and sensor response tests

As analyzed in detail in recent publications in this journal [24,40], the total osmotic swelling pressure Π_{tot} of a smart hydrogel can be obtained by confining it between a porous membrane and the diaphragm of a miniature pressure transducer. In such a sensing scheme, a change in the environmental glucose concentration, as sensed through the pores of the membrane, changes Π_{tot} (see Equation (2)) which must at equilibrium equal the mechanical pressure measured by the pressure transducer. Fig. 2 shows a sketch of

the chemomechanical sensor that was used. The sensor consists of a piezoresistive pressure transducer (model EPX-N01-0.35B, MEAS France, Les Clayes-Sous-Bois, France) with a cylindrical stainless steel sensing area (diameter 3.5 mm) completely covered with a hydrogel film of thickness ≈400 μm. The hydrogel is held in place in the sensor by a cap with a top surface that consists of a replaceable porous membrane through which mass transfer can occur. In keeping with the results obtained from our previous work [40], a stainless steel wire cloth mesh (mesh size 80, wire opening 174 μm, 31% open area) was used as the porous membrane. A GSH was synthesized and cleaned as described above, a circular biopsy tool was used to cut a disc-shaped sample of appropriate diameter, and the sample was then transferred from sugar-free PBS buffer (pH 7.4, ionic strength 0.16 M) to the sensing surface of the pressure transducer using tweezers. The sensor cap with wire mesh was attached to the sensor base by tightening three screws that were adjusted to impose an axial compressive stress on the hydrogel in the sensor. The sensor was then inserted into a large covered environmental bath containing PBS buffer at room temperature and physiological pH and ionic strength. This bath also contained a magnetic stirrer used to minimize external mass transfer resistance to the sensor. Sensor response tests were performed by either injecting solutions of glucose or fructose into the environmental bath and then noting the time-dependent response of the pressure transducer, or by rapidly switching the sensor into another environmental bath at the same ionic strength and pH but with no sugar. The time-dependent pressure signal was captured with an Agilent data acquisition system.

3.4. Total osmotic swelling pressure (Π_{tot}) measurements

The reference environmental solution (infinite bath) was chosen to be phosphate-buffered saline (PBS) solution at 25 °C with ionic strength 0.16 M and pH 7.4. In some cases, the environmental solution also contained 5 mM glucose or 5 mM fructose. Hydrogels of known dry mass m_d were equilibrated with this reference solution, at which point gel swelling pressure Π_{tot} must equal zero. Deswelling of the gels was achieved by enclosing them in a semipermeable membrane (dialysis bag, seamless cellulose tubing; cut off molecular weight: 12 kDa, Sigma Chemical Co., St. Louis, MO, USA). Known concentrations of an osmotic deswelling agent [poly(vinyl pyrrolidone), PVP, M_n = 29 kDa] were added to the environmental solution, and equilibrated with the gel for 8–10 days. The semipermeable membrane prevented penetration of PVP into the gel. At equilibrium, the swelling pressure Π_{tot} of the gel inside the dialysis bag is equal to the known osmotic pressure of the PVP solution outside [41]. Periodically the mass of the gel m_g was measured, and used to calculate the total polymer weight fraction $C = m_d/m_g$ (where m_d is the mass of the dry polymer), with hydrogel swelling ratio $Q \approx 1/C$. Equilibrium was achieved when no further changes in either gel swelling degree or solution composition were detectable. The gel samples were dried at 95 °C. First, the mass of the salt-containing gel was measured. Then the gel was soaked in large excess of distilled water to remove the salt. The swelling ratio was calculated by correcting the measured mass with the known amount of salt.

Reversibility was checked by transferring gels into PVP solutions at different osmotic pressure values.

3.5. Elastic (shear) modulus measurements

Shear modulus data of fully gelled materials were obtained from uniaxial compression measurements using a TA.XT2I HR Texture Analyser (Stable Micro Systems, UK). As discussed in a standard rubber testing handbook [42], torsional measurements of the shear modulus G of fully gelled polymers will be erroneous if sample "slip" occurs at the interface between the solid polymer and the steel rheometer plates, because then the true value of the shear strain exerted on the sample will be unknown. Hence the standard rubber testing handbook recommends lubricating the sample interface to ensure that sample slip does occur, and then determining G in the absence of "barrel" distortion by measuring the force needed to apply compressive strains (uniaxial) on the sample [42].

Equilibrated gel samples were rapidly transferred from the dialysis bag into the TA XT21 HR apparatus, which measures the compressive deformation (precision: ±0.001 mm) as a function of an applied force (precision: ±0.01 N). Stress–strain isotherms were determined at 25 °C in about 3–5 min with no detectable change in gel weight. The absence of sample volume change and barrel distortion was confirmed, and stress–strain isotherms were found to fit the Mooney–Rivlin relation [35,43,44]

$$\sigma = C_1(\Lambda - \Lambda^{-2}) + C_2(1 - \Lambda^{-3}), \quad (5)$$

where σ is the nominal stress (related to the undeformed cross-section of the gel), Λ is the deformation ratio ($\Lambda = L/L_o$, L and L_o are the lengths of the deformed and undeformed specimen, respectively), and C_1 an C_2 are constants. The stress–strain data were determined in the range of deformation ratio $0.7 < \Lambda < 1.0$. The value of C_2 proved to be negligibly small for the gel systems studied. In this situation, the constant C_1 can be identified with the shear modulus (G) of the swollen network.

The swelling and mechanical measurements were carried out at 25 ± 0.1 °C. Repeated measurements showed a mean change in the osmotic swelling pressure and elastic modulus less than 2–3%.

3.6. Hydrogel swelling ratio measurements as a function of temperature

A given hydrogel sample was immersed in a large stirred temperature-controlled vessel containing either sugar-free PBS buffer (pH 7.4, ionic strength 0.16 M), PBS buffer plus 5 mM glucose, or PBS buffer plus 5 mM fructose. Periodically, the gel sample was withdrawn from the solution and weighed after removal of excess surface solution by light blotting with a laboratory tissue. The change in relative swelling ratio for a gel sample subjected to a given change in temperature was calculated as $(m_f - m_0)/m_0$, where m_f is the mass at the final temperature, and m_0 is the mass at the initial temperature. Swelling ratio changes were measured for 3–4 small samples taken from the same reaction mold, and the standard deviation was taken as an estimate of the uncertainty in the measured swelling ratio.

3.7. Small-angle neutron scattering

SANS measurements were made on gels on the NG3 30 m instrument [45] at the National Institute of Standards and Technology (NIST, Gaithersburg, MD, USA). Gel samples were swollen in solutions of heavy water in 2 mm thick sample cells. The sample cell consisted of 1 mm thick quartz windows separated by a 2 mm thick spacer. The beam diameter was 20 mm. The measurements were made at three sample-detector distances, 1.3 m, 4 m and 13.1 m, with incident wavelength 8 Å. The explored wave vector range was $0.003\ \text{Å}^{-1} \le q \le 0.2\ \text{Å}^{-1}$, and counting times from 20 min to 2 h were used. The total counts of neutron at the detector varied in the range 0.5–3 million. After radial averaging, corrections for detector response and cell window scattering were applied. The neutron scattering intensities were calibrated using NIST absolute intensity standards. The incoherent background was subtracted following the procedure described in reference [46]. All SANS experiments were carried out at 25 ± 0.1 °C.

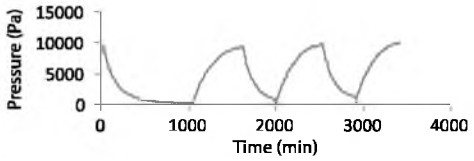

Fig. 3. Time-dependent change in pressure relative to baseline measured by chemomechanical sensor of Fig. 2 in response to cyclic change in glucose at fixed pH 7.4 and fixed ionic strength 0.16 M in 1× PBS buffer. The environmental glucose concentration, which was initially zero, was suddenly increased to 5 mM at time equal zero, suddenly reduced to zero again at time equal 1100 min, and then the cycle was repeated twice more (thermally cured zwitterionic GSH, pre-gel polymer concentration 13 wt.%).

4. Results

4.1. Sugar sensor response results

Fig. 3 shows the response of the chemomechanical sensor (Fig. 2) at 25 °C to cyclic changes in the environmental glucose concentration between zero and 5 mM at fixed pH (7.4) and fixed ionic strength (0.16 M). The response of the same sensor under the same conditions to cyclic changes in environmental fructose concentration between zero and 5 mM is shown in Fig. 4. In both cases, the GSH in the sensor was prepared by thermal curing a pre-gel solution containing 13.0 wt.% polymer in a mold of thickness 400 μm. In Fig. 3, the measured value of Π_{tot} *decreases* in response to the increase in glucose concentration from zero to 5 mM. Note that 5 mM is approximately the normal blood glucose concentration in humans. The average magnitude of the decrease is 9.1 kPa ± 0.05 kPa. The response time in the macrosensor is quite large, but we have already demonstrated elsewhere a response time of order 10 min using the same GSH in a microchip glucose sensor [47]. In Fig. 4, the measured value of Π_{tot} *increases* in response to the increase in fructose concentration from zero to 5 mM. The average magnitude of the increase is 5.6 kPa ± 0.2 kPa. Note that the sensor fructose response magnitude in Fig. 4 is smaller than the sensor glucose response magnitude in Fig. 3, even though we introduced a fructose concentration some 200 times larger than the normal human blood value [31]. Thus when monitoring blood glucose concentration, one can safely neglect fructose interference under most conditions using the GSH of Figs. 3 and 4. In addition, Tierney and co-workers have demonstrated using an optical sensor with the same GSH for glucose recognition that potential interference from physiological concentrations of lactate is negligible, and that the glucose response is essentially the same in human blood plasma as in PBS buffer, provided that the blood plasma does not contain added heparin for anti-coagulation [21].

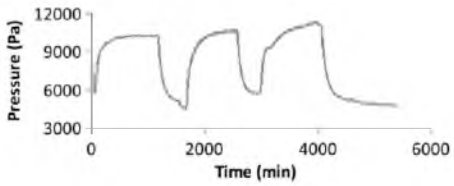

Fig. 4. Time-dependent change in pressure relative to baseline measured by chemomechanical sensor of Fig. 2 in response to cyclic change in fructose at fixed pH 7.4 and fixed ionic strength 0.16 M in 1× PBS buffer. The environmental fructose concentration, which was initially zero, was suddenly increased to 5 mM at time equal zero, suddenly reduced to zero again at time equal 1100 min, and then the cycle was repeated twice more (thermally cured zwitterionic GSH, pre-gel polymer concentration 13 wt.%).

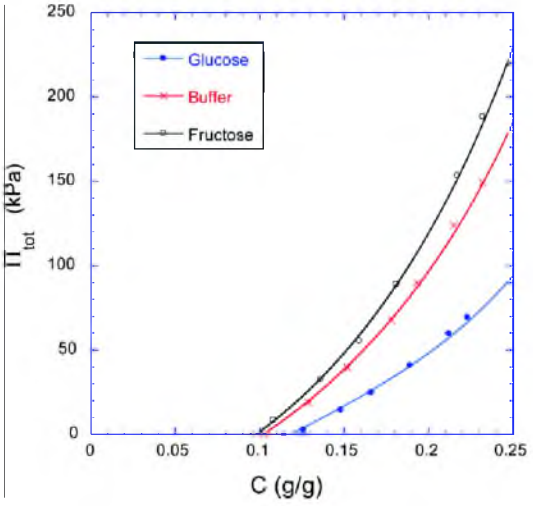

Fig. 5. Total osmotic swelling pressure vs. polymer weight fraction C for thermally cured zwitterionic GSHs at 25 °C in sugar-free 1× PBS buffer (pH 7.4, 0.16 M ionic strength), PBS buffer with 5.0 mM added glucose, and PBS buffer with 5.0 mM added fructose. The continuous curves are least squares fits to Equation (6) in the text (pre-gel polymer concentration 13 wt.%).

This GSH contains both boronic acid moieties (≈8 mol% 3-APB) and pendant tertiary amines (≈10 mol% DMAPAA). As shown elsewhere [14,20,24,32], in the absence of pendant tertiary amines, a similar GSH would swell rather than shrink in response to an increase in glucose concentration, with a magnitude considerably less than the magnitude of the fructose swelling response. Thus the incorporation of a relatively small mole fraction of tertiary amines into the hydrogel is sufficient to dramatically enhance glucose selectivity, as noted by numerous other researchers (Section 1).

It is also important to note that the kinetics of the swelling and shrinking process, which governs the response time of gel biosensors to changes in glucose concentration, strongly depends on the size and geometry of the sample. Fast responses can be obtained by miniaturizing the system. Furthermore, the properties of the network polymer (e.g., chemical quality and distribution of monomers, cross-link density, amounts of charged groups) also influence the dynamic properties.

4.2. Osmotic swelling pressure and elastic shear modulus results

The results of the osmotic deswelling experiments are shown in Fig. 5 where the swelling pressure Π_{tot} of the zwitterionic GSHs is plotted against the polymer weight fraction C, in three different solvents: sugar-free PBS buffer (1×), PBS buffer plus 5 mM added glucose, and PBS buffer plus 5 mM added fructose. It is apparent that the GSH deswells when it is subjected to a given osmotic stress exerted by the PVP solution as described in Section 3.4. The amount of water retained by the GSH has its least value when placed in the glucose solution, and has its greatest value when placed in the fructose solution. The results obtained in sugar-free PBS are intermediate between the results obtained in the fructose and glucose solutions, but closer to the fructose solution results. This is consistent with the sensor results (Figs. 3–4), which show that the GSH exhibits a greater change when transferred from 1× PBS buffer to the 5 mM glucose solution than to the 5 mM fructose solution. One also observes in Fig. 5 that the Π_{tot} value of the zwitterionic GSH

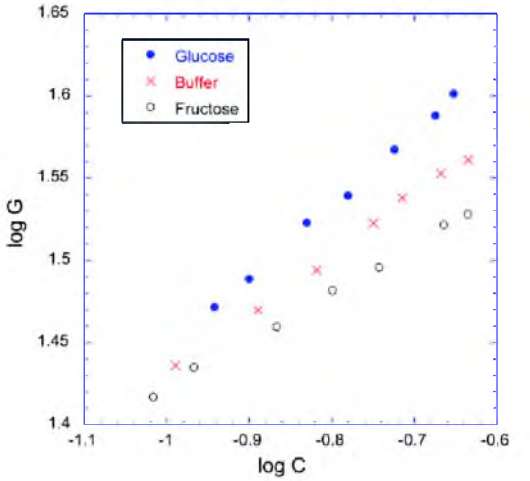

Fig. 6. Logarithmic plot of elastic shear modulus G (in kPa) vs. polymer weight fraction C, as measured in the three different solutions studied in Fig. 5 (thermally cured zwitterionic GSH, pre-gel polymer concentration 13 wt.%).

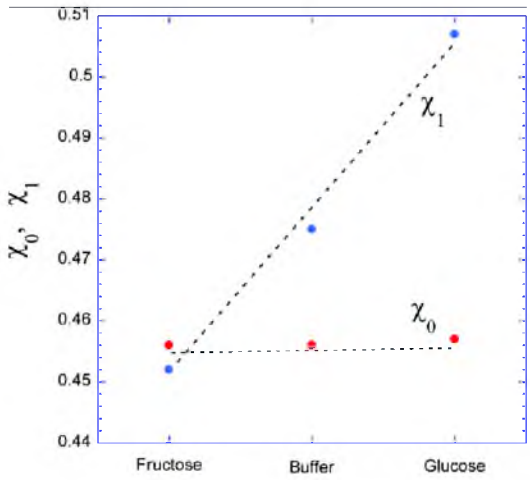

Fig. 7. Values of the Flory–Huggins binary and ternary interaction parameters as obtained by least-squares-fit of the data in Fig. 5 to Equation (6). The broken lines through the data points serve as guides to the eyes.

exhibits a much steeper increase with increasing polymer weight fraction in the fructose solution. This implies that *osmotic modulus* $\left[= C\left(\frac{\partial \Pi_{tot}}{\partial C}\right)_T\right]$ of the GSH, its resistance to having its water content reduced by compression, is larger in the fructose solution.

Combining Equations (2)–(4), one obtains the Flory–Huggins theoretical prediction for the results of Fig. 5:

$$\Pi_{tot} = \Pi_{mix} + \Pi_{el} = -\frac{RT}{V_1}[\ln(1-C) + C + \chi_0 C^2 + \chi_1 C^3] - G. \quad (6)$$

According to Equation (6), Π_{tot} is the sum of a mixing contribution Π_{mix} and an elastic contribution Π_{el}, where the elastic contribution is taken to be the negative of the shear modulus G [36]. The value of G was independently measured as a function of polymer weight fraction in the same three solutions (Section 3). Fig. 6 shows the variation of the shear modulus G with the polymer weight fraction of the zwitterionic GSH. In Fig. 6, at fixed polymer weight fraction C, G is larger in the glucose solution than in sugar-free PBS buffer, as might be expected if glucose-mediated reversible cross-linking is occurring (Section 1). However, we also have the puzzling result that at fixed polymer weight fraction and at (presumably) fixed cross-link density, G is smaller in the fructose solution than in sugar-free PBS buffer. This might be an indication that the network chains are stiffer in the sugar-free PBS buffer than in the fructose solution. A similar result was observed for pH-responsive hydrogels in reference [48].

One can use Equation (6) in conjunction with the shear modulus values of Fig. 6 to perform a least-squares-fit on the measured values of Π_{tot}. The results of this fitting procedure are given by the continuous curves in Fig. 5, and the fit is seen to be excellent. This fitting procedure provides values for the Flory–Huggins binary (χ_0) and ternary (χ_1) interaction parameters, which are shown in Fig. 7 as obtained for the zwitterionic GSH in the fructose solution, in the glucose solution, and in sugar-free PBS buffer. All three χ_0 values are similar, but χ_1 is significantly larger in the glucose solution than in the fructose solution (0.51 vs. 0.43), with an intermediate value observed in sugar-free PBS buffer (0.46). From Equation (3), the larger value of χ_1 implies that Π_{mix}, which depends on thermodynamic mixing interactions rather than on cross-link density, is considerably less favorable for swelling in glucose solutions than in fructose solutions. This is consistent with the observation that the zwitterionic GSH shrinks in response to glucose (Fig. 3), and swells in response to fructose (Fig. 4).

4.3. Small-angle neutron scattering measurements

To obtain information on the spatial organization of the polymer molecules in these zwitterionic GSHs at the nanoscale, we made SANS measurements. Fig. 8 shows the SANS spectra at 25 °C for the thermally cured GSHs of Figs. 3 and 4 swollen to the same extent (12 wt.%) in three different solvents: sugar-free 1× PBS buffer, 1× PBS buffer plus 5 mM added glucose, and 1× PBS buffer plus 5 mM

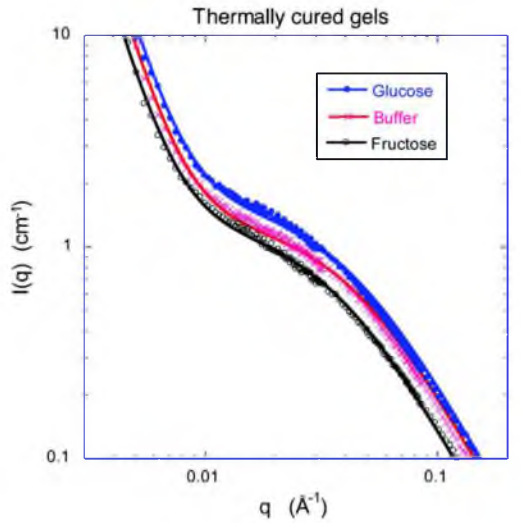

Fig. 8. Comparison of SANS spectra obtained from zwitterionic GSHs at 25 °C in sugar-free 1× PBS buffer (pH 7.4, 0.16 M ionic strength), PBS buffer with 5.0 mM added glucose, and PBS buffer with 5.0 mM added fructose. The GSHs were obtained by thermal curing of a pre-gel solution containing 13.0 wt.% polymer. The continuous curves are least squares fits of Equation (7) to the data.

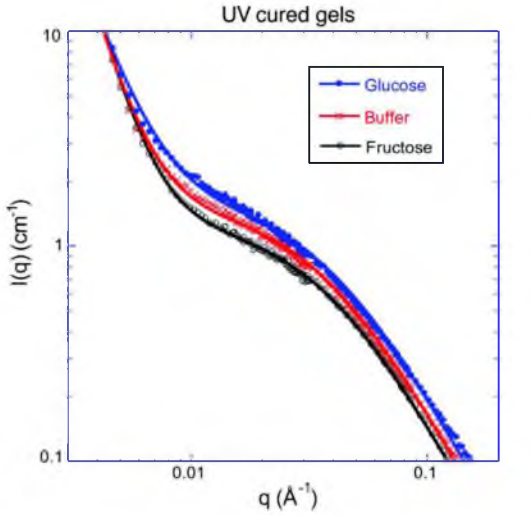

Fig. 9. Comparison of SANS spectra obtained from zwitterionic GSHs at 25 °C in sugar-free 1× PBS buffer (pH 7.4, 0.16 M ionic strength), PBS buffer with 5.0 mM added glucose, and PBS buffer with 5.0 mM added fructose. The GSHs were obtained by UV curing of a pre-gel solution containing 13.0 wt.% polymer. The continuous curves are least squares fits of Equation (7) to the data.

added fructose. Surprisingly, even though the swelling pressure of this GSH responds very differently to fructose and glucose (Fig. 5 vs. Fig. 6), the shape of the SANS spectra (Fig. 8) is similar in fructose and glucose solutions. However, the scattering intensity from the gel swollen in glucose solution is greater than from the corresponding gel swollen in fructose solution by roughly a factor of two. The increase in intensity reflects a decrease in the osmotic modulus, which is consistent with the swelling pressure observations. Fig. 9 shows the SANS response of a UV-cured GSH of the same nominal composition, as obtained after swelling to equilibrium in the same three solvents studied in Fig. 8. Comparing Figs. 8 and 9, one notes that the curing procedure (thermal vs. UV) has a little effect on the hydrogel structure in the low q (<0.007 Å^{-1}) region, where the UV cured gel in glucose solution exhibits a slightly less steep negative slope.

The SANS curves were analyzed using Equation (7), which reproduces the main characteristic features of the scattering curves

$$I(q) = \frac{A_1}{1+q^2\xi^2} + \frac{A_2}{q^s}, \tag{7}$$

where ξ is the polymer-polymer correlation length [49], and A_1, A_2 and s are constants. The intensities A_1 and A_2 are proportional to the average scattering contrast between the polymer and the solvent. In Equation (7) the first term (Lorentzian form factor) is primarily governed by the thermodynamic concentration fluctuations, while the second term arises from large-scale static inhomogeneities frozen-in by the cross-links. These large objects are not expected to make significant contribution to the thermodynamic properties of the system [50,51].

The parameters obtained from the least-squares fit of Equation (7) to the SANS data (continuous lines in Figs. 8 and 9) are listed in Table 1. The apparent invariance of ξ with the solvent composition suggests that glucose induced cross-linking does not affect appreciably the mesh size of these gels.

Table 1
Parameters from fits of Equation (7) to the SANS spectra of thermal cured and UV cured gels.

Sample	A_1 (cm^{-1})	A_2 (cm^{-1})	ξ (Å)	s
T/glucose	0.009 ± 0.002	1.58 ± 0.4	25 ± 3	−3.77
T/buffer	0.009 ± 0.002	1.29 ± 0.3	24 ± 3	−3.76
T/fructose	0.008 ± 0.002	1.24 ± 0.3	23 ± 4	−3.78
UV/glucose	0.008 ± 0.002	1.56 ± 0.5	26 ± 4	−3.35
UV/buffer	0.007 ± 0.002	1.46 ± 0.4	27 ± 4	−3.74
UV/fructose	0.007 ± 0.002	1.24 ± 0.3	28 ± 5	−3.91

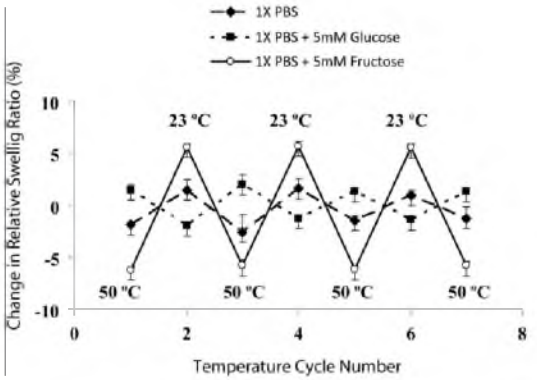

Fig. 10. Response of the relative swelling ratio to cyclic changes in temperature between 50 °C and 23 °C in the solvents given in the legend (UV-cured zwitterionic GSH, pre-gel polymer concentration 20 wt.%).

4.4. Temperature-dependent GSH swelling behavior in fructose and glucose solutions

In Section 4.2, it was shown that the thermodynamic interaction of the zwitterionic GSH is favorable with fructose and unfavorable with glucose (relative to sugar-free PBS buffer). In order to determine if this difference is enthalpic or entropic in origin, we compare the temperature-dependent swelling response of the GSH in 5 mM fructose solution, 5 mM glucose solution, and sugar-free PBS buffer (Fig. 10). An increase in temperature is expected to favor processes that increase entropy relative to processes that reduce enthalpy. Fig. 10 shows the change in the relative hydrogel swelling ratio in response to cyclic changes in temperature between 23 °C and 50 °C. The zwitterionic GSH in sugar-free PBS (1×) shrinks with increase in temperature; the shrinkage is slight (≈2%) but reproducible. This is typical behavior for many water-soluble polymers; it is thought to occur because the water molecules adopt a higher degree of order (lower entropy) near the polymer in order to maintain hydrogen bonding [52]. This structuring of water gives rise to the *hydrophobic interaction force* between polymer chains that is largely entropic in origin. When the GSH is placed in the fructose solution, thereby producing a polymer network containing adsorbed fructose molecules, the degree of hydrogel shrinkage is even larger (≈6%) with increase in temperature. In striking contrast, the GSH polymer network containing adsorbed glucose molecules is observed to swell with increase in temperature (Fig. 10).

5. Discussion

The purpose of this study is to check the widely held assumption [14,18,20,21,24,27,32], first proposed by Alexeev et al. [12], that the shrinkage of zwitterionic GSHs in response to an increase in glucose concentration arises almost entirely due to the formation of

glucose-mediated cross-links (i.e., $|\Delta\Pi_{el}| \gg |\Delta\Pi_{mix}|$). Figs. 5–7 contain the data needed to check this assumption. Consider an increase in environmental glucose concentration from 0 to 5 mM in PBS buffer, which clearly causes the zwitterionic GSH to shrink in the chemomechanical sensor (Fig. 3). At a fixed polymer concentration in the GSH (C=0.15), this increase in glucose concentration results in a decrease in total swelling pressure Π_{tot} of ≈20 kPa (Fig. 5). According to Fig. 6, the decrease in Π_{el} (increase in G) under the same conditions is approximately 3 kPa, thus $\Delta\Pi_{mix}$ is ≈−17 kPa. In other words, when the glucose concentration is increased from zero to 5 mM, 85% of the thermodynamic driving force for the shrinkage of the zwitterionic GSH can be attributed to the decrease in the favorability of thermodynamic mixing interactions, and 15% of the driving force can be attributed to the increase in shear modulus. Note that the sensor signal in Fig. 3 is less than 20 kPa because the hydrogel volume shrinks to some extent within the sensor due to sensor compliance, as discussed in reference [40].

It should be pointed out that the relative contributions of $\Delta\Pi_{el}$ and $\Delta\Pi_{mix}$ might be expected to differ when zwitterionic GSHs of much greater boronic acid content (30 mol.%) than studied here (8 mol.%) are subjected to large changes in environmental glucose concentration (0–40 mM), as in reference [32]. This may explain why the percentage increase in shear modulus due to the increase in glucose concentration reported in reference [32] is much larger than reported here in Fig. 6.

Since the difference between the degree of reversible cross-linking attributable to glucose and fructose is not great for our zwitterionic GSH, an alternate explanation must be found to explain the enhancement in glucose selectivity relative to fructose that is obtained by incorporating tertiary amines into the hydrogel. The results in Fig. 10 provide a clue. In PBS buffer and in the fructose solution, the zwitterionic GSH shrinks with increase in temperature, as expected to occur when water molecules near the GSH are highly ordered in order to preserve a high degree of hydrogen bonding [52]. By contrast, the zwitterionic GSH swells with increase in temperature in the glucose solution. This suggests that the adsorption of glucose molecules by the hydrogel may affect the arrangement of neighboring water molecules in such a way that they do not have lower entropy than bulk water, and do not preserve a high degree of hydrogen bonding. Such a change in water structure would not be apparent in SANS spectra obtained from samples in heavy water. The loss in hydrogen bonding with increase in environmental glucose concentration is probably responsible for the decrease in the osmotic mixing pressure between the network and the solvent that causes the hydrogel to shrink.

6. Conclusions

Copolymerization of tertiary amines (Lewis bases) into glucose-responsive hydrogels containing boronic acid moieties creates a zwitterionic hydrogel with an enhanced selectivity for glucose relative to fructose, and also creates a hydrogel that shrinks rather than swells in response to an increase in environmental glucose concentration. Previously it had been thought that this occurs because glucose can mediate the formation of reversible cross-links in zwitterionic hydrogels, whereas fructose cannot. However, we have shown that another significant factor is the change in the value of Π_{mix}, which reflects the thermodynamic mixing interactions between the network and solvent. The zwitterionic GSH shrinks upon glucose addition and swells upon fructose addition because the change in Π_{mix} is large and negative in the first case, and large and positive in the second case.

Acknowledgements

This research was supported by the Intramural Research Program of the NICHD, NIH. We also acknowledge the support of the National Institute of Standards and Technology, U.S. Department of Commerce, in providing the neutron research facilities used in this work. This work utilized facilities supported in part by the National Science Foundation under Agreement No. DMR-0944772. This project was supported by the National Institutes of Health NHLBI/NIBIB Grant no. 5R21EB008571-02.

References

[1] T. Koschinsky, L. Heinemann, Sensors for glucose monitoring: technical and clinical aspects, Diabetes Metab. Res. Rev. 17 (2001) 113–123.
[2] H.E. Koschwanez, W.M. Reichert, In vitro, in vivo and post explantation testing of glucose-detecting biosensors: current methods and recommendations, Biomaterials 28 (2007) 3687–3703.
[3] A. Glindkamp, D. Riechers, C. Rehbock, B. Hitzmann, T. Scheper, K.E. Reardon, Sensors in disposable bioreactors status and trends, Adv. Biochem. Engin./Biotechnol. 115 (2009) 145–169.
[4] B. Kurtinaitiene, J. Razumiene, V. Gureviciene, V. Melvydas, L. Marcinkeviciene, I. Bachmatova, R. Meskys, V. Laurinavicius, Application of oxygen-independent biosensor for testing yeast fermentation capacity, Biosens. Bioelectron. 26 (2010) 766–771.
[5] Y. Degani, A. Heller, Direct electrical communication between chemically modified enzymes and metal electrodes. 1. Electron transfer from glucose oxidase to metal electrodes via electron relays, bound covalently to the enzyme, J. Phys. Chem. 91 (1987) 1285–1289.
[6] Y. Degani, A. Heller, Direct electrical communication between chemically modified enzymes and metal electrodes. 2. Methods for bonding electron-transfer relays to glucose oxidase and D-amino-acid oxidase, J. Am. Chem. Soc. 110 (1988) 2615–2620.
[7] H. Kudo, T. Sawada, E. Kazawa, H. Yoshida, Y. Iwasaki, K. Mitsubayashi, A flexible and wearable glucose sensor based on functional polymers with Soft-MEMS techniques, Biosens. Bioelectron. 22 (2006) 558–562.
[8] D.A. Gough, L.S. Kumosa, T.L. Routh, J.T. Lin, J.Y. Lucisano, Function of an implanted tissue glucose sensor for more than 1 year in animals, Sci. Traslational Med. 2 (2010) 42–53.
[9] X. Jiang, Y. Wu, X. Mao, X. Cui, L. Zhu, Amperometric glucose biosensor based on integration of glucose oxidase with platinum nanoparticles/ordered mesoporous carbon nanocomposite, Sens. Actuators B: Chem. 153 (2011) 158–163.
[10] F.H. Arnold, W. Zheng, A.S. Michaels, A membrane-moderated conductimetric sensor for the detection and measurement of specific organic solutes in aqueous solutions, J. Membr. Sci. 167 (2000) 227–239.
[11] S.A. Asher, V.L. Alexeev, A.V. Goponenko, A.C. Sharma, I.K. Lednev, C.S. Wilcox, D.N. Finegold, Photonic crystal carbohydrate sensors: low ionic strength sugar sensing, J. Am. Chem. Soc. 125 (2003) 3322–3329.
[12] V.L. Alexeev, A.C. Sharma, A.V. Goponenko, S. Das, I.K. Lednev, C.S. Wilcox, D.N. Finegold, S.A. Asher, High ionic strength glucose-sensing photonic crystal, Anal. Chem. 75 (2003) 2316–2323.
[13] Y.-J. Lee, S.A. Pruzinsky, P.V. Braun, Glucose-sensitive inverse Opal hydrogels: analysis of optical diffraction response, Langmuir 20 (2004) 3096–3106.
[14] A.M. Horgan, A.J. Marshall, S.J. Kew, K.E.S. Dean, C.D. Creasey, S. Kabilan, Crosslinking of phenylboronic acid receptors as a means of glucose selective holographic detection, Biosens. Bioelectron. 21 (2006) 1838–1845.
[15] G.K. Samoei, W. Wang, J.O. Escobedo, X. Xu, H.-J. Schneider, R.L. Cook, R.M. Strongin, A chemomechanical polymer that functions in blood plasma with high glucose selectivity, Angew. Chem. Int. Ed. 45 (2006) 5319–5322.
[16] X. Yang, M.-C. Lee, F. Sartain, X. Pan, C.R. Lowe, Designed boronate ligands for glucose-selective holographic sensors, Chem. Eur. J. 12 (2006) 8491–8497.
[17] M. Lei, A. Baldi, E. Nuxoll, R.A. Siegel, B. Ziaie, A hydrogel-based implantable micromachined transponder for wireless glucose measurement, Diabetes Technol. Ther. 8 (2006) 112–122.
[18] X. Yang, X. Pan, J. Blyth, C.R. Lowe, Towards the real-time monitoring of glucose in tear fluid: holographic glucose sensors with reduced interference from lactate and pH, Biosens. Bioelect. 23 (2008) 899–905.
[19] M.V. Kuzimenkova, A.E. Ivanov, C. Thammakhet, L.I. Mikhalovska, I.Y. Galaev, P. Thavarungkul, P. Kanatharana, B. Mattiasson, Optical Responses, permeability and diol-specific reactivity of thin polyacrylamide gels containing immobilized phenylboronic acid, Polymer 49 (2008) 1444–1454.
[20] S. Tierney, S. Volden, B.T. Stokke, Glucose sensors based on a responsive gel incorporated as a Fabry–Perot cavity on a fiber-optic readout platform, Biosens. Bioelectron. 24 (2009) 2034–2039.
[21] S. Tierney, B.M.H. Falch, D.R. Hjelme, B.T. Stokke, Determination of glucose levels using a functionalized hydrogel-optical fiber biosensor: toward continuous monitoring of blood glucose in vivo, Anal. Chem. 81 (2009) 3630–3636.
[22] X. Huang, S. Li, J.S. Schultz, Q. Wang, Q.A. Lin, MEMS affinity glucose sensor using a biocompatible glucose-responsive polymer, Sens. Actuators B, Chem. 140 (2009) 603–609.

[23] O. Torun, F.C. Dudak, D. Bas, U. Tamer, I.H. Boyaci, Thermodynamic analysis of the interaction between 3-aminophenylboronic acid and monosaccharides for development of biosensor, Sens. Actuators B, Chem. 140 (2009) 597–602.
[24] G. Lin, S. Chang, H. Hao, P. Tathireddy, M. Orthner, J. Magda, F. Solzbacher, Osmotic swelling pressure response of smart hydrogels suitable for chronically-implantable glucose sensors, Sens. Actuators B, Chem. 144 (2010) 332–336.
[25] R. Badugu, J.R. Lakowicz, C.D. Geddes, Ophthalmic glucose sensing: a novel monosaccharide sensing disposable and colorless contact lens, Analyst 129 (2001) 516–521.
[26] J.T. Suri, D.B. Cordes, F.E. Cappuccio, R.A. Wessling, B. Singaram, Continuous glucose sensing with a fluorescent thin-film hydrogel, Angew. Chem. Int. Ed. 42 (2003) 5857–5859.
[27] K.E.S. Dean, A.M. Horgan, A.J. Marshall, S. Kabilan, J. Pritchard, Selective holographic detection of glucose using tertiary amines, Chem. Commun. 350 (2006) 7–3509.
[28] J. Yan, H. Fang, B. Wang, Boronolectins and Fluorescent Boronolectins: an examination of the detailed chemistry issues important for the design, Med. Res. Rev. 25 (2005) 490–520.
[29] K. Kataoka, H. Miyazaki, M. Bunya, T. Okano, Y. Sakurai, Totally synthetic polymer gels responding to external glucose concentration: their preparation and application in on-off regulation of insulin release, J. Am. Chem. Soc. 120 (1998) 12694–12695.
[30] S. Kitano, I. Hisamitsu, Y. Koyama, K. Kataoka, T. Okano, Y. Sakurai, Effect of the incorporation of amino groups in a glucose-responsive polymer complex having phenylboronic acid moieties, Polym. Adv. Technol. 2 (1991) 261–264.
[31] T.H. Kawasaki, H. Akanuma, T. Yamanouchi, Increased fructose concentrations in blood and urine in patients with diabetes, Diabetes Care 25 (2002) 353–357.
[32] S.K. Mujumdar, Ph.D. Thesis, University of Minnesota, 2008.
[33] I. Hisamitsu, K. Kataoka, T. Okano, Y. Sakurai, Glucose-responsive gel from phenylborate polymer and poly(vinyl alcohol): prompt response at physiological pH through the interaction of borate with amino group in the gel, Pharm. Res. 14 (1997) 289–293.
[34] P.J. Flory, Principles of Polymer Chemistry, Cornell University Press, Ithaca, New York, 1953.
[35] K. Dusek, W. Prins, Structure and elasticity of non-crystalline polymer networks, Adv. Poly. Sci. 6 (1969) 1–102.
[36] F. Horkay, I. Tasaki, P.J. Basser, Osmotic swelling of polyacrylate hydrogels in physiological salt solutions, Biomacromolecules 1 (2000) 84–90.
[37] F. Horkay, P.J. Basser, Osmotic observations on chemically cross-linked DNA gels in physiological salt solutions, Biomacromolecules 5 (2004) 232–237.
[38] D.W. Yin, F. Horkay, J.F. Douglas, J.J. De Pablo, Molecular simulation of the swelling of polyelectrolyte gels by monovalent and divalent counterions, J. Chem. Phys. 129 (15) (2008) (art. no. 154902).
[39] I.S. Han, M.-H. Han, J. Kim, S. Lew, Y.J. Lee, F. Horkay, J.J. Magda, Constant-volume hydrogel osmometer: a new device concept for miniature biosensors, Biomacromolecules 3 (2002) 1271–1275.
[40] G. Lin, S. Chang, C.-H. Kuo, J. Magda, F. Solzbacher, Free swelling and confined smart hydrogels for applications in chemomechanical sensors for physiological monitoring, Sens. Actuators B, Chem. 136 (2009) 186–195.
[41] H. Vink, Precision measurements of osmotic pressure in concentrated polymer solutions, Eur. Polym. J. 7 (1971) 1411–1419.
[42] R.P. Brown, Physical Testing of Rubber, second ed., Elsevier, New York, 1986.
[43] M. Mooney, The thermodynamics of a strained elastomer. I. General analysis, J. Appl. Phys. 19 (1948) 434–444.
[44] R.S. Rivlin, Torsion of a rubber cylinder, J. Appl. Phys. 18 (1947) 444–449.
[45] NIST Cold Neutron Research Facility. NG3 and NG7 30-meter SANS Instruments Data Acquisition Manual, January 1999.
[46] F. Horkay, A.M. Hecht, S. Mallam, E. Geissler, A.R. Rennie, Macroscopic and microscopic thermodynamic observations in swollen poly(vinyl acetate) networks, Macromolecules 24 (1991) 2896–2902.
[47] P. Tathireddy, M. Avula, G. Lin, S.-H. Cho, M. Guenther, V. Schulz, G. Gerlacah, J. Magda, F. Solzbacher, Smart hydrogel based microsensing platform for continuous glucose monitoring, in: IEEE Engineering in Medicine and Biology Conference (EMBC), Buenos Aires, Argentina, August 31–September 3, 2010.
[48] F. Horkay, M.-H. Han, I.S. Han, I.-S. Bang, J.J. Magda, Separation of the effects of pH and polymer concentration on the swelling pressure and elastic modulus of a pH-responsive hydrogel, Polymer 47 (2006) 7335–7338.
[49] P.-G. de Gennes, Scaling Concepts in Polymer Physics, Cornell, Ithaca, NY, USA, 1979.
[50] F. Horkay, A.M. Hecht, E. Geissler, Fine structure of polymer networks as revealed by solvent swelling, Macromolecules 31 (1998) 8851–8856.
[51] F. Horkay, G.B. McKenna, P. Deschamps, E. Geissler, Neutron scattering properties of randomly cross-linked polyisoprene gels, Macromolecules 33 (2000) 5215–5220.
[52] J.M. Prausnitz, R.N. Lichtenhaler, E.G. de Azevedo, Molecular Thermodynamics of Fluid-Phase Equilibria, third ed., Prentice Hall, Upper Saddle River, New Jersey, 1999, pp. 94–96.

Biographies

F. Horkay received his Ph.D. in chemistry (1978) from the Loránd Eotvos University (Budapest) and D.Sc. from the Hungarian Academy of Sciences. Prior to joining the National Institutes of Health in 1999, he was a senior research scientist at the Corporate Research and Development Center of the General Electric Corporation (Schenectady, NY, USA). His research interest is to understand the fundamental principles that govern molecular interactions and define structural hierarchy in complex synthetic and biopolymer systems, such as gels, self-assemblies and functional nanostructures. Since 2010 he is the Chair of the Polymer Networks Group, a worldwide organization of polymer physicists, chemists, biologists, materials scientists and engineers.

S.H. Cho is a graduate student in chemical engineering at the University of Utah. She received a B.S. degree in chemical engineering in 2004 from Han Yang University, and a M.S. degree in chemical engineering in 2006 from Han Yang University. Her research area is synthesis and testing of stimuli-responsive hydrogels.

P. Tathireddy received a Bachelor's degree in chemical technology from the Osmania University, Hyderabad, India in 1997. He was a project leader at Computer Maintenance Corporation Private Limited, Hyderabad, India till 1999. He received a Ph.D. degree in chemical engineering in June 2005 from University of Utah. He later joined the Microsystems Laboratory at the University of Utah as a post-doctoral fellow and worked in that position till 2007. He received a Fraunhofer fellowship award in 2007 and was posted as a guest scientist at the Fraunhofer Institute for Biomedical Engineering (IBMT), St. Ingbert, Germany. He currently holds a position as research assistant professor in the Department of Electrical & Computer Engineering at Utah. He has previously contributed to disciplines such as microfluidics and material characterization using impedance spectroscopy while his current research focuses on design, fabrication process development and testing of implantable medical microdevices or BioMEMs. This includes design and development of electronic packaging and new encapsulation techniques of medical devices for chronic use.

L. Rieth received his B.S. degree in materials science from The Johns-Hopkins University, Baltimore, MD, USA in 1994. He received his Ph.D. in materials science and engineering from the University of Florida, Gainesville, FL, USA in 2001. From 2001 to 2003, he was a post-doctoral research associate at the University of Utah, Salt Lake City, UT, USA and continued on at the University of Utah as a research assistant professor in materials science (2003–2005), and electrical and computer engineering (2004–present). His research is focused on deposition and characterization of thin film materials for sensors (chemical, physical, and biological), MEMS, BioMEMS, and energy production.

F. Solzbacher is Director of the Microsystems Laboratory at the University of Utah and an associate professor in electrical and computer engineering with adjunct appointments in materials science and bioengineering. His research focuses on harsh environment microsystems and materials, including implantable, wireless microsystems but also high temperature and harsh environment compatible micro sensors. Prof. Solzbacher received his M.Sc. EE from the Technical University Berlin in 1997 and his Ph.D. from the Technical University Ilmenau in 2003. He is co-founder of several companies such as I2S Micro Implantable Systems, First Sensor Technology and NFocus. He is Chairman of the German Association for Sensor Technology AMA, and serves on a number of company and public private partnership advisory boards. He is author of over 100 journal and conference publications, 5 book chapters and 13 pending patents.

J. Magda is a professor in chemical engineering and in materials science & engineering at the University of Utah. He received his B.S. in chemical engineering in 1979 from Stanford University, and his Ph.D. in chemical engineering and materials science in 1986 from the University of Minnesota in Minneapolis. His areas of interest include stimuli-responsive hydrogels and biomedical sensors for treatment of diabetes and obesity.

CHAPTER 3

EFFECT OF CHEMICAL COMPOSITION ON THE RESPONSE OF ZWITTERIONIC GLUCOSE SENSITIVE HYDROGELS STUDIED BY DESIGN OF EXPERIMENTS

Applied Polymer SCIENCE

Effect of Chemical Composition on the Response of Zwitterionic Glucose Sensitive Hydrogels Studied by Design of Experiments

Seung-Hei Cho,[1] Prashant Tathireddy,[2] Loren Rieth,[2] Jules Magda[1]
[1]Department of Chemical Engineering, University of Utah, Salt Lake City, Utah 84112
[2]Department of Electrical and Computer Engineering, University of Utah, Salt Lake City, Utah
Correspondence to: J. Magda (E-mail: magda@chemeng.utah.edu)

ABSTRACT: A stimuli-responsive hydrogel that contains the anionic monomer 3-acrylamidophenylboronic acid and the cationic monomer *N*-[3-(dimethylamino)propyl]acrylamide binds with cis-diol groups of glucose molecules selectively and reversibly. Even though such hydrogels have good selectivity for glucose, there are still remaining thresholds that should be overcome to enhance the sensitivity (swelling pressure response magnitude) and to reduce the response time (inverse of 1st order rate constant). In this study, the sensitivity and response time of zwitterionic glucose sensitive hydrogels (GSHs) were studied with three factor DOE analysis. The DOE results show that the molar ratio of 3-acrylamidophenylboronic acid/*N*-[3-(dimethylamino)propyl]acrylamide and the wt % of monomer in the pregel solution are the most important factors for enhancing the hydrogel sensitivity. In addition, fast response times can best be achieved by decreasing the molar ratio of cross-linker. The results of this study will be useful as guidelines for the optimal synthesis of glucose sensitive hydrogels. © 2014 Wiley Periodicals, Inc. J. Appl. Polym. Sci. **2014**, *131*, 40667.

KEYWORDS: biomedical applications; biomaterials; radical polymerization; synthesis and processing; stimuli-sensitive polymers

Received 15 January 2014; accepted 2 March 2014
DOI: 10.1002/app.40667

INTRODUCTION

A glucose sensor that responds reversibly and selectively to glucose has good biocompatibility, sufficient durability, and is small enough to be subcutaneously implanted can be used for real time continuous glucose monitoring. To satisfy these requirements, continuous glucose sensing (CGS) devices have been developed for both noninvasive and invasive systems. Noninvasive systems or semi-noninvasive systems use optical sensing methods such as scattering spectroscopy,[1] polarimetry,[2] Raman spectroscopy,[3] or fluorescence measurements.[4] In an invasive CGS system, a glucose sensor is implanted in certain areas of a body, for example, subcutaneously or intravenously. An implantable glucose sensor is capable of continuously measuring glucose concentration changes in any body fluid in real time.

Currently, one of the most promising recognition elements for use in an implantable glucose sensor is a glucose sensitive hydrogel (GSH) containing phenylboronic acid moieties because of its high biocompatibility, nontoxicity, and chemical stability. Pioneering studies on GSHs containing phenylboronic acid were performed by Kataoka et al.[5] This research group developed on/off insulin regulation systems that employed GSHs that swelled in response to increases in glucose concentrations in media solution.[5] However, the selectivity of the GSHs employed for binding of glucose relative to other simple sugars such as fructose, galactose, and mannose was poor.[6,7] In order to enhance selectivity to glucose, zwitterionic GSHs containing phenylboronic acid groups were developed.[8–11] When a zwitterionic GSH containing phenylboronic acid is exposed to an increase of glucose concentration in a media solution, it responds by shrinking rather than swelling. The explanation for this may be that glucose binds to two 3-acrylamidophenylboronic acid (3-APB) moieties within the GSH, thereby acting as a reversible cross-link,[10,12] or that glucose binding changes the structure of water hydrogen bonding in the solution surrounding the hydrogel.[13] In any case, zwitterionic GSHs shrink in response to an increase in glucose concentration and swell in response to an increase in fructose concentration.[10,12]

Although it is now clear that the most selective GSHs should be zwitterionic and contain both anionic 3-acrylamidophenylboronic acid (3-APB) and a cationic tertiary amine such as *N*-[3-(dimethylamino)propyl]acrylamide (DMAPAA), the precise ratio of the charged monomers that will optimize sensitivity and response time needs to be determined. Thus in this article, a statistics-based DOE technique was used to determine the best composition for a zwitterionic GSH with the minimum number of experimental samples. Statistical methods such as DOE have long been used in the industrial field to enhance reliability of products and to increase product

Table I. Comparison of Hydrogel Studies Utilizing DOE Methods

DOE study	Method	Response	Analysis Method
Stanojevic et al.[14]	2 factors and 3 levels Full factorial	Water absorption rate	RSM[18]
Pourjavadi et al.[16]	3 factors and 4 levels Taguchi method	Water absorption rate	ANOVA
Rodrigues et al.[17]	4 factors and 2 levels FFD method	Water absorption rate	ANOVA
Current study	1 factor with 2 levels, 2 factors with continuous levels	Pressure responseInverse of 1st order rate constant	ANOVA RSM[18]

yield subject to limitations in cost and time. However, there are only few papers that report the use of DOE techniques for the optimization of hydrogel/polymer synthesis in the research field.[14–17] Stanojevic et al. used a DOE technique to show that the water absorption rate of pH-sensitive hydrogels increases with increase in the amount of itaconic acid content, and with decrease in the amount of cross-linker.[14] Stanojevic et al. set up a full factorial experimental model with two factors and three levels, and analyzed the response, which in this case was the water absorption rate of the hydrogel, with response surface methodology. Response surface methodology (RSM) is used to determine the tendency of responses using a function which can be achieved from experimental data within the continuous range of variables.[18] DOE using the full factorial method is the best methodology for obtaining reliable results when the system has a small number of factors and levels, but the number of required experiments is excessively large when the system has many input factors and levels. Thus, for analysis of cases having many factors, abbreviated DOE methods have been used to reduce the total number of experiments without sacrifice of accuracy. For example, Pourjavadi et al. optimized the chemical composition of a superabsorbent hydrogel utilizing the Taguchi DOE method.[15,16] Through use of the Taguchi method, these authors greatly reduced the total number of samples. For example, they set up a system with three factors, and four levels. If the DOE had been run by full factorial analysis, the total number of experimental samples would have been 64. However, through use of the Taguchi method, the number of samples was reduced to 16, and the data was still reliable.[15,16] Rodrigues et al. used fractional factorial design (FFD) to find the main factors for composition optimization of an acrylic acid/chitosan base superabsorbent hydrogel.[17] Using FFD, they picked 10 cases from the 16 needed for full factorial analysis, and confirmed that the cross-linker concentration in the pregel solution was the most important factor for determining the water absorption rate.

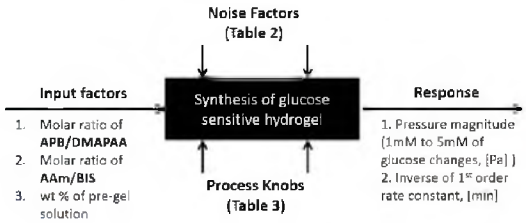

Figure 1. Schematic diagram of the DOE set up with factors that can affect the two outputs.

In this study, DOE was performed to study two types of responses such as swelling pressure and response time using three factors. Two levels were used for one of the factors, and continuously varying levels were used for the two remaining factors. In addition, process knobs and noise factors were strictly controlled in order to reduce errors due to unexpected environment factors. All hydrogel samples were synthesized by a UV polymerization method that is suitable for *in situ* synthesis on small devices. In Table I the different statistical methods are compared for published DOE studies of stimuli-responsive hydrogel composition.

EXPERIMENTAL

Materials

The monomers used for preparation of the gels and solvents were obtained as follows: acrylamide (AAM, Fisher Scientific), *N,N*-methylenebisacrylamide (BIS, Sigma-Aldrich), 3-acrylamidophenylboronic acid (3-APB, Frontier Scientific, Logan, UT), *N*-[3-(dimethylamino)propyl]acrylamide (DMAPAA, Polysciences), 2-hydroxy-4'-(2-hydroxyethoxy)−2-methyl propiophenone (HHMP, Sigma-Aldrich), 1-vinyl-2-pyrrolidinone (V-pyrol, Sigma-Aldrich), D(+)-glucose (Mallinckrodt Chemicals), dimethyl sulfoxide (DMSO, Sigma-Aldrich), 4-(2-Hydroxyethyl)-piperazine-1-ethanesulfonic acid (HEPES, Sigma-Aldrich), and Dulbecco's phosphate-buffered saline (1X PBS, Sigma-Aldrich).

Equipment

Equipment used included a UV lamp (BIB-150P 365nm, Spectroline®), a piezoresistive pressure transducer (EPX series,

Table II. Control Method of Noise Factors

Noise factor	Control method
Transducer variation	All test was performed with one sensor
Glucose concentration changes during experiment due to water evaporation	Test system was sealed to minimize water evaporation
Material contamination	Use fresh monomers for hydrogel synthesis
Synthesis module contamination	Use a fresh parylene coated glass module for each synthesis
Engineering variation	All experiments were obtained by one engineer

Table III. Controlled Value of Process Knobs

Process knob	Value
Synthesis environment	Ar
UV exposure time	3 minutes
UV intensity	10 mW/cm^2
Hydrogel mold thickness	400 μm
Hydrogel conditioning	After washing with DIW, GSH was washed by 1X PBS and 1/3X PBS three times. Sample was stocked in 1X PBS at room temperature
Initial loading pressure	20K Pa

Table IV. Design Factors

Factors	Level	Minimum limitation	Maximum limitation
APB/DMAPAA	Continuous	0.4	5
AAm/BIS	Continuous	7	160
Wt %	discrete	13 (1st level)	30 (2nd level)

Measurement Specialties™), and a data acquisition/switch unit (34970A, Agilent Technologies). Infrared spectroscopy was performed using an ATR-IR spectrometer (iS10, Thermo Scientific), and the DOE software used was JMP 11[24,25] (design of experiment software, SAS Institute, Cary, NC).

DOE

As shown schematically in Figure 1, experiments were designed with consideration of input factors, noise factors, and process knobs that could affect the output. Synthesized GSHs were evaluated by two types of outputs, namely the swelling response magnitude (Pa), and the inverse of 1st order rate constant (min). The chosen input factors were the monomer concentration of the pregel solution, the molar ratio of the two charged monomers 3-APB and DMAPAA, and the mole ratio of the uncharged monomer (acrylamide, AAm) to the cross-linker (*N,N*-methylenebisacrylamide, BIS). Anticipated noise factors were controlled to minimize environment interferences (Table II). Process knobs were also fixed and controlled (Table III).

Factors that affect the sensitivity, selectivity, and response time of glucose sensitive hydrogels are monomer concentration of the pregel solution and copolymer hydrogel composition. Lin et al. previously optimized the swelling response magnitude of GSHs with respect to the mole ratios of the monomers AAm, 3-APB, DMAPAA, and BIS (cross-linker) prepared by free radical polymerization method with redox initiator.[7] Unfortunately, GSH response time was so long that pressure transducer baseline drift may have been substantial. To address this issue, design of experiment (DOE) was set up for GSHs prepared with the same monomers but with both response magnitude and response time used as DOE outputs. The upper and lower limits of the input factors was empirically determined (Table IV). For example, the molar ratio of AAm/BIS used cannot be greater than 160 because this gives a synthesized hydrogel that is too mechanically weak. After choosing the input factor limits, DOE software (JMP 11[24,25]) was used to choose the 12 different GSH samples synthesized (Table V).

Synthesis of Glucose Sensitive Hydrogels

Glucose sensitive hydrogels were synthesized by a UV activated free-radical crosslinking copolymerization process that can be adapted to *in situ* polymerization on micro-fabricated sensors. The free radical initiator used was HHMP/V-pyrol, which can be activated by UV at 365 nm. All monomers were dissolved in the 10 wt % DMSO/HEPES solvent, after which the solution was purged with Ar gas for 10 min. The synthesis mold was also purged with Ar gas for 10 min. Mold thickness was controlled with a 400 μm Teflon spacer. The pregel solution was injected into the synthesis mold and then the transparent mold was exposed to UV at 365 nm for 3 min (Table III). Synthesized

Table V. List of Synthesized Hydrogel Samples Chosen by DOE and Responses

Sample	APB/DMAPAA (mole/mole)	AAm/BIS (mole/mole)	wt % Pregel solution	Magnitude (Pa)	Inverse of 1st order rate constant (min)
G041613	0.4	160	13	1527 (±35)	35 (±2)
G042513	0.4	25	13	6149 (±230)	71 (±8)
G081630	0.8	160	30	3051 (±220)	42 (±7)
G080713	0.8	7	13	2736 (±240)	163 (±16)
G082013	0.8	20	13	2994 (±130)	147 (±5)
G082530	0.8	25	30	17043 (±1670)	153 (±3)
G084013	0.8	40	13	5006 (±380)	73(±3)
G134013	1.25	40	13	5402 (±740)	114 (±13)
G161213	1.6	12	13	4310 (±450)	76 (±12)
G251613	2.5	160	13	0	none
G254013	2.5	40	13	6934 (±580)	69 (±2)
G502530	5	25	30	2491 (±150)	104 (±20)

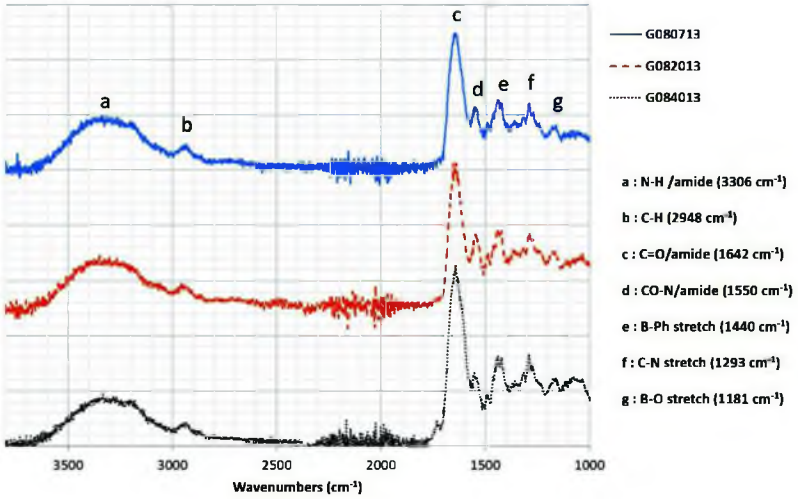

Figure 2. ATR-IR spectra of dried glucose sensitive hydrogels. [Color figure can be viewed in the online issue, which is available at wileyonlinelibrary.com.]

hydrogels were washed first with distilled water, and then they were washed three times with PBS buffer (Table III).

Response Measurement

Hydrogel swelling pressure response was measured for a glucose concentration change between 1 m*M* and 5 m*M* in 1X PBS buffer, because the normal fasting blood glucose level is ≈3.8 to 5.5 m*M*. Swelling pressure response was measured with a piezoresistive pressure transducer.[7,11,19] Glucose responsive hydrogels react to glucose in the surrounding environment by either swelling or deswelling. If the hydrogel is in a confined space in between a rigid porous membrane and a piezoresistive diaphragm, the swelling pressure change results in a mechanical pressure change which is transduced into a measurable voltage. The time-dependent value of this voltage was captured on a PC using the Agilent data acquisition system.

Reaction Kinetics of Glucose Sensitive Hydrogels

As in previous studies,[7] it was found that the time-dependent swelling response of the stimuli-responsive hydrogels could be fit with the first-order kinetic model of Quintana,[26] as given below:

$$\frac{d[P]}{dt} = k_1[P_\infty - P] \quad (1)$$

P: Time-dependent pressure measured with a piezoresistive pressure transducer ≡ [Pa]

P_∞: Pressure measured with a piezoresistive pressure transducer after equilibrium is reached after a glucose concentration change ≡ [Pa]

k_1: Proportionality constant between swelling rate and the swelling capacity ≡ (time^{-1})

The inverse of the first order rate constant was used as a measure of response time.

RESULTS AND DISCUSSION

Characterization of Hydrogels by ATR-IR

Glucose sensitive hydrogels were synthesized using eleven different pregel solution compositions (Table V), and then were characterized by ATR-IR in order to confirm the actual chemical composition within the hydrogels after

Table VI. Comparison of Estimated Ratio and IR Absorbance Ratio of Functional Groups

	C—N stretch from amide groups		B—O stretch from APB		CO-N from AAm, and BIS amides		C=O	
Sample	Pregel	IR[a]	Pregel	IR[b]	Pregel	IR[c]	Pregel	IR[d]
G080713	1.34	1.39	2.00	2.00	1.00	1.00	1.00	1.00
G082013	1.04	1.06	1.00	1.24	1.19	1.16	1.19	1.08
G084013	1.00	1.00	1.00	1.18	1.17	1.15	1.17	1.04

Pregel: estimated value from monomer composition of pregel solution.
[a] C—N stretch from amide and amine groups (relative absorbance ratio of *f*).
[b] B—O stretch from boronic acid group (relative absorbance ratio of *g*/*e*).
[c] CO—N from amide groups (AAm, BIS) (relative absorbance ratio of *d*/*b*).
[d] C=O (relative absorbance ratio of *c*/*b*).

Table VII. Evaluation of Input Factors

	P-values	
Parameters	Response magnitude	Inverse of 1st order rate constant
The ratio of APB/DMAPAA	0.037	0.23
The ratio of AAm/BIS	0.081	0.012
wt % Pregel solution	0.002	0.18

polymerization. Figure 2 shows the ATR-IR spectra of samples G080713, G082013, and G084013. The absorption peaks were identified using Ref. 22. According to Beer's Law, the chemical composition can be estimated by comparison of the absorbance ratio of the functional groups' peaks.[20,21,23] By comparison of IR absorbance ratio of functional group peaks from DMAPAA, APB, and BIS, the chemical composition of the hydrogel can be compared with the chemical composition of the pregel solution. Table VI shows that IR absorbance ratio exhibits the same trends as the molar ratio of pregel solution.

Determination of Contributive Factors by ANOVA

For each of the eleven different GSH compositions, experimental results for the swelling response magnitude (P_a) and the inverse of 1st order rate constant (min) are given in Table V. The main contributive factors for these two responses were determined from *P*-values that were estimated by Analysis of Variance (ANOVA, Table VII), with significant factors corresponding to *P*-values < 0.05 (ANOVA stats with null hypothesis. A value for *P* less than 0.05 implies that the response tendency depends on the variable studied). The results in Table VII show that the molar ratio of 3-APB/*N*-[3-(dimethylamino)propyl]acrylamide and the wt % of monomer in the pregel solution are the most important factors for enhancing the hydrogel sensitivity, and that a fast response times can best be achieved by decreasing the molar ratio of cross-linker. The results of the statistical analysis are summarized by the following equations for predicting response magnitude and response time obtained using JMP 11[24,25] [constant A: (APB/DMAPAA-2.7)/2.3, B: (AAm/BIS-83.5)/76.5, & C: (wt % −21.5)/8.5].

Magnitude estimation equation:

$$Y = 3286 - 4577A - 6906B - 571C - 2661(A \times B) - 5426(A \times C) - 3221(B \times C) \quad (2)$$

Inverse of 1st order rate constant estimation equation:

$$Y = 490 + 436A + 556B + 23C + 681(A \times B) + 57(A \times C) - 56(B \times C) \quad (3)$$

In leverage plots (Figures 3 and 4), the distance from dots and the blue dash corresponds to expected residual value when the effect is removed. Red dash lines are showing significance at *P*-value < 0.05 level. Thus, when two dash lines are cross each other, the data points should be meaningful.

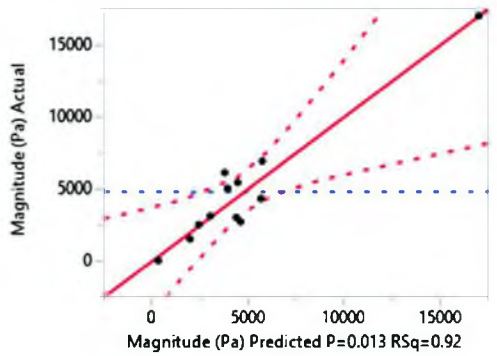

Figure 3. Leverage plot of response magnitude (Rsquared value: 0.92). Red line: predicted value (eq. (2)), black points: actual value, red dash: significance, and blue dash: anticipated residual when the effect is removed. [Color figure can be viewed in the online issue, which is available at wileyonlinelibrary.com.]

Sensitivity Control Factor

The surface plot from statistical analysis (Figure 5) shows that enhanced sensitivity of zwitterionic GSHs was achieved by increase of either the molar ratio of 3-APB/DMAPAA or of the pregel solution monomer concentration. The best sensitivity of zwitterionic GSHs in the DOE set was achieved when the ratio of 3-APB/DMAPAA was 0.8 (with fixed AAm/BIS = 25, and pregel monomer wt % = 30, sample G082530) in IX PBS (pH = 7.4). However, a drop in sensitivity is observed in Figure 5 at the highest values of the molar ratio of 3-APB/DMAPAA studied (above 2.5). This can probably be explained as follows. An increase in the ratio initially increases the sensitivity of the GSH by increasing the number of boronic acid groups that reversibly bind to glucose. However, if the ratio becomes too large, then the fraction of boronic acid groups that are charged probably decreases because the mole ratio of cationic tertiary amines becomes too small. The function of the

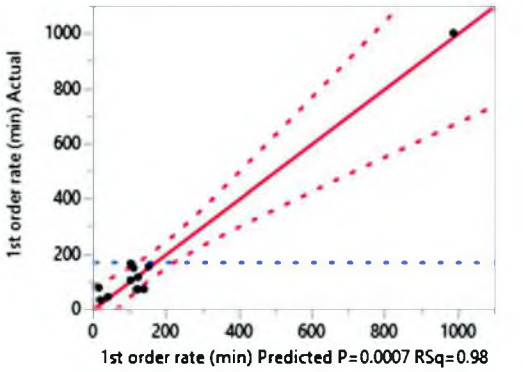

Figure 4. Leverage plot of inverse of 1st order rate constant (Rsquared value: 0.98). Red line: predicted value (eq. (3)), black points: actual value, red dash: significance, and blue dash: anticipated residual when the effect is removed. [Color figure can be viewed in the online issue, which is available at wileyonlinelibrary.com.]

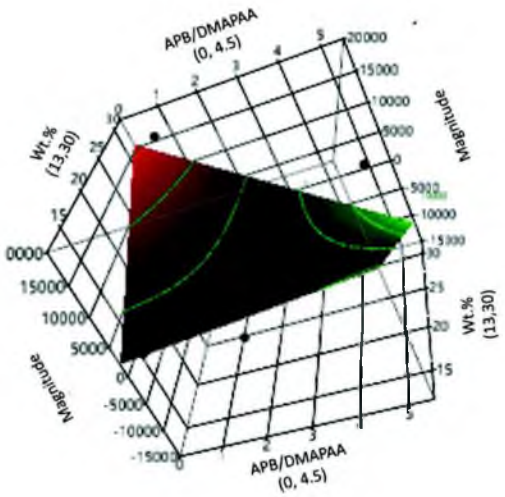

Figure 5. Surface plot of response magnitude to the glucose concentration change in 1X PBS buffer (from 1 to 5 m*M*) vs. the molar ratio of 3-APB/DMAPAA and wt % of pregel solution (dot: actual data points). [Color figure can be viewed in the online issue, which is available at wileyonlinelibrary.com.]

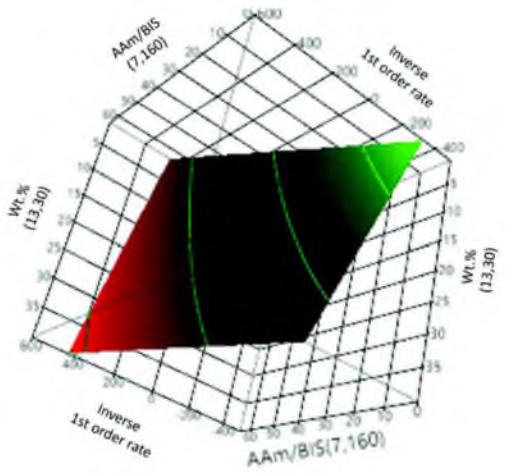

Figure 7. Surface plot of inverse of 1st order rate constant to the glucose concentration change in 1X PBS buffer (from 1 to 5 m*M*) vs. the molar ratio of AAm/DMAPAA and wt % of pregel solution (dot: actual data points). [Color figure can be viewed in the online issue, which is available at wileyonlinelibrary.com.]

cationic tertiary amines is to increase the acidity of neighboring boronic acid groups. In addition, an increase in the monomer concentration in the solution used to synthesize GSHs from 13 wt % to 30 wt % increases the glucose sensitivity of the GSH when the chemical composition is fixed. This can be explained by the increase that occurs in the amount of glucose-binding moieties per unit volume in gels synthesized from pregel solutions containing higher monomer concentrations. In support of this idea, Figure 6 shows that the water content of GSHs synthesized from pregel solutions containing 30 wt % of monomer is lower than the water content of GSHs synthesized from presolutions containing 13 wt % of monomer, which implies that the polymer weight fraction and the number of glucose-binding moieties per unit volume in the synthesized gel is larger. This explains why the glucose response magnitude is larger for GSHs synthesized from solutions containing 30 wt % monomer than from GSHs synthesized from 13 wt % monomer.

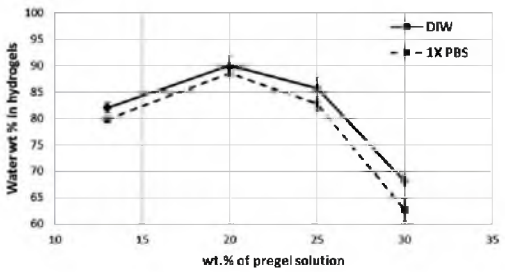

Figure 6. Water wt % of synthesized hydrogels vs. wt % of pregel solution (circles: gel swollen in DIW, squares: gel swollen in 1X PBS).

Response Time Control Factor

The surface plot from statistical analysis (Figure 7) shows that a reduced response time for zwitterionic GSHs can be achieved by decreasing the crosslinker mole ratio AAm/BIS. This is reasonable because the entanglement spacing of the hydrogel network increases with decrease in the density of crosslinks, making it easier for glucose to diffuse into the gel, and also reducing the viscoelastic response time. However, if the chosen amount of cross-linker is too small, the hydrogel is likely to lose mechanical integrity in long-term applications. For our sensor design, in which the hydrogel was confined between a porous steel mesh and a piezoresistive diaphragm, we found that a mole ratio of AAm/Bis of 40 or less was necessary to obtain sufficient mechanical strength for a reversible response.

CONCLUSIONS

Experiments chosen and analyzed using DOE methods show that the molar ratio of 3-APB/DMAPAA and the monomer wt % of the pregel solution are the dominant factors that determine the magnitude of response of zwitterionic GSHs to an increase in glucose concentration from 1 to 5 m*M*. The best glucose sensitivity was achieved when the ratio of 3-APB/DMAPAA was increased from 0.4 to 2.5 in 1X PBS with fixed values of other factors. In addition, GSHs synthesized from 30 wt % pregel solutions show better glucose sensitivity than GSHs synthesized from pregel solutions containing 13 wt % monomer. DOE statistical analysis of experiments also shows that the molar ratio of AAM/BIS is the primary factor for determining the value of the inverse of 1st order rate constant in this study. Faster glucose responses can be obtained by decreasing the amount of cross-linker (BIS). The results of this study will be useful for the design of an implantable continuous glucose sensor that employs zwitterionic GSHs.

REFERENCES

1. Heinemann, L.; Krämer, U.; Klötzer, H.; Hein, M.; Volz, D.; Heise, T.; Rave, K. *Diabetes Technol. Ther.* **2000**, *2*, 211.
2. Cameron, B. D.; Anumula, H. *Diabetes Technol. Ther.* **2006**, *8*, 156.
3. Dieringer, J. A.; McFarland, A. D.; Shah, N. C.; Stuart, D. A.; Whitney, A. V.; Yonzon, C. R.; Young, M. A.; Zhang, X.; Van Duyne, R. P. *Faraday Discuss.* **2006**, *132*, 9.
4. Mansouri, S.; Schultz, J. S. *Biotechnology* **1984**, *2*, 885.
5. Hayakawa, Y.; Kataoka, M. *J. Am. Chem. Soc.* **1998**, *120*, 12694.
6. Gu, Y. Ph.D thesis, Swelling Properties of Phenylboronic Acid-containing Hydrogels and Their Application in Microfluidic Drug Delivery Devices, University of Minnesota, **2003**.
7. Lin, G.; Chang, S.; Hao, H.; Tathireddy, P.; Orthner, M.; Magda, J.; Solzbacher, F. *Sens. Actuators B Chem.* **2010**, *144*, 332.
8. Horgan, A.; Marshall, A.; Kew, S.; Dean, K.; Creasey, C.; Kabilan, S. *Biosen. Bioelectron.* **2006**, *21*, 9, 1838.
9. Yang, X.; Pan, X.; Blyth, J.; Lowe, C. *Biosens. Bioelectron.* **2008**, *23*, 6, 889.
10. Tierney, S.; Volden, S.; Stokke, B. *Biosens. Bioelectorn.* **2009**, *24*, 7, 2034.
11. Lin, G.; Chang, S.; Kuo, C. H.; Magda, J.; Solzbacher, F. *Sens Actuators B Chem.* **2009**, *136*, 186.
12. Alexeev, V. L.; Sharma, A.; Goponenko, A.; Das, S.; Wilcox, C.; Finegold, D.; Asher, S. *Analy. Chem.* **2003**, *75*, 2316.
13. Horkay, F.; Cho, S.; Tathireddy, P.; Reith, L.; Solzbacher, F.; Magda, J. *Sens Actuators B Chem.* **2011**, *160*, 1, 1363.
14. Stanojevic, M.; Krusic, M. K.; Filipovic, J.; Parojcic, J.; Stupar, M. *Drug Deliv.* **2006**, *13*, 1.
15. Pourjavadi, A.; Salimi, H.; Amini-Fazl, M. S.; Kurdtabar, M.; Amini-Fazi, A. R. *J. Appl. Polym. Sci.* **2006**, *102*, 4878.
16. Pourjavadi, A.; Soleyman, R.; Bardajee, G. R.; Ghavami, S. *Bull. Korean Chem. Soc.* **2009**, *30*, 11, 2680.
17. Rodrigues, F.; Pereira, A.; Fajardo, A.; Muniz, E. *J. Appl. Polym. Sci.* **2013**, 3480.
18. Bradley, N. Ph.D. thesis, The response surface methodology, Indiana University of South Bend, **2007**.
19. Guenther, M.; Gerlach, G.; Wallmersperger, T.; Avula, M. N.; Cho, S. H.; Xie, X.; Devener, B. V.; Solzbacher, F.; Tathireddy, P.; Magda, J. J.; Scholz, C.; Obeid, R.; Armstrong, T. *Adv. Sci. Technol.* **2013**, *85*, 47.
20. Mathias, L. J.; Hankins, M. G.; Bertolucci, C. M.; Grubb, T. L.; Muthiah, J. *J. Chem. Edu.* **1992**, *69*, 8, A217.
21. McKelvy, M. L.; Britt, T. R.; Davis, B. L.; Gillie, J. K.; Graves, F. B.; Lentz, L. *Analy. Chem.* **1998**, *70*, 119R.
22. Pavia, D. L.; Lampman, G. M.; Kriz, G. S. Introduction to Spectroscopy: A Guide for Students of Organic Chemistry, 3rd ed.; Brooks/Coles: Fort Worth, Texas, 2001.
23. Faniran, J. A.; Shurvell, H. F. *Can. J. Chem.* **1968**, *46*, 2089.
24. Sall, J.; Lehman, A.; Stephens, M.; Creighton, L. JMP Start Statistics: A Guide to Statistics and Data Analysis Using JMP, 5th ed.; SAS Institute (ISBN 978-1-61290-307-1, electronic book), 2012.
25. Smith, M. Medical Malpractice: Descriptive Statistics, Graphics, and Exploratory Data Analysis, SAS Institute.
26. Quintana, J. R.; Valderruten, N. E.; Katime, I. *Langmuir* **1999**, *15*, 4728.

CHAPTER 4

EFFECT OF GAMMA RAYS AND NEUTRON IRRADIATION ON THE GLUCOSE RESPONSE OF BORONIC ACID CONTAINING "SMART" HYDROGELS

Reprinted from, Polymer Degradation and Stability, 99, Jules Magda, Seung-Hei Cho, Seth Streitmatter,Tatjana Jevremovic, Effects of gamma rays and neutron irradiation on the glucose response of boronic acid-containing "smart" hydrogels, 219-222, 2014, with permission from Elsevier.

Medical products must be sterilized completely to prevent infection by microorganisms, such as bacteria, viruses and fungi. Various sterilization methods are used because the appropriate sterilization procedure depends on the material composition of the medical products (Table 4.1). For example, high temperature steam sterilization cannot be used for products made of thermoplastic polymers, such as polyimide and polycarbonate. Gamma radiation sterilization is commonly used for pharmaceutical and medical devices because it can ionize material by initiating chemical reactions at any temperature, pressure or phases without using additional chemicals. Gamma rays can even be used for packaged products because of their ability to penetrate packing material. This reduces the number of steps in the packaging process. Gamma rays are emitted by Cobalt-60 (^{60}Co) or Cesium-137 (^{137}Cs). The ^{60}Co is produced in nuclear power reactors by irradiation of ^{59}Co with fast neutrons (equation 4.1, [20]). Because ^{60}Co is unstable following neutron capture, it decays to ^{60}Ni by emitting a photon, which ionizes the target material.

$$_{27}Co^{59} + n^{1} \rightarrow {}_{27}Co^{60} \tag{4.1}$$

However, it has been reported that gamma radiation affects the chemical structure of polymers, such as poly(vinyl chloride), poly(methyl methacrylate) and polycarbonate, by changing their crosslinking structure [22]. The crosslinking network can be more increased or scission of the network can occur because gamma rays reactivate radical polymerization [21]. Thus, a study of polymer degradation by gamma irradiation is required before the development of new medical devices. Therefore, the effects of gamma irradiation on zwitterionic glucose-responsive hydrogels was studied, and the results will be discussed in this chapter.

Table 4.1 Classification of sterilization methods (adapted from [19])

Method	Control factors	Subjects	Mechanism
Autoclave	• Temperature (126-138 °C) • Pressure (~ 3 atm) • Time (~15 min)	High temperature resistant material	Irreversible denaturation of protein by water steam
Dry-heat sterilization	• Temperaure (160-180 °C) • Time (~180 min)	Nonaqueous high temperature resistant material	Oxidation of cell constituents
Filtration	• Filter pore size (< 0.22 um) • Filter material	Thermo labile solution	Filtering
Radiation	• Radiation dose (gamma radiation: 25 KGy)	Active ingredients, Drug products, Medical devices	Ionization of molecules in microorganisms
Gas (Ethylene Oxide)	• Concentration of gas • Humidity • Time • Temperature	Thermoplastics	Alkylation of cell constituents

In addition, the effect of neutron irradiation on hydrogels was also studied for the boron neutron capture therapy (BNCT) application. BNCT was developed for localized brain cancer treatment. Irradiated ^{10}B, which is ^{11}B, by neutrons produces alpha particles and ^{7}Li recoil nuclei. Cancer cells are killed by the fission products of ^{11}B. The zwitterionic glucose-responsive hydrogels can be used as boron carriers with minor modifications. The neutron irradiation effect study was performed to examine the possibility of applying hydrogels to BNCT.

Polymer Degradation and Stability 99 (2014) 219–222

Contents lists available at ScienceDirect

Polymer Degradation and Stability

journal homepage: www.elsevier.com/locate/polydegstab

Effects of gamma rays and neutron irradiation on the glucose response of boronic acid-containing "smart" hydrogels

Jules Magda [a,*], Seung-Hei Cho [a], Seth Streitmatter [b], Tatjana Jevremovic [a,b]

[a] Department of Chemical Engineering, University of Utah, Salt Lake City, UT 84112, USA
[b] University of Utah Nuclear Engineering Program (UNEP), Salt Lake City, UT 84112, USA

ARTICLE INFO

Article history:
Received 27 August 2013
Accepted 1 November 2013
Available online 12 November 2013

Keywords:
Hydrogels
Gamma rays
Stimuli-responsive
Boron neutron capture therapy
Nuclear reactor
Glucose

ABSTRACT

If a biomaterial is to be implanted in the body, it must be subjected to a sterilization procedure which often involves gamma irradiation. We report results for the effects of γ-irradiation on the glucose response of a hydrogel with glucose-binding boronic acid moieties. This 'smart" hydrogel is of a type suitable for use in non-enzymatic glucose sensors. In addition, the effect of neutron irradiation on the glucose response of these hydrogels is also of interest, because the hydrogels could be used with minor modification to deliver boron to tumors during boron neutron capture therapy (BNCT). We show that the glucose response of the smart hydrogels is unaffected by exposure to neutrons in the dose range typical for BNCT. The effect of gamma rays on the glucose response depends on the method used to cure the smart hydrogel. If the hydrogel is cured with a thermal free-radical-initiator, then the hydrogel can be sterilized by gamma irradiation with no adverse effects upon the glucose response. However, if the hydrogel is cured with a UV-initiated free radical initiator, then the glucose response decreases in magnitude with increase in the gamma radiation dose.

1. Introduction

Radiation sterilization is a common means of microbial control and sterilization for single-use bioprocess systems and devices [1]. Gamma irradiation is the application of electromagnetic radiation emitted from radionuclides such as Cobalt 60 or Cesium 137 isotopes. This ionizing radiation damages the nucleic acids of microorganisms, and leaves no residual radioactivity within the biomaterial or device. In order to satisfy the sterility assurance level of the United States Pharmacopeia, the recommended gamma dose is 25.7 kGy or larger [1].

Boron neutron capture therapy (BNCT) is a treatment protocol for cancer in which non-radioactive boron atoms (isotopic ^{10}B) are delivered to tumors and then exposed to thermal neutrons, such as those produced by nuclear reactors [2]. The resultant fission reactions produce short-ranged alpha-particles that destroy all cells located within 10 μm of the ^{10}B nuclei. Currently, low molecular weight pharmaceuticals such as boronophenylalanine (BPA) or sodium borocaptate (BSH) are used to deliver ^{10}B nuclei to the site of a tumor. However, because the concentration of ^{10}B nuclei that can be delivered by BPA or BSH to tumor cells is limited to about 100 ppm, there is interest in increasing BNCT therapeutic effectiveness by using high molecular weight delivery agents that contain multiple boron atoms such as polymers, dendrimers, or micelles [3].

One possible type of high molecular weight agent for delivering high concentrations of boron atoms to tumors is a polymer hydrogel nanoparticle containing the monomer 3-acrylamido phenylboronic acid (3-APB), as synthesized by precipitation polymerization [4]. A hydrogel of this type is also glucose-responsive, meaning that it has a degree of equilibrium swelling that reversibly changes in response to the environmental glucose concentration [5–8], and thus can be used in a wireless non-enzymatic glucose sensor when coupled with a suitable transduction mechanism [7]. The hydrogel is glucose responsive because the phenylboronic acid moieties present in the hydrogel reversibly bind to glucose molecules. Enzymatic glucose-responsive hydrogels, on the other hand, employ the enzyme *glucose oxidase* to bind glucose, and cannot be exposed to sterilization protocols involving gamma irradiation, because the gamma rays will degrade the enzyme. Hence the first aim of the current study is to determine whether or not glucose-responsive hydrogels that employ phenylboronic acid moieties to reversibly bind glucose can be subjected to γ-sterilization without loss of glucose sensitivity. The second aim of the current study is to

* Corresponding author. 50 S Central Campus Dr, Rm 3290, University of Utah, Salt Lake City, UT 84112, USA. Tel.: +1 801 581 7536; fax: +1 801 585 9291.
E-mail address: jj.magda@utah.edu (J. Magda).

0141-3910/$ – see front matter © 2013 Elsevier Ltd. All rights reserved.
http://dx.doi.org/10.1016/j.polymdegradstab.2013.11.002

determine whether or not the same hydrogel retains its glucose sensitivity when subjected to simultaneous irradiation by both thermal neutrons and gamma rays, at the relative dose levels expected to be present during BNCT. In previous studies, the effect of gamma sterilization on the water content, swelling pressure, or drug release rate from polymer hydrogels has been studied Fernandez-Carballido et al. [9], Kanjickal et al. [10], Elijarrat-Binstock et al. [11], and Guenther et al. [12]. Generally, γ-irradiation is found to be less disruptive to hydrogel properties than competing sterilization technologies, particularly when γ–irradiation is performed on freeze-dried samples at lower temperatures [9,11]. Nonetheless, ESR [13] and ATR-FTIR measurements [14] clearly show that γ-irradiation produces free radicals which may either degrade covalent bonds such as amides [14] or induce chemical crosslink formation [15]. As far as we know, there have been no previous reports of the effects of γ-irradiation on boronic acid-containing smart hydrogels, nor of the effects of neutron irradiation on any type of hydrogel.

2. Materials and methods

2.1. Materials and hydrogel synthesis

The monomers used for preparation of the gels were obtained as follows: acrylamide (AAM, Fisher Scientific), *N,N*-methylenebisacrylamide (BIS, Sigma–Aldrich), 3-acrylamido phenylboronic acid (3-APB, Frontier Scientific, Logan, UT, USA), and *N*-(3-dimethylaminopropyl acrylamide) (DMAPAA). The monomers were used as received. 2-hydroxy-4'-(2-hydroxyethoxy)-2-methyl propiophenone (HHMP, Sigma–Aldrich), 1-vinyl-2-pyrrolidinone (V-pyrol, Sigma–Aldrich), N,N,N′,N′-tetramethylethylenediamine (TEMED; Sigma–Aldrich), ammonium persulfate (APS; Sigma–Aldrich), D(+)-glucose (Mallinckrodt Chemicals), dimethyl sulfoxide (DMSO, Sigma–Aldrich), 4-(2-Hydroxyethyl)piperazine-1-ethanesulfonic acid (HEPES, Sigma–Aldrich), and Dulbecco's phosphate-buffered saline solution (1X PBS, Sigma–Aldrich) were also used as received.

A pre-gel solution was formed by gentle stirring at room temperature of the monomers AAM, DMAPAA, 3-APB, and BIS in the mole ratio 80:10:8:2, respectively in the mixed solvent HEPES buffer/DMSO. The amount of solvent in the pre-gel solution was 20 wt%; the amount of free radical initiator was 2 wt%. This is the same monomer composition that has previously been used with different free-radical initiators to prepare glucose-responsive hydrogels for use in glucose sensors [7,8]. In the current study, for gels that were thermally cured (12 h at 25 °C), we used APS and TEMED as the free-radical initiator and reaction accelerator, respectively. For gels that we cured by UV irradiation (3 min of UV exposure at wavelength 365 nm), we used HHMP as the free-radical initiator [16,17]. In order to enhance HHMP solubility, an amount of V-pyrol equal to 10 mol% of the HHMP was also added to the pre-gel solution. For both thermal and UV curing, monolithic gel films were synthesized by injecting the monomer solution into a mold of thickness 400 μm and then initiating free-radical crosslinking copolymerization [5,6]. After curing, the gels were washed multiple times in deionized water and PBS buffer to remove residual monomer and initiator. Precipitation polymerization [4] can be used in the future to prepare hydrogel nanoparticles of the same composition for use in BNCT. However, hydrogels that are monolithic films are more convenient for material characterization, as needed in the current study. These hydrogels have been shown to contain about 90% water at physiological pH and ionic strength [7,8], and hence about 10,000 ppm by wt. of boron, based on the nominal monomer composition.

2.2. Exposure of smart hydrogels to thermal neutrons and/or gamma rays

Hydrogels synthesized by both thermal and UV curing methods were placed in separate glass vials containing PBS buffer and were irradiated at room temperature with gamma rays emitted from a J.L. Shephard Mark I ^{137}Cs irradiator in the Department of Pathology at the University of Utah School of Medicine. Gamma doses ranged from 70 Gy to 25.7 kGy, as calculated using a conversion factor of 10 mGy/R in water. Note that for each dose value, a separate hydrogel sample (from the same synthesis batch) was employed. In order to simulate BNCT conditions, hydrogels synthesized by both thermal and UV curing methods in separate polypropylene microcentrifugation tubes containing deionized water were placed for 30 min in the University of Utah TRIGA Reactor (UUTR) operating at 90 kW. Different vials were placed within the thermal neutron irradiation (TI) port, and within the fast neutron (FNIF) irradiation port. Table 1 shows the doses of both neutrons and gamma rays in the TRIGA reactor, as calculated by the Monte Carlo simulation code MCNPX [18].

2.3. Measurement of hydrogel glucose response

Hydrogels with the compositions described above are already known to be glucose-responsive hydrogels that shrink with increase in the environmental glucose concentration at fixed pH and ionic strength [7,8]. This apparently occurs because an increase in the environmental glucose concentration increases the fraction of negatively charged boronic acid moieties within the hydrogel, thereby changing the structuring of water molecules within the hydration sphere surrounding the hydrogel [8]. As in Lin et al. [6], the variation in hydrogel osmotic swelling pressure with change in glucose concentration was measured by placing the hydrogel film in a "macrosensor". The macrosensor consists of an off-the-shelf piezoresistive pressure transducer (Endevco model 8510B-2, San Juan Capistrano, CA, USA, full-scale pressure 2 psig) with a cylindrical stainless steel sensing area (diameter 3.2 mm) that is completely covered with the hydrogel film (thickness ≈ 400 μm). The hydrogel is held in place with a cap having a top surface that consists of a rigid porous membrane through which mass transfer occurs. Glucose response tests were performed by placing the macrosensor in a well-stirred temperature-controlled continuous-flow test platform that allows us to vary the glucose concentration of the aqueous environment without handling the sensor. The environmental glucose concentration was varied at room temperature between zero and 5.0 mM (the normal physiological value) at a fixed pH of 7.4 and at a fixed ionic strength of 150 mM. The change in hydrogel osmotic swelling pressure with change in environmental glucose concentration was detected as a change in the mechanical pressure measured by the pressure transducer. Measurements were performed on hydrogels from the same synthesis batch both before and after exposure to radiation.

3. Results

3.1. Effect of gamma irradiation

Fig. 1 shows the time dependence of the glucose response for a UV-cured hydrogel, both before and after exposure to gamma rays

Table 1
Hydrogel doses in TRIGA reactor.

Irradiation port	Neutron dose (kGy)	Gamma dose (kGy)	Total dose (kGy)
TI	66.8	1.92	68.7
FNIF	844	2.16	846

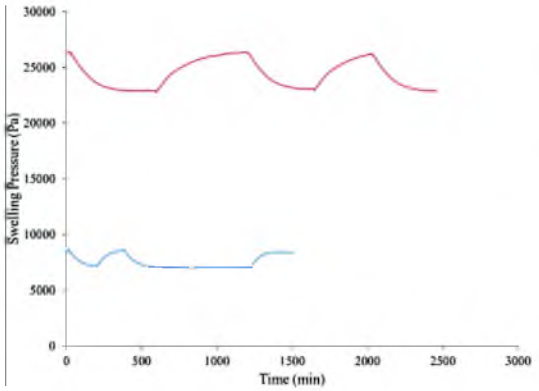

Fig. 1. Time dependence of the change in swelling pressure of the UV-cured hydrogel as environmental glucose concentration is cycled three times between zero and 5 mM; prior to irradiation (top curve); after 70 Gy of gamma irradiation (bottom curve). The initial value of the glucose concentration was zero; the curves have been shifted vertically to enhance clarity.

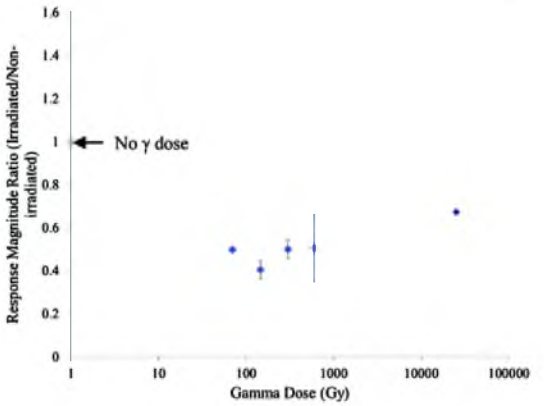

Fig. 3. For UV-cured hydrogels, magnitude of the swelling pressure response to a glucose concentration change (zero to 5 mM) vs. gamma irradiation dose. The swelling pressure magnitude has been normalized by the dose free value.

(70 Gy). These results were obtained when the environmental glucose concentration was varied between zero and 5 mM at fixed pH and ionic strength, starting at an initial value of zero. As expected from previous work [7,8], the osmotic swelling pressure of a hydrogel sample decreases when the glucose concentration increases. In Fig. 1, the magnitude of this decrease is larger for the hydrogel sample that has not been irradiated than it is for the irradiated sample from the same synthesis batch (4 kPa vs. 2 kPa, respectively).

Fig. 2 shows the time dependence of the glucose response, both before and after exposure to gamma rays (70 Gy), for a thermally-cured hydrogel having the same composition as the UV-cured gel of Fig. 1. In this case, exposure to gamma rays does not have a detrimental effect on the glucose response, and may even enhance it. In Fig. 2, a hydrogel sample that has not been irradiated exhibits a glucose swelling response of about 5 kPa, whereas an irradiated sample from the synthesis batch exhibits a glucose response of about 7 kPa. However, the uncertainty in the glucose response magnitude is of order 1 kPa, so it is difficult to discern a trend solely on the basis of the results in Figs. 1 and 2. Hence in Fig. 3, the dose-dependent effect of γ-irradiation on UV-cured gels is explored using results for multiple samples from two nominally identically synthesis batches. In Fig. 3, the dose-dependent glucose response magnitude is normalized by the value observed for a non-irradiated sample from the same synthesis batch.

The results in Fig. 3 clearly show that γ-irradiation reduces the response sensitivity of the UV-cured smart hydrogels by approximately 50%. However, for thermally-cured gels having the same composition, a similar plot yields quite different results (Fig. 4).

In Fig. 4, unlike Fig. 3, smart hydrogel response magnitude shows a small increase with increasing gamma dose, but the amount of the increase is comparable to the measurement uncertainty. However, one can at least conclude that exposure to gamma irradiation at sterilization levels does not have a detrimental effect on the sensitivity of these thermally-cured glucose-responsive hydrogels.

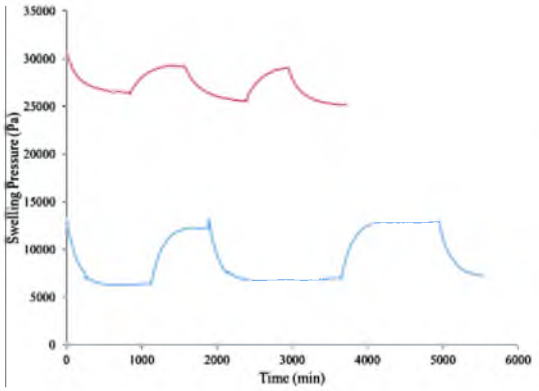

Fig. 2. Time dependence of the change in swelling pressure of the thermally-cured hydrogel as environmental glucose concentration is cycled three times between zero and 5 mM; prior to irradiation (top curve); after 70 Gy of gamma irradiation (bottom curve). The initial value of the glucose concentration was zero; the curves have been shifted vertically to enhance clarity.

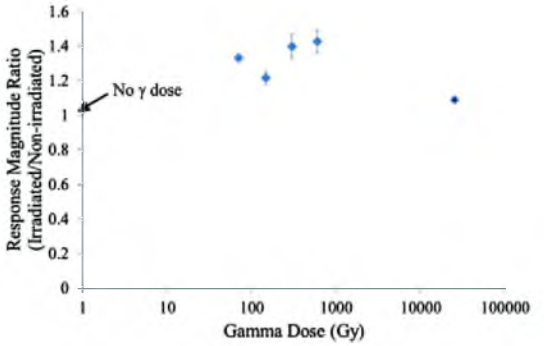

Fig. 4. For thermally-cured hydrogels, magnitude of the swelling pressure response to a glucose concentration change (zero to 5 mM) vs. gamma irradiation dose. The swelling pressure magnitude has been normalized by the dose free value.

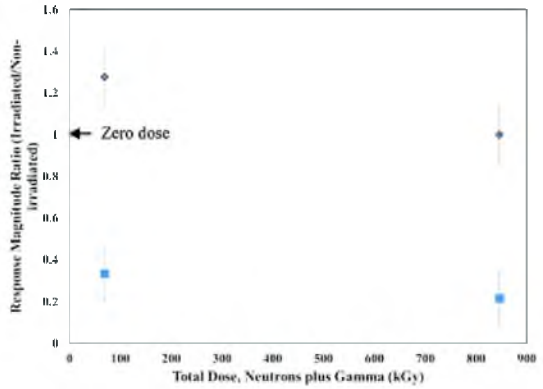

Fig. 5. Magnitude of the swelling pressure response to a glucose concentration change (zero to 5 mM) vs. total radiation dose in the nuclear reactor (neutrons + gamma) for thermally-cured hydrogels (diamonds) and UV-cured hydrogels (squares). The swelling pressure magnitude has been normalized by the dose free value.

3.2. *Effect of exposure to neutrons and gamma rays in the nuclear reactor*

The effect of the simultaneous exposure to both neutrons and gamma rays in the UUTR is shown in Fig. 5, which contains a plot of the normalized glucose response vs. the total dose for both types of glucose-sensitive hydrogels. The intermediate value of the total dose was obtained for samples placed at the thermal neutron (TI) port of the nuclear reactor, whereas the larger dose was obtained for samples placed at the fast neutron (FNIF) port. As shown in Table 1, the gamma dose was approximately 2 KGy at both ports, but the neutron dose was much larger at the FNIF port, two orders of magnitude larger than the gamma dose. Nonetheless, similar results were obtained for hydrogel samples placed at both nuclear reactor ports. According to Fig. 5, exposure to radiation in the nuclear reactor reduces the sensitivity of the UV-cured glucose-responsive gels by approximately 70%, which is similar to the effect of γ-irradiation alone (Fig. 3). Exposure to radiation in the nuclear reactor has minimal effect on the sensitivity of the thermally-cured glucose responsive gels.

4. Discussion

Exposure to gamma rays has been shown to produce free radicals within hydrogels [13], and these free radicals may either induce hydrogel crosslinking reactions [15], or degrade covalent amide bonds [14] similar to those present in the glucose-responsive hydrogels studied here. According to thermodynamic considerations [6], an increase in crosslink density decreases the response sensitivity of a smart hydrogel, all other factors being unchanged. Therefore, one can explain the different trends in Figs. 3 and 4 by assuming that gamma ray exposure increases the crosslink density of our UV-cured gels, but has no effect on our thermally-cured gels. This might be the case because of the presence of the UV sensitizer in the former, or because the gels were incompletely crosslinked prior to gamma exposure, even though we followed the standard UV curing protocol [16,17]. The results in Fig. 5 for hydrogels simultaneously exposed to both neutrons and gamma rays are not substantially different than the results observed for gamma exposure alone, even though the neutron dose is orders of magnitude larger. This suggests that the combined effects of radiation on the hydrogels in the TRIGA reactor is primarily determined by the gamma component of the dose.

5. Conclusions

Thermally-cured glucose-responsive hydrogels containing pendant boronic acid moieties are essentially unaffected by exposure to either thermal neutrons or sterilization levels of gamma rays. This is good news for the possible use of these materials in BNCT [2] or in continuous glucose sensors for bioreactors [7]. However, when smart hydrogels of the same type are prepared following a standard UV-curing protocol [16,17], exposure to gamma rays reduces the glucose response sensitivity by over 50%, possibly due to the formation of additional hydrogel crosslinks. Therefore it may be necessary to modify the UV-curing protocol for smart hydrogels that will eventually be subjected to gamma sterilization.

Acknowledgments

This research was supported by the Neopanora Institute Network of Energy Technologies, and the University of Utah Nuclear Engineering Program (UNEP).

References

[1] Bio-process Systems Alliance, Irradiation and Sterilization Subcommittee. 2008 guide to irradiation and sterilization validation of single-use bioprocess systems. Bioproc Int 2008 May 10–22;(Suppl.).
[2] Hopewell JW, Morris GM, Schwint A, Coderre JA. Boron neutron capture therapy: application of radiobiological principles. In: Sauerwein WAG, Wittig A, Moss RL, Nakagawa Y, editors. Textbook of neutron capture therapy. Berlin: Springer; 2012.
[3] Cambre JN, Sumerlin BS. Biomedical applications of boronic acid polymers. Polymer 2011;52:4631–43.
[4] Stringer RC, Gangopadhyay S, Grant SA. Comparison of molecularly imprinted particles prepared using precipitation polymerization in water and chloroform for fluorescent detection of nitroaromatics. Analytica Chim Acta 2011;703:239–44.
[5] Gehrke SH. Synthesis, equilibrium swelling, kinetics, permeability and applications of environmentally responsive gels. Adv Poly Sci 1993;110:81–144.
[6] Lin G, Chang S, Kuo C-H, Magda J, Solzbacher F. Free swelling and confined smart hydrogels for applications in chemomechanical sensors for physiological monitoring. Sens Actuators B Chem 2009;136:186–95.
[7] Lin G, Chang S, Hao H, Tathireddy P, Orthner M, Magda J, et al. Osmotic swelling pressure response of smart hydrogels suitable for chronically implantable glucose sensors. Sens Actuators B Chem 2010;144:332–6.
[8] Horkay F, Cho SH, Tathireddy P, Rieth L, Solzbacher F, Magda J. Thermodynamic analysis of the selectivity enhancement obtained by using smart hydrogels that are zwitterionic when detecting glucose with boronic acid moieties. Sens Actuators B Chem 2011;160:1363–71.
[9] Fernandez-Carballido A, Puebla P, Herrero-Vanrell R, Pastoriza P. Radiosterilisation of indomethacin PLGA/PEG-derivative microspheres: protective effects of low temperature during gamma-irradiation. Int J Pharm 2006;313:129–35.
[10] Kanjickal D, Lopina S, Evancho-Chapman MM, Schmidt S, Donovan D. Effects of sterilization on poly(ethylene glycol) hydrogels. J Biomed Mater Res A 2008;87A:608–17.
[11] Elijarrat-Binstock E, Bentolila A, Kumar N, Harel H, Domb AJ. Preparation, characterization, and sterilization of hydrogel sponges for iontophoretic drug-delivery use. Polym Adv Technol 2007;18:720–30.
[12] Guenther M, Schulz V, Gerlach G, Wallmersperger T, Solzbacher F, Magda JJ, et al. Hydrogel-based piezoresistive biochemical microsensors. Proc SPIE 2010;7642. 764227-1:9.
[13] Kanjickal D, Lopina S, Evancho-Chapman MM, Schmidt S, Inbaraj JJ, Cardon TB, et al. Electron spin resonance studies of the effects of sterilization on poly(ethylene glycol) hydrogels. J Biomed Mater Res A 2008;88A:409–18.
[14] Tyan Y-C, Liao J-D, Lin S-P, Chen CC. The study of the sterilization effect of gamma ray irradiation of immobilized collagen polypropylene nonwoven fabric surfaces. J Biomed Mater Res A 2003;67A:1033–43.
[15] Park S-E, Nho Y-C, Lim Y-M, Kim H-I. Preparation of pH-sensitive poly(vinyl alcohol-g-methacrylic acid) hydrogels by gamma ray irradiation and their insulin release behavior. J Appl Polym Sci 2004;91:636–43.
[16] Fedorovich NE, Alblas J, De Wijn JR, Hennink WE, Verbout AJ, Dhert WJA. Hydrogels as extracellular matrices for skeletal tissue engineering: state-of-the-art and novel application in organ printing. Tissue Eng 2007;13:1904–25.
[17] Tse JR, Engler AJ. Preparation of hydrogel substrates with tunable mechanical properties. In: Bonifacino JS, editor. Current protocols in cell biology. Somerset, NJ: Wiley; 2010.
[18] Pelowitz BD. MCNPX user's manual 2011; v2.7.0 LA-CP-11–00438. Los Alamos: Los Alamos National Laboratory.

[19] Rutala WA, Weber DJ. Guideline for disinfection and sterilization in healthcare facilities, 2008. Healthcare Infection Control Practices Advisory Committee (HICPAC): 58-79.

[20] Laughlin WL, Boyd AW, Chadwich KH, Donald JC, Miler A. Dosimetry for radiation processing. NY: Taylor & Francis Ed: 1989.

[21] Vinhas GM, Souto-Maior RM, Almeida YMB, Neto BB. Radiolytic degradation of poly(vinyl chloride) systems. Polym Degrad Stabil 2004; 86: 431-6.

[22] Schnabel W. Polymer degradation-principles and practical applications. NY: Macmillan Co: 1981.

CHAPTER 5

OPTIMIZATION OF FERROMAGNETIC PARTICLE ALIGNMENT AND SYNTHESIS OF MAGNETIC FIELD PRODUCING HYDROGELS FOR A GLUCOSE SENSOR

5.1 Abstract

Magnetometers can be used as signal transducers of chemical sensors because of many advantages such as high sensitivity, small size and low price. Nevertheless, previous studies rarely adopted magnetometers as transducers because it is difficult to develop materials that change their magnetic flux density in response to stimuli. In this study, magnetic particle-embedded, zwitterionic glucose-responsive hydrogels were developed to enable a magnetometer to serve as a signal transducer. The alignment of ferromagnetic particles was optimized by computer simulation (Comsol 4.3). Responses of glucose-responsive hydrogels were measured by a magnetoresistive transducer. The hydrogels produced different magnetic flux densities due to volume changes in response to glucose. In particular, a hydrogel containing horizontally aligned ferromagnetic particles showed good sensitivity be detecting physiologically relevant (~10 mM) glucose concentrations. The glucose sensitivity test results agreed with the modeling results.

5.2 Introduction

A chemical sensor consists of a target analyte sensitive material and a signal transducing device. The choice of signal transducer depends on the types of signals produced by the target analyte sensitive material in response to stimuli. The most common methods used are electrochemical sensing systems, such as potentiometric [1], amperometric [2], or conductometric [2] devices. Electrochemical transducers are useful for quantifying target analytes because electrical signals can be numerically interpreted. Researchers often use optical sensors as well. Optical sensors are useful for simple on/off systems. For example, such sensors can be used when one needs to detect the presence or absence, rather than quantity, of a particular material, e.g., in the case of explosives. Optical sensors can be used as high resolution chemical sensors. [3] synthesized chromophore-containing polymers for a 2,4-dinitrotoluene sensor. The UV wavelength of the chromophore-containing polymer was changed by 2,4-dinitrotoluene. The sensor was designed to detect, rather than quantify, the target analyte. The sensor was able to detect 2,4-dinitrotoluene down to the ppb level. Some researchers have used pressure-sensing devices as transducers by using materials capable of producing pressure changes, such as hydrogels [4]-[6]. The volume of hydrogels is changed by swelling or shrinking in response to the target analyte. The volume changes exert different forces on a pressure sensor in a confined space.

Magnetic flux-sensing devices (magnetometers) also can be a good signal transducing method because of their many advantages, such as small size, high sensitivity, low price and low power usage. To use a magnetometer as a signal transducer, magnetic field-producing materials must first be created. Magnetic particles

have been studied in some areas, especially for drug delivery [7], bioseparation [8], and cancer treatment [9]. However, most of the studies did not use magnetic field-producing materials, but magnetic field-responsive materials. For example, [7] embedded cobalt ferrite nanoparticles in a polyacrylamide (PAA) hydrogel to detect hydrogel responses magnetically. The ferro-hydrogel shrank or swelled in response to a magnetic field because the ferro-hydrogel acted as a cross-linker in this case. This research suggests that it may be possible to use external magnetic fields to control the release of drugs to a target area in the body.

In this study, magnetic field-producing hydrogels were developed by embedding ferromagnetic particles within a zwitterionic glucose-responsive hydrogel. Unlike previous studies, ferromagnetic particles were aligned within the glucose-response sheet of the hydrogel. The key idea is that the volume changes of the hydrogel will cause magnetic flux density changes because a magnetic flux density proportionally decreases as distance from the flux source increases. Computer modeling was performed to optimize the alignment method/direction of magnetic particles within the hydrogel. Glucose responses of the hydrogels were then measured by a magnetoresistive transducer (HMC 5883L, Honeywell).

5.3 Experiments

5.3.1 Materials

The monomers used for preparation of the gels and solvents were obtained as follows: acrylamide (AAM, Fisher Scientific), N,N-methylenebisacrylamide (BIS, Sigma-Aldrich), 3-acrylamidophenylboronic acid (3-APB, Frontier Scientific, Logan,

UT, USA), N-(3-dimethylaminopropyl acrylamide) (DMAPAA, Polysciences Inc.), 2-hydroxy-4'-(2-hydroxyethoxy)-2-methyl propiophenone (HHMP, Sigma-Aldrich), 1-vinyl-2-pyrrolidinone (V-pyrol, Sigma-Aldrich), D(+)-glucose (Mallinckrodt Chemicals), dimethyl sulfoxide (DMSO, Sigma-Aldrich), 4-(2-Hydroxyethyl)piperazine-1-ethanesulfonic acid (HEPES, Sigma-Aldrich), and Dulbecco's phosphate-buffered saline (1X PBS, Sigma-Aldrich). Ferromagnetic particles were donated by Hoosier Magnetics Inc. (Ogdensburg, NY)

5.3.2 Polymerization of Magnetic Particles Embedded Hydrogels

Figure 5.1 illustrates the synthesis procedure of ferromagnetic particle embedded hydrogels. First, ferromagnetic particles (5 wt% of pre-gel solution) were aligned in a hydrogel synthesis module by magnets. The preparation method of the pre-gel solution followed [10] (chemical components molar ratio: AAM/BIS/3-APB/DMAPAA=80/2/8/10). Prepared pre-gel solution was injected into the magnetic particle-aligned module. Next, the module was exposed to UV light (365 nm, 10 mW/cm2) for 5 minutes to initiate the process of radical polymerization. When polymerization was complete, a second layer of hydrogel was polymerized after changing a Teflon spacer. Figure 5.2 shows the synthesized magnetic particles-embedded, glucose-responsive hydrogels.

5.3.3 Modeling of Magnetic Flux as a Particle Alignment

Computation (Comsol 4.3 (Comsol Multiphysics®)) was performed to observe the effects of configuration differences of magnetic particle alignment on magnetic flux.

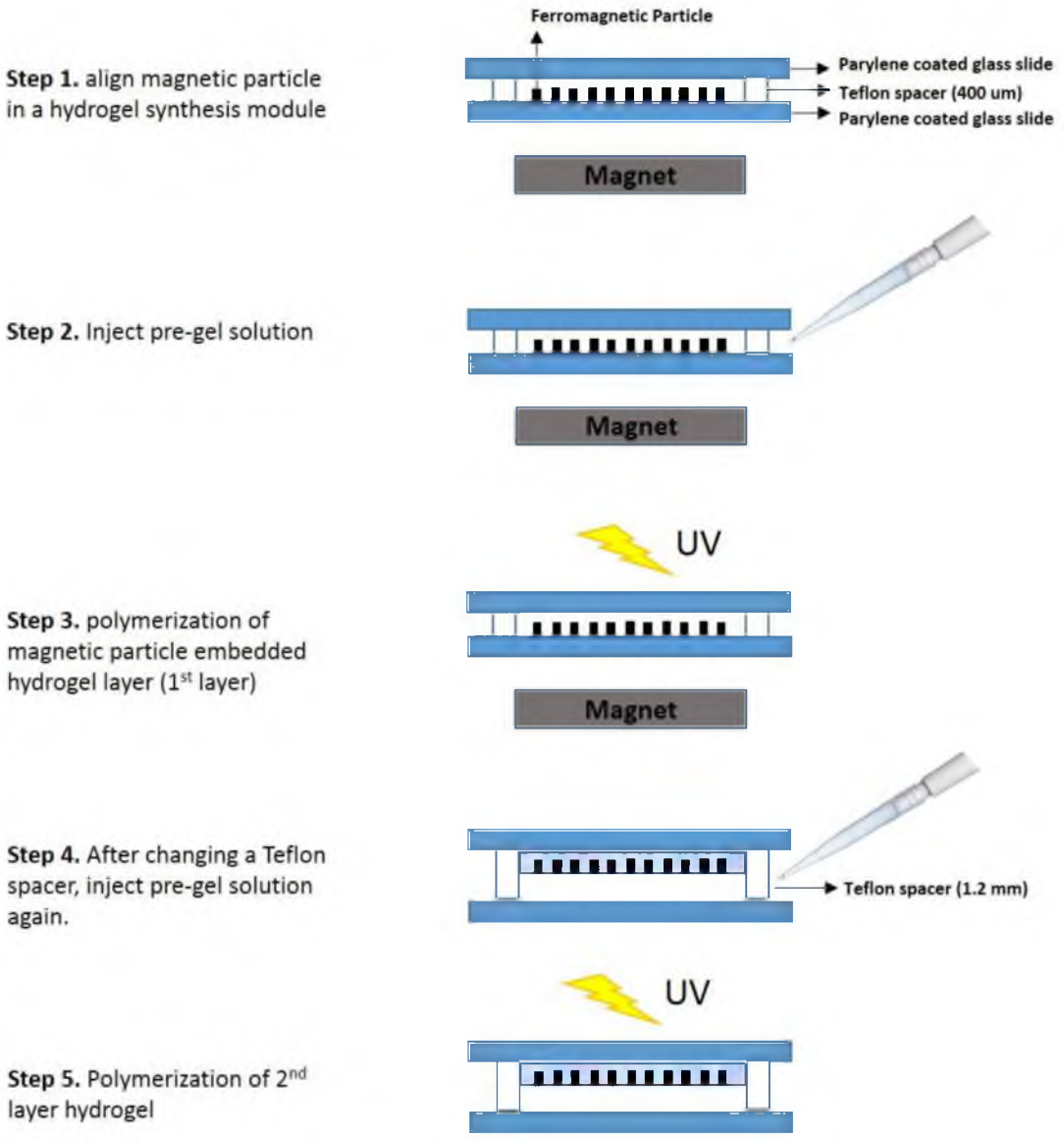

Figure 5.1 Schematic synthesis procedure of ferromagnetic particle-embedded, glucose-responsive hydrogel.

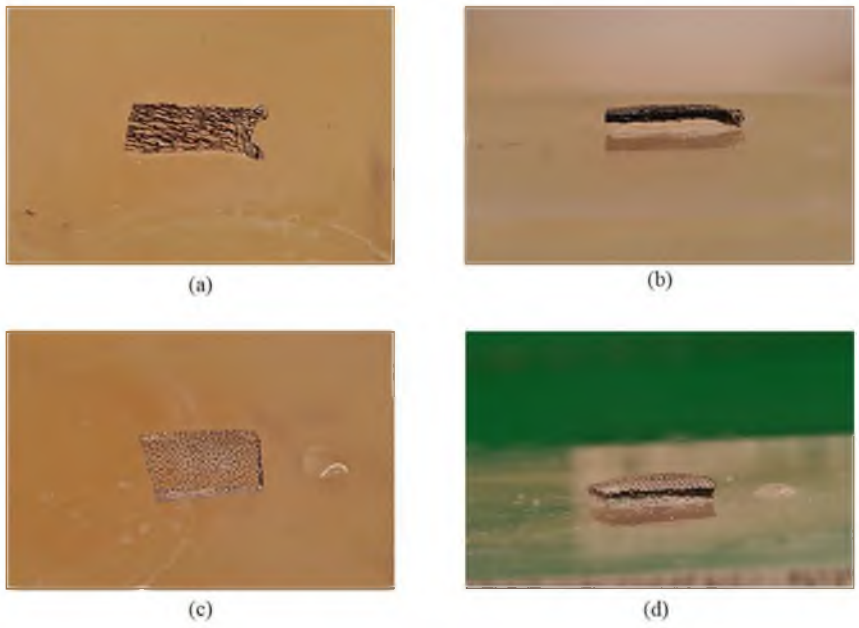

Figure 5.2 Synthesized ferromagentic particle-embedded glucose-reponsive hydrogels. (a) and (b): xy-direction aligned magnetic particles; (c) and (d): z-direction aligned magnetic particles.

Domains were divided into two parts: the ferromagnetic domain and the surrounding environment, which was a glucose-responsive hydrogel. Figure 5.3 shows the geometry of these domains.

With the assumption that magnetic fluxes can only be produced by ferromagnetic particle layers within the hydrogel ($\nabla \times \mathbf{H} = 0$), the model was defined in the Magnetic Fields, no current interface module of the program. Parameter values were estimated by the density of magnetic particles in the hydrogel (5 wt%) (Table 5.1).

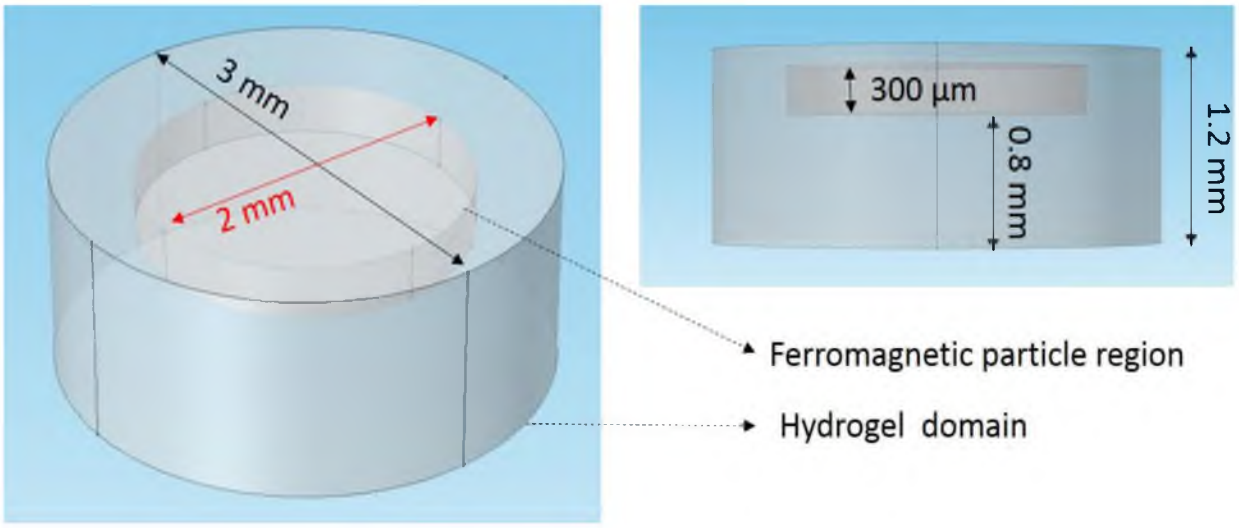

Figure 5.3 Geometry of model domains.

Table 5.1 Parameter values for magnetic field simulation

	Commercial hard ferrite magnet	Magnetic particle within a hydrogel (estimated value)
Density ≡ [g/cm^3]	5	1
Magnetic field density (B) ≡ [T]	0.35	0.07
Magnetic field strength (H) ≡ [kA/m]	150	30

5.3.4 Measurement of Glucose Responses of Hydrogels

Figure 5.4 illustrates the glucose response measurement system with a magnetoresistive transducer (HMC 5883L, Honeywell). Small pieces of ferromagnetic particle-embedded, glucose-responsive hydrogel (3 mm diameter) were loaded on the magnetoresistive transducer. The transducer was submerged in an experimental media. The data receiver remotely collected signals from the magnetoresistive transducer.

5.4 Results and Discussion

5.4.1 Magnetic Flux as a Ferromagnetic Particle Alignment

The alignment direction of ferromagnetic particles determined the magnetic flux direction in this study. For example, if magnetic particles were aligned in the x-direction, the magnetic force was exerted in the x-direction (horizontal). Modeling results (Figure 5.5 and Figure 5.6) show that the formation of magnetic flux within the hydrogel depended on the alignment direction of ferromagnetic particles. Figure 5.5 (a) shows that the magnetic flux was center-oriented when magnetic particles were aligned in the x-direction.

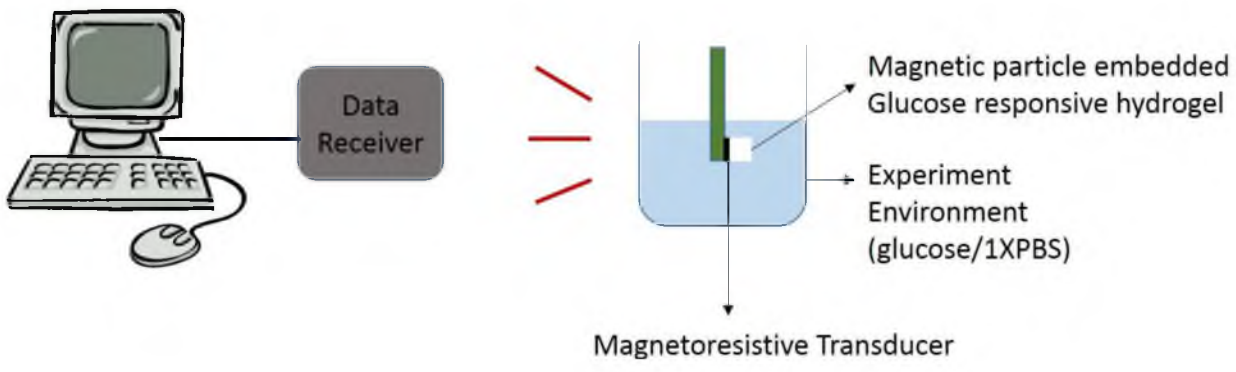

Figure 5.4 Illustration of the glucose response measurement system with a magnetoresistive transducer.

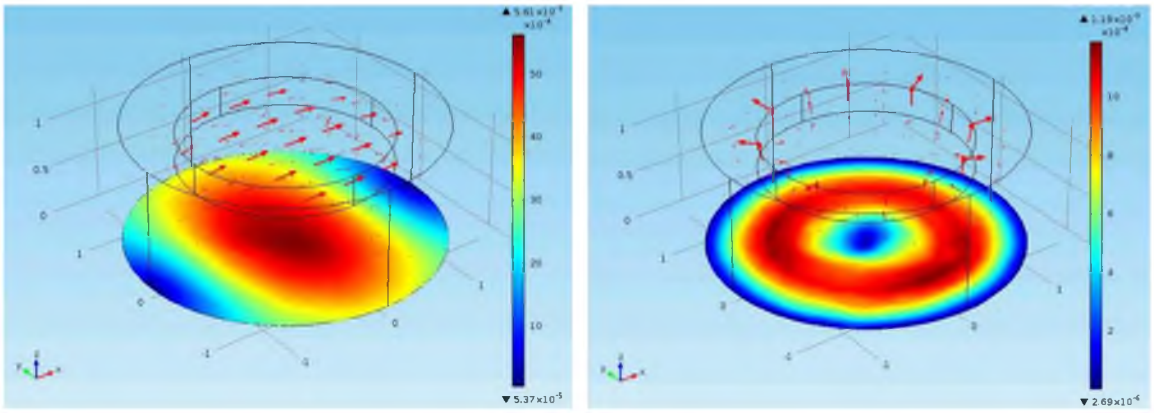

(a) (b)

Figure 5.5 Magnetic fluxes with alignment directions of ferromagnetic particles. (a) Magnetic flux of x- direction aligned magnetic particles within a hydrogel (unit: T), (b) Magnetic flux of z-direction aligned magnetic particles within a hydrogel (unit: T).

In addition, magnetic flux density in the glucose response area (0 to 0.8 mm) decreased linearly with increasing distance from the magnetic particle layer (Figure 5.6 (a)). Therefore, a magnetoresistive transducer will detect changes in the magnetic flux density as the thickness of the glucose0responsive hydrogel changes (Figure 5.4). This result shows that the horizontal alignment method can be used for magnetic particle-embedded hydrogels using a magnetometer as a signal transducer. In contrast, when particles were aligned in the z-direction (perpendicular) within the hydrogel, the magnetic flux was oriented at the edge of a concentric circle (Figure 5.5 (b)). Although the magnetic flux density of z-direction aligned particles also decreased linearly with increasing distance from the magnetic particle layer, it did not cover all of the glucose response area (Figure 5.6 (b)). Moreover, the flux density of the x-direction method was five times greater than that of the y-direction method in the glucose response area (0 - 0.8mm from the bottom of hydrogel samples, which is under the ferromagnetic particle layer, Figure 5.3).

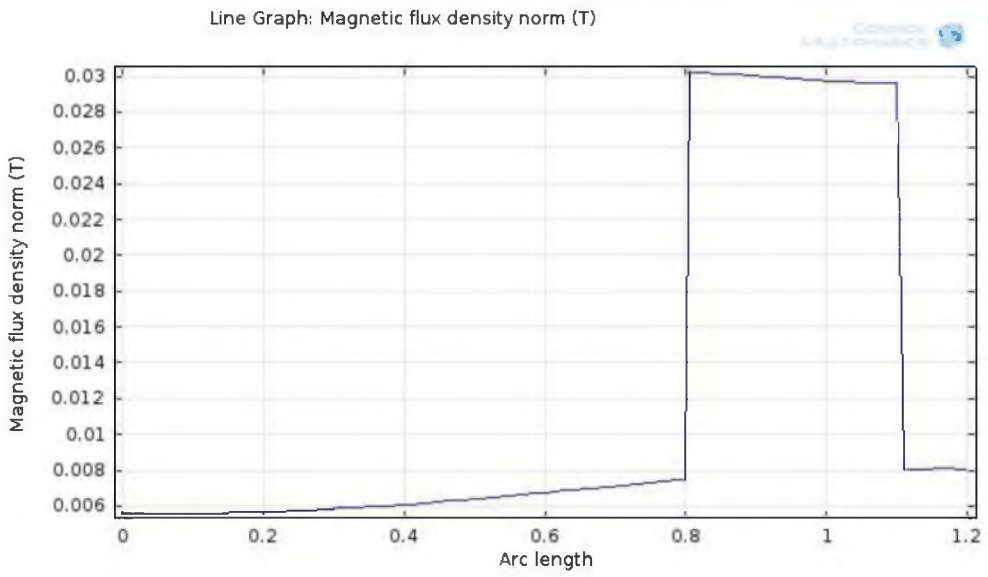

(a)

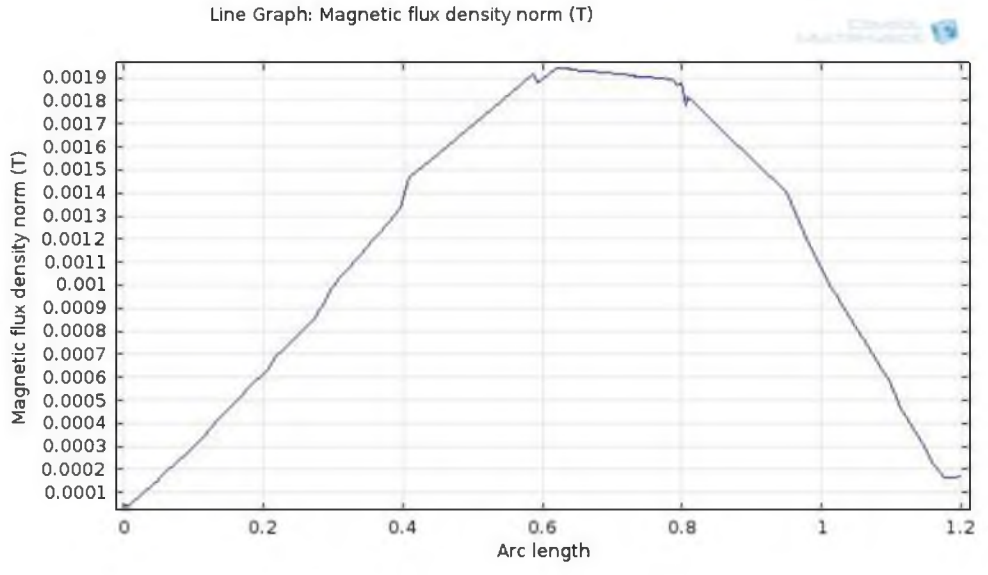

(b)

Figure 5.6 Magnetic flux density versus distance from magnetic particle layer within a hydrogel. (a) Magnetic flux density versus distance (x-direction aligned particles), (b) Magnetic flux density versus distance (z-direction aligned particles).

5.4.2 Glucose responses

Glucose-responsive hydrogels reversibly swell or shrink as the glucose concentration in the surrounding media changes. Specifically, zwitterionic glucose-responsive hydrogels shrink when they are exposed to more glucose molecules [6, 11, 12]. This reduces the thickness of the glucose-response area. Thus, the magnetic flux density from ferromagnetic particle-embedded, zwitterionic glucose-responsive hydrogels will increase with increasing glucose concentrations. Figure 5.7 shows reversible glucose responses with the alignment direction of ferromagnetic particles. As expected from computer simulations, the hydrogel with the horizontal ferromagnetic layer showed a good reversible response (Figure 5.7 (a)). Response magnitudes linearly increased with increasing glucose concentrations in the physiological range (3-10 mM). Moreover, the inverse first order rate was about 9 (± 1) minutes. This is a remarkable improvement when compared to our previous studies [6, 10]. [6] developed a continuous glucose-sensing (CGS) system with a 400 μm thick zwitterionic glucose-responsive hydrogel (AAM/BIS/3-APB/DMAPAA=80/2/8/10, same composition in this study) and a piezoresistive pressure transducer. The study showed a good reversible binding from 0 to 5 mM glucose concentration. Unfortunately, the inverse first order rate was about 65 (±15) [6]. However, although the hydrogel thickness in this study was twice as thick as the gel in the study of [6], response times were only one-seventh as long.

5.5 Conclusions

A magnetometer is a good signal transducing device for chemical sensors because of its many advantages. However, it is rarely used as a transducer because it is difficult to

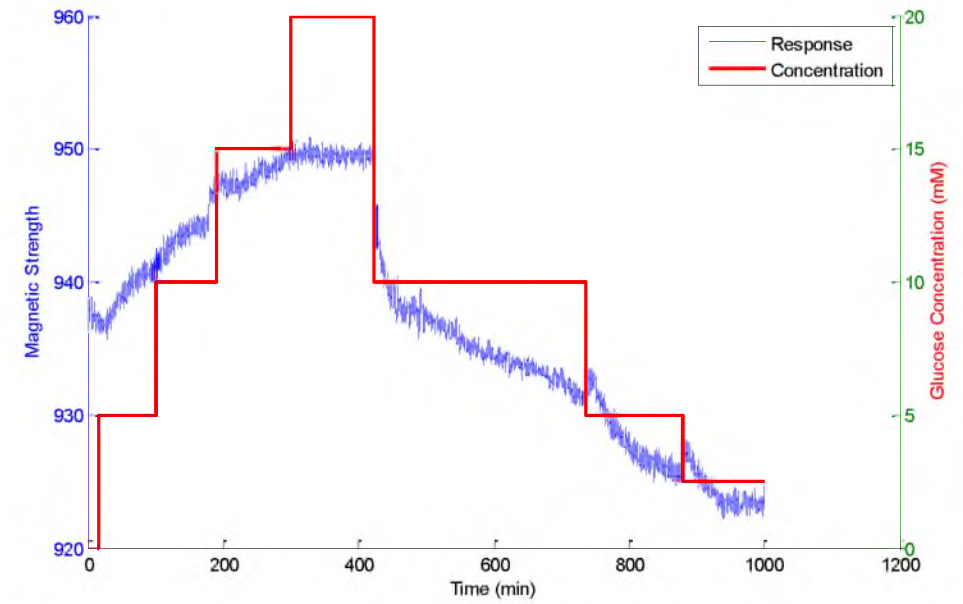

(a)

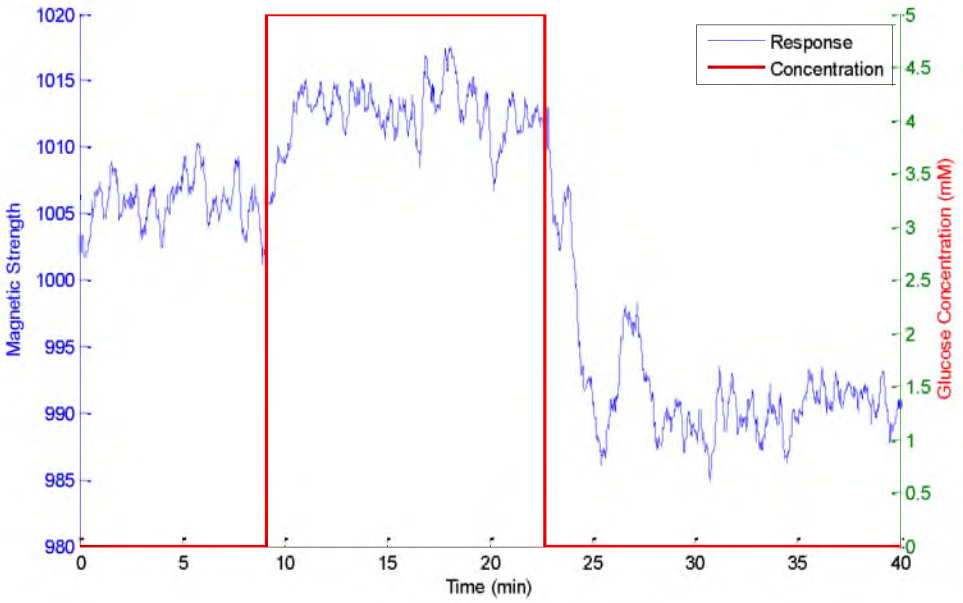

(b)

Figure 5.7 Glucose responses of magnetic particle-embedded, zwitterionic glucose-responsive hydrogel as measured by a magnetometer. (a) Glucose responses of a hydrogel containing x-direction aligned magnetic particles, (b) Glucose responses of a hydrogel containing y-direction aligned magnetic particles.

develop materials that can produce magnetic fields in response to stimuli, although there are many studies of magnetic field-responsive materials. Thus, we invented a magnetic field-producing, zwitterionic glucose-responsive hydrogel for a diabetic sensor application by embedding ferromagnetic particles within the hydrogel. The ferromagnetic particle alignment method was optimized by a computer simulation, and glucose responses were measured by magnetoresistive transducer. The hydrogel with horizontally aligned ferromagnetic particles showed good sensitivity in the physiological glucose range (~10 mM). Moreover, we reduced the response time by almost seven-fold with this magnetic field-producing hydrogel.

5.6 References

[1] Anzai, J.; Chung, C. Carboxylated Poly(vinyl chloride)/Plasticizer Composite Membranes as Chemical Sensor Materials: Potentiometric Response and Water Uptake Properties. *Polymer Communications* **1990,** 31, 375-377

[2] Lange, U.; Roznyatovskaya, N. V.; Mirsky, V. M. Conducting Polymers in Chemical Sensors and Arrays. *Analytica Chimica Acta* **2008,** 614, 1-26.

[3] Chen, A.; Sun, H.; Pyayt, A; Zhang, X.; Luo, L.; Jen, A.; Sullivan, P. A.; Elangovan, S.; Dalton, L. R.; Dinu,R.; Jin, D.; Huang, D. Chromophore-Containing Polymers for Trace Explosive Sensors. *Journal of Physical Chemistry C* **2008,** 112, 8072-8078.

[4] Herber, S.; Eijkel, J.; Olthuis, W.; Bergveld, P.; Van den Berg, A. Study of Chemically Induced Pressure Generation of Hydrogels under Isochoric Conditions using a Microfabricated Device. *Journal of Chem. Phy.* **2004,** 212, 2746-2751.

[5] Porter, T. L.; Stewart, R.; Reed, J.; Morton, K. Models of Hydrogel Swelling with Applications to Hydration Monitoring. *Sensors* **2007,** 7, 1980-1991.

[6] Lin, G.; Chang, S.; Hao, H.; Tathireddy, P.; Orthner, M.; Magda, J.; Solzbacher, F. Osmotic Swelling Pressure Response of Smart Hydrogels Suitable for Chronically-Implantable Glucose Sensors. *Sensors & Actuators, B, Chem.* **2010,** 144, 332–336.

[7] Berkum, S. V.; Dee, J. T.; Philipse, A. P.; Erne, B. H. Frequency-Dependent Magnetic Susceptibility of Magnetite and Cobalt Ferrite Nanoparticles Embedded in PAA Hydrogel. *International Journal of Moelcular Sciences* **2013,** 14, 10162-10177.

[8] Katz, E.; Willner, I.; Wang, J. Electroanalytical and Bioelectroanalytical Systems Based on Metal and Semiconductor Nanoparticles. *Electroanalysis* **2004,** 16, 19-44.

[9] Shinkai, M. Functional Magnetic Particles for Medical Application. *Journal of Bioscience and Bioengineering* **2002,** 94, 606-613.

[10] Magda, J.; Cho,S-H.; Streitmatter, S.; Jevremovic, T. Effect of Gamma Rays and Neutron Irradiation on The Glucose Response of Boronic Acid-Containing "Smart" Hydrogels. *Polymer Degradation and Stability* **2014,** 99, 219-222.

[11] Alexeev, V.L.; Sharma, A.C.; Goponenko, A.V.; Das, S.; Lednev, I.K.; Wilcox, C.S. High Ionic Strength Glucose-Sensing Photonic Crystal. *Anal. Chem.* **2003,** 75, 2316-2323.

[12] Tierney, S.; Volden, S.; Stokke, B.T. Glucose Sensors Based on a Responsive Gel Incorporated as a Fabry-Perot Cavity on a Fiber-Optic Readout Platform. *Biosens. Bioelectron.* **2009**, 24, 2034–2039.

CHAPTER 6

MOLECULARLY IMPRINTED POLYMER USING THE INTERACTION OF CO^{2+} AND GLUTATHIONE FOR A GLUTATIONE SENSOR

6.1 Abstract

Glutathione (GSH) is a tri-peptide consisting of glycine, cysteine and glutamic acid. GSH deficiency in cells contributes to oxidative stress, which plays a key role in aging and the pathogenesis of many diseases such as Alzheimer, Parkinson, diabetes and other ailments. Hence, a glutathione sensor that is able to monitor GSH levels in body fluid could be an important tool for preventing such diseases. This research focuses on the possibility of devising a new mechanism for testing GSH sensible material in saliva that can be used to determine GSH levels. Two main strategies used in the research are molecularly imprinting technology (MIT) and Co^{2+}-imidazole mediated binding complex (Co-MIP). The polymeric matrices obtained using MIT, which are called molecularly imprinted polymers (MIP), can be strong molecular recognition elements able to mimic natural recognition entities such as antibodies and biological receptors. The structure of metal ion and imidazole binding on the other hand is useful for aqueous environments (such as saliva) because of the high stability of the binding structure. For this research, Co-MIP was used for enhancing sensitivity of glutathione-imprinted polymer (GSH-MIP) to GSH molecules in saliva. GSH-MIP was successfully synthesized by radical

polymerization, and a sensitivity test of GSH-MIP showed promising results for inventing a glutathione sensor MIP effect was confirmed when the sensitivity of GSH-MIP was compared with nonimprinted polymer. Also, Co-MIP showed the highest sensitivity to GSH in physiological condition buffer solution (1X PBS).

6.2 Introduction

Glutathione (GSH) is a low molecular weight thiol existing in cytosol, mitochondria, nuclear matrix, and peroxisomes of cells. GSH is an important component for cellular reactions [1]. It mainly works as:

- Scavenger of free radicals and other reactive oxygen species
- Insulin sensitizing agent
- Removal of formaldehyde
- Main component for the conversion of prostaglandin H_2 in cells

GSH also involves in important body regulation such as DNA synthesis, cytokine production, immune response, and so forth. Thus, each cell component should maintain a certain concentration of GSH. Plus, the ratio of GSH and oxidized GSH (GSSG) should be over 10 in a normal physiological condition [1], [2] because GSH deficiency can be a cause of serious diseases such as Alzheimer, Parkinson's disease, ADHD, Autism, immune disorders, diabetes, etc. (Table 6.1).

Although the importance of monitoring GSH levels has been emphasized for a long time, there are only a few studies reported about GSH sensing materials or devices [4], [5] (Section 1.2.11 Glutathione Sensors). Therefore, GSH sensitive polymer was developed to devise a glutathione sensor for this research. Two strategies were tried to

Table 6.1 Glutathione deficiency caused diseases (adapted from [3])

Organ	Disease
Brain	Alzheimer, Parkinson OCD, ADHD, Autism, Migraine, Stroke, Trauma, Cancer
Lung	Asthma, COPD, Allergies, ARDS, Cancer
Joints	Rheumatoid, Osteo-Arthritis, Psorisis
Kidney	Chronic Kidney Disease, Renal Graft, Nephritis
Skin	Skin Ageing, Sunburn, Psoriasis, Melanoma
Heart	CHD, Cardiac Fibrosis, Hypertension, Ischemia
Eyes	Macular Degeneration, Retinal Degeneration
Multi-organ	Diabetes, Ageing, Chronic Fatigue
Blood vessels	Endothelial Dysfunction, Hypertension, Restenosis
Immune system	Chronic Inflammations, Auto Immune Disorders, Lupus, IBD, MS

achieve a good GSH sensitivity. First of all, a molecularly imprinted polymer (MIP) method was used to enhance GSH selectivity and sensitivity. MIP is a polymer matrix has cavities resembling target analyte during MIP polymerization process [6], [7]. When MIP is exposed to the target analytes, it forms binding complex with them selectively. MIP has been applied in many areas such medicine, environmental analysis, sensor and drug delivery because of the high selectivity. Second of all, chelating complex was used for GSH binding sites to enhance sensitivity in an aqueous environment. In most of the MIP studies, hydrogen bonding was used for target analyte binding sites because hydrogel bonding is the strongest reversible binding force [8]. However, hydrogen bonding can be easily interrupted by other molecules, especially in an aqueous media

(such as body fluid). Thus, chelating complex was adapted to reduce the interference. Metal ions strongly attract ligand molecules because molecules distribute an electrons to be in electro neutral state [9]. As a result, a chelating complex can be a strong and sensitive reversible binding sites in MIPs. Thus, many MIPs studies based on a water environment are using metal complexes for binding sites to enhance sensitivity. For example, [10] adopted peptide-Ni(II) interaction as a binding site for developing a protein purification system with MIP. They confirmed sensitivity improvement by using peptide-Ni(II) interaction in a water based system [10]. [11] synthesized Co^{2+}-imidazole combined MIPs for an organophophate pesticide detection. They reported that Co^{2+}-imidazole complex bound with organophosphotriester by hydrolyzation. They were expecting their MIP polymer could be used for an organophophate compounds monitoring system [11]. These previous studies supported that sensitivity of GSH imprinted polymer in aqueous media can be improved by involving metal ions. Thus, we also adopted a metal ion complex in this research. Metal ions were immobilized by a first chelating ligand (imidazole) within the MIP structure, and then glutathione molecules can become a second chelating ligand to form chelation structure.

6.3 Experiments

6.3.1 Materials

The monomers used for synthesis of the molecularly imprinted polymer were purchased as follows: Methacrylic acid (MAA) (Polysciences. Inc., Warrington, PA), acrylic acid (AA) (Polysciences. Inc., Warrington, PA) 1-vinylimidazole (VI) (Sigma-Aldrich, Louis, MO), ethylene glycol dimethacrylate (EGDMA) (Polysciences. Inc.,

Warrington, PA), 2,2'-azobisisobutyronitrile (AIBN) (Sigma-Aldrich, Louis, MO), ammonium persulfate (APS) (Sigma-Aldric, Louis, MO), reduced glutathione (GSH) (Sigma-Aldrich, Japan), oxidized glutathione (GSSG) (Sigma-Aldrich, Japan), cobalt(II) chloride (Sigma-Aldrich, UK), copper(II) chloride (Sigma-Aldrich, Louis, MO), zinc chloride (Sigma-Aldrich, Louis, MO), chromium(II) chlrodie (Sigma-Aldrich, Louis, MO), methanol (MeOH) (Mallinckrod chemicals, Phillipsburg, NJ), acetonitrile (Mallinckrod chemicals, Phillipsburg, NJ), and Dulbecco's phosphate-buffered saline solution (1X PBS) (Sigma-Aldrich, Louis, MO).

6.3.2 Equipment

Equipment used included a PowerSpin LX centrifuge, UNICO (3.5K rpm, 2 minutes and 30 sec), a multipurpose rotator (Thermo Scientific), and an ultrasonic cleaner (Brnsonic, B-1200R-1). An Au-sputter (Sputter coater 108auto, Cressington Scientific Instrument Ltd), a scanning electron microscope (FEI NanoNova Scanning Electron Microscope), a Nikon optical microscope (Nikon microphot V series) were used for microscope imaging. A PerkinElmer Lambda 750 UV/VIS spectrophotometer (resolution: 2nm) was used for estimation of glutathione binding affinity.

6.3.3 Synthesis

6.3.3.1 Synthesis of a Glutathione-Imprinted Polymers

All monomers (Table 6.2) were dissolved in 90 vol.% of acetonitrile (the monomer mixture concentration should be 15 wt.%). After adding radical initiator (AIBN) in the monomer mixture, the mixture was purged by Ar gas for 10 minutes. Then,

Table 6.2 Monomer compositions (molar ratio, monomer composition of GSH-MIP was based on [8].

Monomer	GSH-NIP	GSH-MIP*	VI-NIP	VI-MIP	Co-NIP	Co-MIP
MAA	4	4	0	0	0	0
AA	0	0	4	4	4	4
EGDMA	20	20	20	20	20	20
GSH	0	1	0	1	0	1
VI	0	0	1	1	1	1
AIBN	0.1	0.1	0.1	0.1	0.1	0.1
$CoCl_2$	0	0	0	0	0.5	0.5

polymerization was processed for 24 hours at 60°C by a precipitation method. Reflux system was used to recover evaporated acetonitrile during polymerization. When polymerization was done, a washing step followed to get rid of imprinted GSH. The synthesized GSH-MIP particles were washed by fresh methanol (MeOH), and the washing solution was centrifuged to recollect GSH-MIP particles. This washing step was repeated three times. Finally, synthesized GSH-MIP was dried in an oven at 50°C for removing residual washing solvent. Nonimprinted polymer (GSH-NIP) was prepared by same procedure as described above without GSH template.

6.3.3.2 Synthesis of Chelating Ligand Containing MIP

VI, GSH, and $CoCl_2$ ($CuCl_2$, $CrCl_2$, or $ZnCl_2$) were dissolved in 90 vol% acetonitrile, and stirred for 30 minutes with Ar purging. After adding AA, EGDMA, and AIBN in the previous mixture (the final concentration of monomer mixture was 15 wt%), the mixture was purged with Ar for 10 minutes more before starting polymerization. Polymerization was processed with same method of GSH-MIP in the previous Section.

6.3.4 Microscope imaging

6.3.4.1 Scanning Electron Microscope

Synthesized particle mixture (0.1 wt%) was prepared with acetonitrile. The diluted MIP particle emulsion was dropped on a clean Si wafer after sonication for 1 minute. Then, it was left in the air with a cover to protect contamination until acetonitrile was evaporated. After sputtering of Au on the prepared specimen, imaging was performed by a scanning electron microscope (FEI NanoNova Scanning Electron Microscope)

6.3.4.2 Optical Microscope

Synthesized particle mixture (0.1 wt%) was prepared with 1X PBS. The diluted MIP particle emulsion was dropped on a clean optical microscope slide glass having a micro ruler. Imaging was performed by an optical microscope (Nikon microshot V series).

6.3.5 Estimation of Binding Affinity

Sensitivity comparison was done by plotting of scatchard plot for each sample [15]. The scatchard plot was based on the binding kinetics of antigen-antibody at equilibrium of the system.

$$N_t + F \overset{K_a}{\rightarrow} B \tag{6.1}$$

$$B = \frac{F \cdot B_{max}}{K_D + F} \Longrightarrow \frac{B}{F} = -\frac{B}{K_D} + \frac{B_{max}}{K_D} = -BK_a + B_{max}K_a \tag{6.2}$$

N_t (B_{max}): The total number of binding sites, maximum binding ≡ [mmole/g]

F: The concentration of free (unbound) target molecule at equilibrium ≡ [mM]

B: The concentration of bound target molecule at equilibrium ≡ [mM]

K_a: Binding affinity ≡ [1/mM]

K_D: Dissociation constant ≡ [mM]

6.3.6 Sensitivity Test

Figure 6.1 illustrates the sensitivity test procedure. One wt% of sample emulsions were prepared with 1X PBS and the samples were incubated on a shaker for 1 hour at room temperature. After adding GSH (concentration range: 5, 2.5, 1, 0.5, 0.25 mM) solution into the sample emulsions, the samples were incubated for 2 hours at room temperature. Then supernatant of each sample were taken after centrifuging them at 4000 rpm for 2.5 minutes. The GSH concentration of supernatant reflects the amount of unbound GSH at the equilibrium. It was measured by a UV-Vis spectroscopy (PerkinElmer Lambda 750 UV/VIS spectrophotometer).

6.4 Results and Discussion

6.4.1 Optimization of Synthesis Conditions

6.4.1.1 Solvent Polarity and Synthesis Temperature

Functional monomers, the amount of cross-linker, porogenic solvent, and synthesis temperature are key factors determining sensitivity and selectivity of MIPs. Functional monomers consists of target analyte-binding sites. The amount of cross-linker determines not only rigidity of MIPs, but also shape of binding cavity. Initially, hydroxyl group of MAA was used for functional binding sites to optimize other factors in this study. In addition, the molar ratio of cross-linker (EGDMA) and backbone (MAA) was

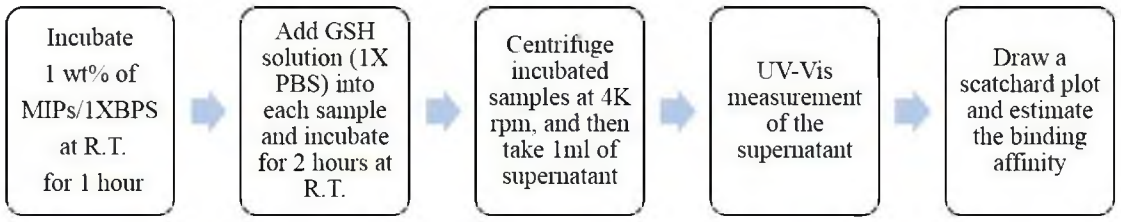

Figure 6.1 Sensitivity experiment flow.

fixed (EGDMA/MAA=4) because [8] achieved the best GSH sensitivity with the molar ratio. Except these two fixed factors, progenic solvent and synthesis temperature are also very important factors for MIPs because solvent polarity and environment temperature will change interaction and binding shape of target analytes-functional monomer complexes [12], [13]. However, they were not studied before. Thus, three different solvents were chosen to see binding affinity changes as solvent polarity, and polymerization was tried at two different temperatures to optimize synthesis temperature (Table 6.3).

GSH binding affinity (K_a) of each sample can be estimated by a scatchard plot (Figure 6.2). A scatchard plot shows the ratio of bound/unbound mobile GSH versus bound GSH concentration at equilibrium. According to equation 6.2, the slope of a scatchard plot will be a binding affinity of the sample. Thus, all binding affinity values in Table 6.3 were estimated by drawing a scatchard plot for each sample. Experiment results showed that polarity and temperature effect was considerably huge. The binding affinity of GSH-MIP was decreased as decreasing of solvent polarity (Table 6.3). Polarity effect was even bigger than MIP effect. Nonimprinted polymer synthesized in acetonitrile showed four times higher binding affinity than GSH imprinted polymer synthesized in

Table 6.3 Glutathione sensitivity comparison as polymerization conditions.

Sample	GSH-NIP	GSH-MIP			
Solvent	Acetonitrile	Acetonitrile	Acetonitrile	Chloroform	IPA
Synthesis Temperature (°C)	60	60	27	60	60
Polarity of solvent	5.8	5.8	5.8	4.1	3.9
Binding affinity K_a [mM^{-1}]	10.05	17.59	2.74	4.8	2.72

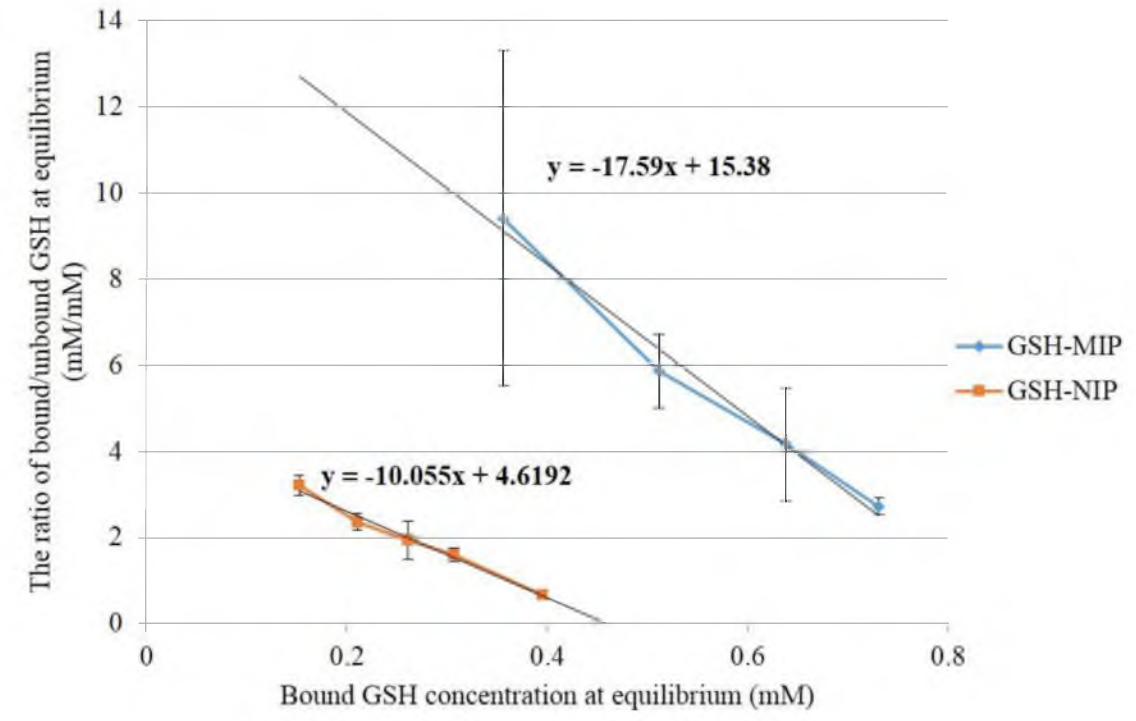

Figure 6.2 Scatchard plots of GSH-MIP and GSH-NIP (the ratio of bound/unbound mobile GSH vs. bound GSH at equilibrium, based on equation 6.2).

IPA. In addition, the binding affinity of GSH-MIP synthesized at 60 °C was seven times higher than GSH-MIP synthesized at 27 °C.

6.4.1.2 Metal ions for chelating complex

Although transition metal complex follows Lewis acid-base rule such as "hard bases stabilize high oxidation states and soft bases stabilize low oxidation states" the best chelate for GSH should be chosen by experimentally. Thus, metal ions having thiolate and imidazole as chelating ligands such as Co^{2+}, Cu^{2+}, and Zn^{2+} were investigated.

Imidazole already inserted MIP structure during polymerization, and metal ions were immobilized at the imidazole sites within MIP structure. Then, the immobilized metal ions became mobile GSH binding sites because these metal ions also form chelating structure with thiol groups of GSH. Table 6.4 shows the binding affinity depending on metal ions. The best binding affinity to GSH was achieved when Co^{2+} was involved as chelate.

6.4.2 Morphology of GSH-MIPs

Morphology of synthesized GSH-MIP particles was confirmed by microscope imaging (Figure 6.3). Spherical shape GSH-MIP particles (2-5 μm diameter) were achieved by precipitation method (Figure 6.3 (a)), and Co-MIP particles were twice as big (about 10μm) than GSH-MIP (Figure 6.3 (b)). This is a good improvement of particle

Table 6.4 Binding affinity comparisons as metal ions

	GSH-MIP synthesized in acetonitrile at 60°C		
Binding Affinity Ka [mM^{-1}]	Co^{2+}	Cu^{2+}	Zn^{2+}
	25.36	20.44	10.14

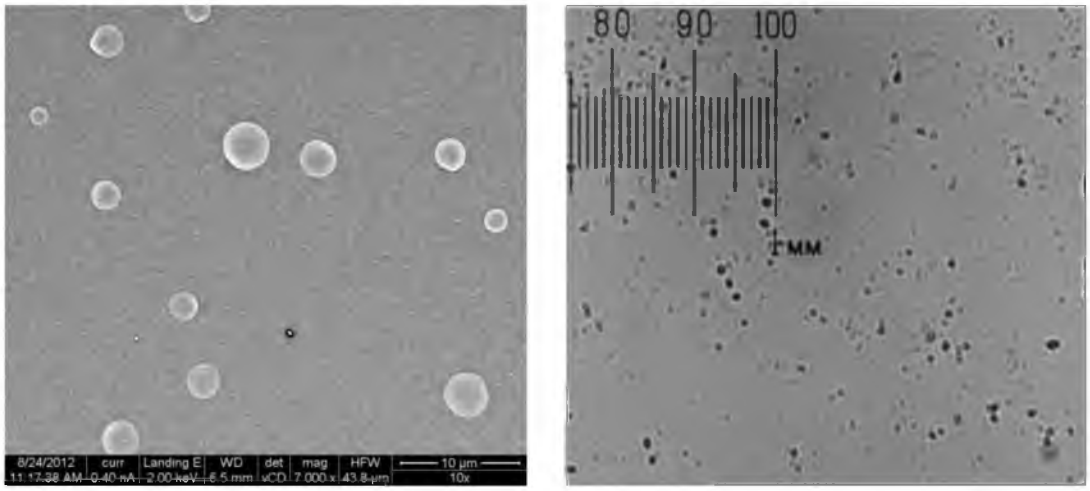

(a) (b)

Figure 6.3 Microscope images of GSH-MIP: (a) GSH-MIP (FEI NanoNova Scanning Electron Microscope), (b) Co-MIP (Nikon microshot V series).

type MIPs polymerization. Most of MIPs synthesis methods have been developed in monolith type in previous studies [6], [7]. Thus, [8] ground monolith type GSH-MIP to get particle type sample and then sieved the ground particles to control particle size. However, we directly achieved particle type GSH-MIPs by precipitation method in this research.

6.4.3 MIP and Co^{2+} chelating complex effect on GSH sensitivity

MIP effect was confirmed by comparison of binding affinities with the MIPs synthesis condition optimization experiment (Section 6.4.1). Binding affinity of GSH-MIP was 1.7 times higher than GSH-NIP when hydroxyl groups were used for binding sites (Figure 6.2). Moreover, GSH-MIP showed good GSH selectivity. Relative sensitivity (K_a/K_{ag}) of GSH-MIP was almost twice as high than GSH-MIP (Table 6.5).

Binding affinity was also improved by involving Co^{2+}-GSH chelating complex.

Table 6.5 Glutathione sensitivity comparisons

Sample	GSH-MIP	GSH-NIP	Co-MIP	Co-NIP	unit
Binding affinity to GSH (K_a)	17.59	10.05	20.70	15.92	1/mM
Total number of binding sites for GSH [a]	109.30	57.46	917.39	915.45	μmole/g
Binding affinity to GSSG (K_{ag})	1.94	10.12	20.55	51.66	1/mM
Total number of binding sites for GSSG	43.81	57.09	200.00	465.66	μmole/g
Relative sensitivity [b] : GSH selectivity (K_a/K_{ag})	1.81	0.99	1.01	0.31	

[a] The total number of binding sites was estimated from x-axis intercept of a scatchard plot.
[b] Relative sensitivity is the binding affinity ratio of GSH/GSSG

Particularly, there was a huge enhancement of the total number of binding sites for GSH. Even without MIP process, the binding affinity and total number of binding sites for GSH was improved with Co^{2+}-GSH chelating complex (see Co-NIP data). However, Co-MIP also showed a good binding affinity to GSSG although MIP helped to achieve GSH selectivity when relative sensitivities of Co-MIP (1.01) and Co-NIP (0.31) were compared. Large number of GSH binding sites of Co-MIP can be the cause of the selectivity drop. Co^{2+} forms chelating complex with thiol group of GSH. GSH has one thiol group, and GSSG has two thiol groups. Thus, binding affinity to GSSG must be greater than GSH without the MIP process. Actually, GSH selectivity was improved by the MIP process in this research. However, if too many chelate binding sites are surrounding GSSG, GSSG will tend to form Co^{2+}-thiol group complex.

6.5 Conclusions

GSH deficiency is the cause of many diseases such as Alzheimer, Parkinson, and diabetes. Therefore, GSH sensitive material was developed in this research for a GSH monitoring system. To achieve GSH sensitivity and selectivity in an aqueous media such as body fluid, two main strategies were tried: molecularly imprinting technology (MIT) and Co^{2+}-GSH chelating complex (Co-MIP). Polymerization conditions were optimized with precipitation method, and GSH sensible polymer particles were successfully synthesized. MIP effect was confirmed from both of GSH-MIP and Co-MIP, and GSH sensitivity was improved by involving Co^{2+} chelate complex. In particular, the total number of binding sites for GSH of Co-MIP is almost nine times greater than samples without the chelate complexes. However, this is also the cause of losing GSH selectivity to GSSG.

6.6 References

[1] Wu, G.; Fang, Y. Z.; Yang, S.; Lupton, J. R.; Turner, N. D. Glutathione Metabolism and Its Implications for Health. *Recent Advances in Nutritional Sciences* **2003,** 489-492.

[2] Dringen, R. Metabolism and Functions of Glutathione in Brain. *Progress In Neurobiology* **2000,** 62, 649-671.

[3] Townsend, D. M.; Tew, K. D.; Tapiero, H. The Importance of Glutathione in Human Disease. *Biomedicine & Pharmacotherapy* **2003,** 57, 145-155.

[4] Tian, D.; Qian, Z.; Xia, Y.; Zhu, C. Gold Nanocluster-Based Fluorescent Probes for Near Infrared and Turning on Sensing of Glutathione in Living Cells. *Langmuir* **2012**, 28, 3945-3951.

[5] Oztekin, Y.; Ramanaviciene, A.; Ramanavicius, A. Electrochemical Glutathione Sensor Based on Electrochemically Deposited Poly-Maminophenol. *Electroanalysis* **2011**, 23, 701-709.

[6] Bossi, A.; Bonini, F.; Turner, A.P.F.; Piletsky, S.A. Molecularly Imprinted Polymers for the Recognition of Proteins. *The State of the Art Biosensors and Bioelectronics* **2007,** 22, 1131-1137.

[7] Pichon, V.; Chapuis-Hugon, F. Role of Molecularly Imprinted Polymers for Selective Determination of Environmental Pollutants—A review. *Analytica Chimica Acta* **2008,** 622, 48-61.

[8] Tong, Y. J.; Xin, Y.; Yang, H. L.; Zhang, L.; Zhang, Y.R.; Chen, Y.; Xia, X.L.; Wang, W. Preparation and Performance Research on Glutathione Molecularly Imprinted Polymers. *Chromatographia* **2011,** 74, 443-450.

[9] Bell, C.F. Principle and Application of Metal Chelation, Oxford Clarendon Press, 1977.

[10] Bradley, R.; Kenneth, J. S. Synthetic Peptide Receptors: Molecularly Imprinted Polymers for the Recognition of Peptides Using Peptide–Metal Interactions. *Journal of America Chemical Society* **2001,** 123, 2072-2073.

[11] Yamazaki, T.; Yilmaz, E.; Mosbach, K.; Sode, K. Towards the Use of Molecularly Imprinted Polymers Containing Imidazoles and Bivalent Metal Complexes for the Detection and Degradation of Organophosphotriester Pesticides. *Analytica Chimica Acta* **2001,** 435, 209-214.

[12] Joshi, V. P.; Karmalkar, R. N.; Kylkarni, M. G.; Mashelkar, R. A. Effect of Solvents on Selectivity in Separation Using Molecularly Imprinted Adsorbents: Separation of Phenol and Bisphenol A. *Ind. Eng. Chem. Res.* **1999,** 38, 4417-4423.

[13] Song, X.; Want, J.; Zhu, J. Effect of Porogenic Solvent on Selective Performance of Molecularly Imprinted Polymer for Quercetin. *Material Research* **2009,** 12, 299-304.

[14] Dan, R.; Wang, Y.; Du, L.; Du, S.; Huang, M.; Yang, S.; Zhang, M. The Synthesis of Molecular Imprinted Chitosan-Gels Copolymerized with Multiform Functional Monomers at Three Different Temperatures and the Recognition for the Template Ovalbumin. *Analyst* **2013,** 138, 3433-3443.

[15] Burton, M. E. Applied Pharmacokinetics & Pharmacohydnamics: Principles of Therapeutic Drug Monitoring, Lippincott Williams & Wilkins: 2006; p 83.

CHAPTER 7

CONCLUSIONS AND FUTURE DIRECTIONS

7.1 Conclusions

Motivation for this research was to devise biomedical sensors that can be used for diagnosis or treatment of diseases because medical treatment and operation processes can be simplified by biomedical sensors. For example, diabetic patients can continuously monitor their blood glucose levels without concern about pain and infection if they use a body implantable continuous glucose monitoring system (CGMS). People can also keep watching their body conditions and for the potential possibility of getting certain diseases such as Alzheimer's, Parkinson's, and diabetes by using a glutathione (GSH) monitoring system. Therefore, a glucose responsive hydrogel was developed for a CGMS in this research. In addition, glutathione sensitive material was also synthesized to develop a GSH sensor.

First, the binding mechanism of boronic acid groups and sugar molecules was studied in Chapter 2. Glucose selectivity of zwitterionic glucose responsive hydrogel was confirmed by previous research. However, the binding mechanism was not clearly understood. Therefore, a thermodynamic approach was used to explain the glucose selectivity of zwitterionic glucose responsive hydrogels. Many prior studies already mentioned that glucose molecules acted as extra cross-linking structure within the

zwitterionic glucose responsive hydrogel by forming of double binding structure with two boronic acid groups. This explained the elastic contribution factor (Π_{el}) effect to glucose selectivity. However, the importance of a mixing contribution (Π_{mix}) factor was confirmed by this study. In particular, ternary interaction parameter (χ_1) of a Flory-Huggins equation in a glucose solution (≈ 0.51) is larger than a fructose solution (≈ 0.45). This research result was published in *Sensors and Actuators* B (160 (2011) 1363-1371).

Second, chemical composition effect was studied to enhance sensitivity and selectivity of zwitterionic glucose responsive hydrogels in Chapter 3. Particularly, design of experiments (DOE) method was used for this study. DOE has been used in an industrial area for a long time because it is useful in getting reliable data with limited cost and samples. Statistical analysis of experimental results confirmed that the molar ratio of 3-APB/DMAPAA and the monomer wt.% of the pre-gel solution determined sensitivity of the hydrogels. In addition, the molar ratio of AAM/BIS determined response time (inverse of first order rate). Faster glucose responses were achieved by decreasing the amount of cross-linker (BIS). This study will be useful in developing a body implantable CGMS using zwitterionic glucose responsive hydrogels.

Third, the effect of gamma rays and neutron irradiation on glucose responsive hydrogels was studied in Chapter 4. Glucose responsive hydrogels must be sterilized to be used as a part of biomedical devices. Gamma irradiation is the most common sterilization method for medical devices. However, it has been reported that gamma irradiation can effect the cross-linking structure of polymer. Therefore, a degradation study of glucose responsive hydrogels should be conducted before developing an implantable CGMS. Study results showed that gamma ray exposure increases the

crosslink density of UV-cured hydrogels, but there was no effect on thermally-cured hydrogels. It is possible that the remaining UV initiator within the hydrogel structure can be reactivated by gamma irradiation. Additionally, the neutron irradiation effect was also studied because zwitterionic glucose responsive hydrogels containing boronic acid moieties can be used for a boron neutron capture therapy (BNCT) with a minor modification. After exposure to both gamma rays and neutrons, glucose responses of the hydrogels were not different from the responses of hydrogels only exposed to gamma ray.

Fourth, magnetic field producible hydrogels were developed by embedding ferromagnetic particles within a zwitterionic glucose responsive hydrogel in Chapter 5. A magnetometer can be a good signal transducer for a chemical sensor because of good sensitivity, high resolution, low price, and minimal size. For adopting a magnetometer as a glucose response transducer, magnetic field producible hydrogels were synthesized. By embedding ferromagnetic particles, the zwitterionic glucose responsive hydrogel can produce a different magnetic flux density in response to glucose. The ferromagnetic particles embedding method was optimized by a computer simulation. Glucose responses were measured by a magnetoresistive transducer. The hydrogel with horizontal aligned ferromagnetic particles showed good sensitivity in the physiological glucose range (~10 mM). This result agrees with the computer simulation result. By adopting a magnetometer as a glucose response transducer, the response time was reduced (almost seven times shorter than piezoresistive pressure transducing method) with this magnetic field producing hydrogel.

Fifth, glutathione (GSH) sensitive polymer was developed by adopting a molecularly imprinted polymer (MIP) method and metal ion (Co^{2+}) chelating complex in

Chapter 6. Monitoring of GSH level in a body fluid is important to prevent diseases because the deficiency of GSH causes Alzheimer's, Parkinson's disease, ADHD, Autism, immune disorders, diabetes, etc. Particle type GSH sensitive polymers were achieved by a precipitation method. By creating a scatchard plot, MIP effect was confirmed from both of GSH imprinted polymer (GSH-MIP), and Co^{2+} chelate containing GSH-MIP (Co-MIP). Co^{2+} chelate binding sites helped to improve GSH binding affinity and total number of GSH binding sites. However, Co-MIP showed a good binding affinity to GSSG also.

7.2 Future Directions

A body implantable continuous glucose monitoring system (CGMS) is the best solution for diabetic treatment unless an innovative drug or medical operation is created to recover the disease completely. Currently, few semi-invasive CGMSs are commercialized and successfully used by diabetic patients [1-2]. However, the current CGMS product still has limitations. First, it has a short life time. Thus, patients should change the device every 10 days. Second, it should be calibrated by using a finger prick glucometer 2-3 times a day because the response is not accurate. Third, it still has quite a long lag time. According to a report [3], signal processing time normally takes 10 minutes. Therefore, patients cannot monitor their glucose level in real-time. Fourth, the majority of CGMS devices are designed to measure glucose levels of interstitial fluid, not blood, because it is installed on some body parts such as arm, or thigh. Thus, the values from the device cannot directly reflect blood glucose level changes. A body implantable CGMS is the only solution to overcome these limitations. Developing of glucose

responsive hydrogel and merging with an appropriate signal transducer is one approach to invent an implantable CGMS. However, there are still many tasks that must be completed in future research.

1) Sensing device should be scale down for body implantation.

2) Biocompatibility of all materials used in the sensing device should be confirmed.

3) Sensing device must have a long life time, such as patient's life time.

4) Response manipulation should be processed in real time.

Although these remaining tasks can be completed, clinical level experiments should be followed to prevent unexpected medical emergencies. While there is a long way to go, the ideal CGMS can be created through accumulating small steps of research.

Glutathione (GSH) roles for cell constructions and their importance have been studied in nutritional and medical sciences for many years. The regulation mechanism and function of GSH were confirmed about 40 years ago [4]. Interestingly, there are few studies that have tried to develop GSH sensing devices. In this research, GSH sensing devices are studied by developing GSH sensitive materials. Therefore, finding an appropriate signal transducing system for a GSH sensor and merging of GSH sensitive materials and a transducer should be followed first in order to further the research.

7.3 References

[1] Deiss, D.; Bolinder, J.; Riveline, J.P.; Battelino, T.; Bosi, E.; Tubiana-Rufi, N.; Kerr, D.; Phillip, M. Improved Glycemic Control in Poorly Controlled Patients with Type 1 Diabetes using Real-Time Continuous Glucose Monitoring. *Diabetes Care* **2006**, 29, 2730–2732.

[2] Garg, S.; Zisser, H.; Schwartz, S.; Bailey, T.; Kaplan, R.; Ellis, S.; Jovanovic, L. Improvement in Glycemic Excursions with a Transcutaneous, Real-Time Continuous Glucose Sensor: A Randomized Controlled Trial. *Diabetes Care* **2006**, 29, 44–50.

[3] Thome-Duret, V.; Reach, G.; Gangnerau, M.N.; Lemonnier, F.; Klein, J. C.; Zhang, Y.; Hu, Y.; Wilson, G. S. Use of a Subcutaneous Glucose Sensor to Detect Decreases in Glucose Concentration Prior to Observation in Blood. *Anal Chem.* **1996,** 68, 21, 3822-3826.

[4] Arias, I.M.; Jakoby, W.B. (Eds.), Glutathione: Metabolism and Function, Raven Press, New York, 1976, p. 77.